UNIVERSITY OF CASSINO AND SOUTHERN LAZIO

Ph.D. in Methods, models and technologies for engineering

XXXII Cycle

Ph.D. thesis

Exposure to airborne Particles: estimation of dose and Excess Lung Cancer Risk of populations living in Western countries

Supervisor
Prof. Giorgio Buonanno

Ph.D. student
Antonio Pacitto

Coordinator
Prof.ssa Wilma POLINI

A.A. 2018/2019

ABSTRACT

In the present thesis, six experimental campaigns were carried out to better understand the influence of the lifestyle in the exposure to airborne particles and to estimate the typical received daily dose of different populations. Moreover, a risk assessment based on an Excess Lung Cancer Risk (ELCR) model was performed taking into account two crucial environments: school environments and street canyons. In addition, an evaluation of the effectiveness of some possible solution to reduce the ELCR was performed taking into account two solution: (i) personal protectors (facemasks) for outdoor environments, and (ii) air purifiers and ventilation strategies for indoor environments.

The daily dose in terms of particle surface area received by citizens living in five cities in Western countries (Barcelona, Cassino, Guilford, Lund and Brisbane), characterized by different lifestyle, culture and climate, was evaluated and compared. Non-smoking volunteers performing non-industrial jobs were considered in the study. Particle concentration data allowed obtaining the exposure of the “typical citizen” for each city. Such data were combined in a Monte Carlo method with the time activity pattern data characteristics of each population and inhalation rates to obtain the most probable daily dose in terms of particle surface area as a function of the population gender, age, and nationality. Indoor Air Quality (IAQ), and in particular cooking and eating activities, was recognized as the main influencing factor in terms of exposure (and thus dose) of the population: then confirming that lifestyle (e.g. time spent in cooking activities) strongly affect the daily dose of the population.

Looking at outdoor environments/activities, one of the most influencing microenvironments/activity to airborne particle exposure is "transport". To better understand this environment Vehicular Indoor Air Quality (VIAQ) was investigated inside 14 diesel/non-diesel taxi pairs operating simultaneously and under normal working condition over six weekday hours (10:00-16:00) in the city of Barcelona.

Parameters measured included PM_{10} mass and chemistry, particle number concentration (PNC) and size, lung deposited surface area (LDSA), black carbon (BC), CO_2, CO, and a range of volatile organic compounds (VOCs). Keeping the windows open or close has shown the dominant influence of the air exchange rates on VIAQ. Median values of PNC and LDSA were reduced to around 10^4 #/cm^3 and <20 μm^2/cm^3 respectively under closed conditions, but more than doubled with windows open and sometimes approached 10^5 #·cm^{-3} and 240 μm^2/cm^3.

In urban areas, the coexistence of nanoparticle sources and particular street-building configurations can lead to very high particle exposure levels. An innovative approach for the evaluation of lung cancer incidence in street canyons due to exposure to traffic-generated particles was proposed. To this end, the literature-available values of particulate matter, PAHs and heavy metals emitted from different type of vehicles were used to calculate the ELCR at the tailpipe. The estimated ELCR was then used as input data in a numerical CFD (Computational Fluid Dynamics) model that solves the mass, momentum, turbulence and species transport equations, in order to evaluate the cancer risk in every point of interest inside the street canyon. Thus, the influence of wind speed and street canyon geometry (H/W, the height of the building, H and width of the street, W) on the ELCR at street level was evaluated by means of a CFD simulation. It was found that the ELCR calculated on the leeward and windward sides of the street canyon at a breathable height of 1.5 m, for people exposed 15 minutes per day for 20 years, is equal to 1.5×10^{-5} and 4.8×10^{-6}, respectively, for wind speed of 1 m/s and H/W equal to 1. The ELCR at street level results higher on the leeward side for aspect ratios equal to 1 and 3, while for aspect ratio equal to 2 it is higher on the windward side. In addition, the simulations showed that with the increasing of wind speed the ELCR becomes lower everywhere in the street canyon, due to the increased in dispersion.

Moving the attention on the indoor environments, schools may be classified as a critical microenvironment in terms of IAQ due to the proximity to outdoor particle sources and the frequent lack of proper ventilation and filtering systems. Moreover, the population exposed in schools (i.e. children) represents a susceptible population due to their age. Measurements in terms of PNC, LDSA, and PM fraction

concentrations were measured inside and outside schools in Barcelona (Spain) and Cassino (Italy). Simultaneously, PM samples were collected and chemically analyzed to obtain mass fractions of carcinogenic compounds. School time airborne particle doses received by students in classrooms were evaluated as well as their ELCR due to a five-year primary school period. Median surface area dose received by students during school time in Barcelona and Cassino resulted equal to 110 mm^2 and 303 mm^2, respectively. The risk related to the five-year primary school period was estimated about 2.9×10^{-5} and 1.4×10^{-4} for students of Barcelona and Cassino, respectively.

Different solutions were taken into account to reduce personal as well as collective exposure to airborne particles. An individual protective measure against particle pollution may be represented by face masks. A custom experimental set-up was developed in order to measure the effectiveness of nine different respirators under real environmental conditions in terms of particle mass concentration below 2.5 microns ($PM_{2.5}$), PNC, LDSA and BC. Facemask performances were assessed in a typical traffic affected urban background environment in the city of Barcelona under three different simulated breathing rates to investigate the influence of flow rate. Results showed a median face mask effectiveness for $PM_{2.5}$ equal to 48% in a range of 14-96%, 19% in a range of 6% - 61% for BC, 19% in a range of 4% - 63% for PNC and 22% in a range of 5% - 65% for LDSA.

A collective and indoor-adaptable solution to reduce exposure to airborne particles could be represented by air purifiers and ventilation strategies. To evaluate the effect of different ventilation methods (natural ventilation, manual airing) and the use of air purifiers in reducing the indoor concentrations of different airborne particles and gaseous pollutants in indoor environments an experimental campaign was performed. The samplings were carried out in two naturally-ventilated school gyms in Barcelona (Spain) of different volumes and different distance to major urban roads. Indoor and outdoor measurements of PNC, BC and PM_{1-10} concentrations were performed as well as indoor measurements of CO_2 and NO_2 concentrations. The study revealed that the use of air purifier with windows kept closed (natural ventilation) can lead to a significant reduction in terms of indoor-to-outdoor concentration ratios. In the smaller gym (air changes per hour of the purifiers, ACH, equal to 9.2 h^{-1}) the I/O ratios were

reduced by 93% and 95% in terms of particle number and PM_{1-10}, respectively; whereas in the larger school gym (ACH=1.7 h^{-1}) the corresponding reductions were 70% and 84%. For manual airing scenarios, the effect of the air purifiers on outdoor-generated sub-micron particles is reduced; in particular, for low ACH values (i.e. ACH=1.7 h^{-1}), the reduction is quite negligible (6%).

TABLE OF CONTENTS

LIST OF FIGURES

LIST OF TABLES

1 INTRODUCTION

1.1 Air quality

Human beings need a regular and continuous supply of air, and every day human adult breathes:

- In rest condition around 13 l/min;
- During moderate activity around 29 l/min;
- During high-intensity activity around 53 l/min.

Therefore, given its obvious importance to human existence, it is imperative that air remains unpolluted [1]. This requires the control of the environmental air quality and where necessary, the enforcement of emission limitations for air pollutants. Since the antiquity, humans started to recognize some correlation between poor air quality and human disease, but only in the twenty century, the adverse health effect of air pollution entered the world consciousness. This problem started to be present in the public opinion in 1930 when emissions of sulfur dioxide (SO_2) mixed with dense fog in the Meuse Valley in Belgium lead to 60 people died [2]. Another episode where people have been could notice the relation between air pollution and human health was in London, in 1952, wherefrom December to February 12000 people died after exposure to dense smog containing SO_2 and smoke particulate [3]. The first major regulatory effort aimed at both studying and setting limits on emission and air pollution was in America in 1970 with the Clean Air Act (CAA). On this occasion, the CAA defined the National Ambient Air Quality Standards that set limits on six primary pollutants found in the air: Carbon Monoxide “CO”, Lead “Pb”, Nitrogen Dioxide “NO_2”, Ozone “O_3”, Sulfur Dioxide “SO_2” and Particulate Matter “PM” [4].

Inhalation and consequent absorption of airborne particles and chemicals may have direct consequences for human health. Nevertheless, adverse health effect can also be indirectly influenced by the deposition of air pollutants in environmental media and

uptake by plants and animals. This lead to entering the food chain or being present in drinking water of the chemicals and thereby constituting additional sources of human exposure. Recognizing the need for humans to unpolluted air the WHO published the first *"air quality guidelines for Europe"* in 1987 [5]. To this reason in recent decades, major efforts have been made to reduce air pollution, declined significantly the emission of the main air pollutants. For example, the reduction of SO_2 was about 50% in the period 1980-1995 [6, 7], and this reduction is reflected by declining concentrations in ambient air in urban areas. Instead of the trend concentration of others pollutants, as PM or NO_2, less clear and it is envisaged that these pollutants still constitute a risk to human health [8, 9].

1.2 Human exposure to particulate matter

People can be exposed to a high concentration of airborne particles both in indoors and outdoors. Many studies highlighted the link between inhalation (and consequent deposition) of airborne particles in human respiratory tracts and health effects, such as respiratory diseases and inflammation [10, 11], cardiovascular diseases [12], diabetes [13], higher systolic blood pressure and pulse pressure [14], and decreased cognitive function in older men [15]. Moreover, the International Agency for Research on Cancer (IARC) has recently classified the particular matter (PM) as carcinogenic to humans (group 1) on the basis of the evidence presented by studies that showed a significant correlation between lung cancer and the exposure to PM [16, 17].

PM is a complex mixture of small solid particles and liquid droplets that are suspended in the air and vary in size, shape, surface area, chemical composition, solubility and origin. Particles with aerodynamic diameter <2.5μm are often considered more harmful than larger-sized particles because it can penetrate in the deeper parts of human's respiratory track like bronchi and Alveoli [18]. Main contributors to PM in urban areas are mainly emissions from combustion processes, industries and power generation plants, but also by atmospheric photochemical reactions and conversion processes [19]. Ultrafine particles (UFPs) are defined as those having diameters <0.1 μm. Typically, a higher concentration of UFPs is recorded close to the emission sources [20] and can decrease rapidly as the distance from the emission source

increases [21-24]. Their ability to penetrate in the deepest areas of the human respiratory tract can cause various adverse effects, possibly release in the bloodstream toxic and potentially carcinogenic substances [25, 26]. Particle Number Concentration (PNC) and Surface Area (SA) have been identified as more appropriate metrics for UFP-related health effects [27-29] and the biological response may be more related to the SA of the particle deposited in the lungs than the other metrics [30, 31]. Another component of fine particles is Black Carbon (BC): a primary PM component that is emitted from incomplete combustion as small sphere in a range size from 1 to 50 nm, and aggregates to particles of larger size, from 0.1 to 1μm [32]. BC can be considered a better indicator of harmful particulate substance caused by combustion sources than PM_{10} and $PM_{2.5}$ [33]. A number of studies indicated that traffic-related policy measures should focus on the reduction of BC concentration [33-35]. In a moderately polluted urban area, BC concentration values are in the range of a few $\mu g \cdot m^{-3}$, while in a heavily polluted area can reach up to tens of $\mu g \cdot m^{-3}$ under unfavorable meteorological conditions. Many studies have revealed a link between exposure to BC and increasing adverse health effects in cardiovascular diseases such as cardiac and ventricular arrhythmias, lowered heart rate variability, changes in blood pressure and increase of cardiovascular mortality [36-39] or negative effects on the respiratory system [40]. In addition, recent studies on spatial and temporal evolution of BC concentration in urban areas, report the significance of BC contribution in UFPs concentrations [35, 41-43], but also that in high insolation urban areas nucleation of secondary particles highly influence the PNC [44]. The harmful potential of airborne particles stems from their ability to penetrate, and deposit in the deepest areas of human respiratory tract, causing irritation, inflammation, and possibly translocate to the blood system, carrying with them carcinogenic and toxic compounds [45], and depositing in secondary organs [46] including brain tissues [15]. Even though the scientific community has not reached a definitive conclusion whether morphology, size or chemical composition of the particles are the key factor in affecting human health, the focus of scientific studies has shifted from super-micron particles (whose contribution is expressed in terms of mass concentrations of particles smaller than 10 and 2.5 μm, i.e. PM_{10} and $PM_{2.5}$) [47, 48] to sub-micron (PM_1) and UFP whose

contribution is better related to PNC [49, 50] and SA concentration [29] than mass concentration. In fact, numerous toxicity-based studies have shown that surface area is a more appropriate metric for UFP-related health effects [27, 51] and that the biological response depends more on the SA of the particles deposited in the lungs than on other exposure metrics [30, 31]. This could be due to their large surface area and the related high probability to carry and transmit toxic compounds [52, 53]. In order to evaluate the health effect of the exposure to airborne particles, a dose-response relationship is needed [54]. To this purpose the daily dose of airborne particles received by people, along with the toxicity of such particles, is a key parameter to be evaluated and provided to medical experts [27, 55, 56]. Moreover, the airborne particle daily dose is the main input data for a human health risk model [57]. Airborne particle doses received by population can be evaluated based on exposure measurements. Nonetheless, even though the scientific community is moving from particle mass-based to PNC and SA-based metrics, the current legislation is still limited to outdoor concentration of PM_{10} and $PM_{2.5}$; further, such measurements are limited to a number of fixed outdoor sampling points (FSPs) located in specific regions of interest in the urban area [58, 59]. The number of FSP is a function of the population density, without links to climate nor the community lifestyle, and therefore is not properly representing the actual exposure of citizens to PM [60]. Moreover, PM_{10} and $PM_{2.5}$ measurements at FSPs cannot be considered proxies for exposure to sub-micron and UFP since they present different dynamics (e.g. dilution, deposition) and sources (e.g. sub-micron particles are mainly generated by combustion processes whereas super-micron particles are mostly emitted by mechanical processes, [23, 24, 61, 62]).

Traffic is considered one of the main source of air pollutants in cities, and with urban inhabitants already accounting for a majority of the total global population (https://data.worldbank.org/indicator/SP.URB.TOTL.IN.ZS, UN Population Division) the effects of breathing vehicular gas and particle emissions have grown to become one of our most challenging environmental health problems (e.g. [63, 64]. Traffic-related air pollutants (TRAPs) source from both exhaust and non-exhaust (such as brakes and tyre wear [65]) emissions and their distribution is typically highly variable in time and space (e.g; [61, 62]. There are consequently notable differences

in the exposure of individual city commuters to TRAPs during their travel through the city. For the traveler outdoors the most important of these factors is proximity to the sources of traffic emissions, whereas for the commuter inside a road vehicle exposure to TRAPs will depend primarily on air exchange rates (e.g. [66-68]). In Moreno, et al. [69] authors compared pollutant exposure when travelling by different public transport options (bus, tram, subway) in Barcelona to improve the understanding of how real-time air pollutant concentrations regularly inhaled by urban commuters vary depending on how they choose to travel.

Commonly, one of the most critical urban configurations in the cities in which the air quality get worse is the so-called street canyon, which is a typical urban configuration of a street flanked by buildings on both sides. In a street canyon, air exchange provided by natural ventilation may become weak with consequent formation of high particle concentration zones. For these reasons, urban microenvironments may increase human exposure to high particle concentrations, and significantly contribute to the increase of the daily dose[70] likely leading to pulmonary and cardiovascular diseases, as well as to lung cancer cases[71-73].

There are several studies in scientific literature addressing the evaluation of air quality in urban street canyons by means of numerical simulations and dedicated experimental campaigns. Numerical simulations of pollutant dispersion inside street canyons of different typologies were carried out by Kikumoto and Ooka [74] and Hertwig, et al. [75], finding that the canyon geometry strongly influence the ventilation efficiency and then the pollutant dispersion. Similar results were found in Scungio, et al. [76], where the fluid flow patterns and the dispersion of UFPs inside street canyons of different aspect ratios (H/W, height of building, H and width of the street, W) with different turbulence modelling techniques were calculated[76, 77].

Mediterranean cities are recognized to be densely populated and trafficked suffering from higher levels of $PM_{2.5}$ than those of Northern Europe [78, 79]. Thus, citizens in these cities live generally close to main roads and are exposed to high exhaust and non-exhaust vehicle emissions. Such high density of urbanization also causes short distance from schools to major roads leading to non-negligible near-road pollution exposure at schools of children as evidenced by the international UPTECH

(Ultrafine Particle from Traffic Emission on Children Health; [80] and BREATHE (BRain dEvelopment and Air polluTion ultrafine particles in scHool childrEn; [81-83] projects. Indeed, children are the most vulnerable population in terms of air pollution exposure [84, 85] due to their higher inhalation rates resulting in larger specific doses than adults [86-89]. Therefore the long exposure time in schools (children spend from 175 to 220 days and from 5 to 8 hours at school [90] could significantly affect the overall dose received by students attending schools located near highly-trafficked urban roads. Indeed, high indoor particle concentrations may result from the significant outdoor-to-indoor infiltration of sub-micron particles (with indoor/outdoor ratios roughly varying in the 0.6-0.9 range), which depends on the levels of outdoor pollutants, physical barriers of the building, type of ventilation and particle physic-chemical properties and size [66, 91-103].

Since schools represent a crucial environment in terms of air quality assessment a number of studies have been carried out by the scientific community to measure and evaluate the Indoor Air Quality (IAQ) in schools [104, 105]. For many years, most of these papers proposed a simplified evaluation of the IAQ just considering the CO_2 concentrations and thermal comfort as main parameters; nonetheless their negative effects can be merely restricted to students' vigilance and cognitive performances [106-109]. Moreover, European standards, providing guidelines on ventilation rates, still adopt the CO_2 concentration as main design parameter [110] since it is unanimously considered as a good proxy of the IAQ [111, 112]. This approach is not adequate from a scientific point of view since the CO_2 behavior (i.e. sources, dynamics, removal) cannot be considered representative of all the different pollutants typically present in schools [113, 114]. Indeed, the IAQ in schools is influenced by several pollutants, including both gaseous species and airborne particles. Some of the gaseous pollutants are indoor-generated (e.g. radon, VOCs), thus, their behavior can be roughly treated as the CO_2 one; whereas, other gases are outdoor-generated as they are typically related to vehicular traffic (e.g. NO_2) then penetrating the building envelope on the basis of the airtightness and ventilation system of the buildings [91]. Particularly in the context of urban areas of developed countries, the different metrics of the airborne particles affect the school air quality in different manners: super-micron

particles (better described in terms of PM_{10}, i.e. mass concentration of particles smaller than 10 μm) can be treated as an indoor-generated pollutant due to the high emission indoor (e.g. resuspension phenomena), whereas sub-micron particles (better described in terms of PNC and BC concentrations) may be mostly driven by outdoor-generated pollutants as they represent the aerosol metrics characteristics of secondary atmospheric PM formation and tailpipe traffic emissions [113-115]. These pollutants, unlike CO_2, can cause serious health effects such as respiratory and cardiovascular problems as well as lung cancer [11, 31, 116-120], thus, their concentration should be monitored and reduced. As an example, outdoor-generated pollutants may results in high concentration in schools when they are located near to highly trafficked roads [83, 121] due to the high outdoor-to-indoor penetration. Such high exposures can lead to not negligible sub-micron particle doses received by the children in schools and, consequently, to risks and effects higher than acceptable levels [105].

The penetration of outdoor-generated pollutants is strongly affected by the ventilation system adopted in the schools. Indeed, schools worldwide are typically naturally-ventilated buildings, thus, on the basis of the perceived indoor air quality, people working in classrooms adopt random airing strategies that easily reduce the indoor-generated pollutants but lead to simultaneous increase of the outdoor-generated ones [115]. In order to guarantee a simultaneous reduction of all the pollutants (both produced indoors and outdoors) ventilation retrofit should be adopted by installing mechanical ventilation systems able, at the same time, to increase the air exchange rate of environment and to filter the fresh air [122]. Nonetheless, ventilation retrofit represents an expensive solution, therefore, it should be supported (on national basis) by the regulatory authorities through policies and incentives: to date, such incentives mainly supported energy saving solutions (e.g. renewable energy, building insulation), whereas the improvement of the air quality was less frequently adopted [123].

A possible easy-to-use solution to reduce pollutant concentrations in indoor environments is adopting air purifiers, i.e. systems made up of fans (or pumps) pulling the indoor air through a series of filters that remove airborne particles and gases and then circulating the purified air back into the indoor environment [124-130]. Air purifier can work according to different operating principles and present different

filtration methods, nonetheless, those characterized by the highest performances (able to trap sub-micron particles and UFP) include high-efficiency particulate air (HEPA) filters which permanently remove airborne particles from the sucked air. Several household appliance producers recently launched on the market their own air purifiers characterized by different filtration systems, flow rates, control strategies (e.g. remote control, sensor-based control, etc.), geometry, size, design. The producers typically characterize the effectiveness of their own purifiers through in-house tests carried out in *ad-hoc* test-chambers then providing rough indication regarding the maximum suggested floor area/volume of the micro-environment where the air purifier can be used. Even if the recommendations provided by the producers result approximate and inhomogeneous (for example the air purifier flow rate values spanning from about 1.5-fold to >10-fold the room volume to be purified), represent a key information since, to date, no standards are available to choose the characteristics of the air purifier to be installed as a function of the indoor micro-environment.

In order to reduce the level of urban air pollution, a common strategy is to encourage public to use sustainable public transport and also active transport such as cycling or walking. However, cyclists and pedestrians may be exposed to higher concentrations of air pollutants due to their proximity to vehicle emissions. Moreover, cyclists exhibit higher breathing rate (cyclist ≈40 $L \cdot min^{-1}$) compared to car drivers (≈12 $L \cdot min^{-1}$) or bus passengers (≈13 $L \cdot min^{-1}$) [131], other study found a mean (standard deviation) value of real-word breathing rate for cyclist equal to 59.1(13.7) $L \cdot min^{-1}$ and 46.2 (10.6) $L \cdot min^{-1}$ for man and woman respectively [132]. For this reason, the use of personal Respiratory Protectors (RP) is becoming more and more common in recent years. Respiratory protectors as face masks can be summarized in two macro categories, for occupational settings (professional face masks) and for non-occupational settings (commercial face masks). In many countries, in occupational settings, people have to use RP in order to safeguard their health. In addition, these professional facemasks have to meet national and international standards (e.g. EN 149:2001, EN 140:1998 in Europe). The use of RP in non-occupational setting is not supported by legal enforcement, so commercial face masks do not have to respect such

standards as professional ones but they reflect market laws following trends of fashion rather than human health.

2 OBJECTIVES

The aims of this thesis are to evaluate the influence of the lifestyle on the exposure to ultrafine particles (by means a “direct exposure assessment approach”) and the estimation of daily doses in terms of particles SA received by people, taking into account different characteristics of the populations; as gender, age and origin. Moreover, based on the data of received dose and data on chemical characterization a risk assessment as a consequence of the exposure to airborne particles was obtained by means an excess lung cancer risk (ELCR) model for two crucial environments (i) school environment for children that are attending 5-years primary school, and (ii) in a common urban configuration usually called street canyons. Both environments represent a critical and crucial environment for different reasons; (i) school environments, as said above, for their vulnerable population (the children), and (ii) transport environments for their high concentrations of airborne particles which people could be exposed. In addition, an evaluation of the efficiency of some possible solutions to reduce the ELCR by means reducing the received dose of the people were taken into account. The solutions taken into account are (i) a personal protection by means personal RPs as facemasks, usually used in outdoor environments, and (ii) a collective protection by means air purifiers and/or ventilation strategies, usually applied in indoor environments.

To achieve the above-mentioned objectives, six experimental campaigns have been developed and performed in which the following aspects have been investigated and evaluated:

- The evaluation of the influence of the lifestyle in airborne exposure, characterizing and comparing the sub-micron particle daily dose, in terms of surface area received by the population living in five different cities in western countries;

- The evaluation of the air quality inside vehicles (VIAQ) mostly used to move through the city, taking into account parameter as BC, PM, PNC, LDSA, CO, CO_2 and VOCs;
- Estimation of the lung cancer risk of people exposed to traffic-generated particles inside street canyon;
- Evaluation of IAQ and estimation of ELCR in different primary schools located in two European cities, Barcelona and Cassino;
- Evaluation of airborne particle exposure reduction by means personal RPs as facemasks in outdoor environments and ventilation strategies including air purifiers in indoor one.

3 THE INFLUENCE OF LIFESTYLE ON AIRBORNE PARTICLE SURFACE AREA DOSES RECEIVED BY DIFFERENT WESTERN POPULATIONS

A better representativeness of the overall human exposure to sub-micron and ultrafine particles can be obtained through personal monitoring able to quantify the exposure in indoor micro-environments too. Such an approach is very demanding from a technical-economic point of view since a large sample (in terms of people involved in the experiments) is needed to represent the exposure of an entire population: indeed, the different lifestyles of the people result in exposures to different pollutant sources, in many different microenvironments (both outdoor and indoor), where they live, spend time or pass through during the day [133-135]. Thus, exposure data are essential to evaluate the dose of airborne particles received by population, but information on the type of activity is also needed to estimate the inhalation and consequent deposition of particles in the different regions of the lungs [136], as well as time activity pattern data (i.e. time spent in each microenvironments). As an example, in previous studies [137] the tracheobronchial and alveolar doses received by Italian and Australian populations were estimated on the basis of an "indirect exposure assessment approach", i.e. characterizing the exposure to airborne particles through fixed monitors (not personal monitoring) placed in each microenvironments where people reside during the typical day [138], and evaluating the deposition fraction of such particles as a function of their size through the deposition model proposed by the International Commission on Radiological Protection [136]. That study demonstrated a significant difference between the two populations in terms of daily dose, highlighting the effect of both lifestyle and air quality of the local microenvironments.

Previous studies opened up the question about the main parameters affecting the airborne particle doses received by the populations. They also pointed out to the need for further efforts to fill the gap in knowledge about the effect of lifestyle (e.g. culture) and geographical location (e.g. climate, outdoor concentration) in this respect.

To this end, the aim of the present study is to characterize and compare the sub-micron particle daily dose, in terms of surface area, received by population living in five different cities in Western countries: Barcelona (Spain), Cassino (Italy), Guilford (United Kingdom), Lund (Sweden) and Brisbane (Australia). These cities/populations were selected in order to highlight the possible effect of local pollution concentration and population lifestyles; indeed, some of these cities were previously characterized in term of background particle concentrations. The study was limited to non-smoking population (smoking population should be analyzed separately due to the large dose they typically receive, [139]) and non-industrial working environments.

The study was performed with a "direct exposure assessment approach" measuring the exposure to airborne particle concentrations through personal "portable" monitors capable of measuring the exposure at a personal scale [133, 140]. To this end, several volunteers were selected amongst the five populations to perform personal monitoring and obtain the exposure representative of the population living therein. Exposure data were combined in a Monte Carlo method along with statistics on time activity patterns of the citizens to obtain the statistically most probable dose received by such five populations.

3.1 Methodology

3.1.1 Study area

Measurements were carried out in Barcelona (Spain), Cassino (Italy), Guilford (United Kingdom), Lund (Sweden) and Brisbane (Australia). Barcelona (inhabitants: 1.6 million; city area: 101 km^2), located on the northeast coast of the Iberian Peninsula (41°23′N 2°11′E), is characterized by a subtropical-Mediterranean climate with warm summers and mild winters. Climate and position contribute to typical low airborne particle concentrations [69, 141] in spite of its numerous pollutant sources, e.g. industrial activities, road transport lines, and high vehicle density (5800 cars/km^2).

Cassino (inhabitants: 36000; city area: 83 km²) is located in Central Italy (41°29′30″N 13°50′00″E) in the Liri Valley. Climate and topography of the area contribute to frequent temperature inversion phenomena in winter resulting in high pollutant concentrations [60, 133]. Lund (inhabitants: 82000; city area: 26 km²) is situated in the southern part of Sweden (55°42′14″N 13°11′42″E) 15 km north from the coast of Baltic sea. Oceanic climate and typically low pollutant concentrations characterize the city [141, 142]. Guildford (inhabitants: 137000) is located in the Surrey County, 43 km southwest of London (51°14′N 0°34′W) and about 50 km north of the ocean (English Channel). The climate is classified as oceanic, and the pollutant concentrations in Surrey County area are generally low [141, 143]. Brisbane (inhabitants: 2.3 million; city area: 15826 km²), located 20 km west of the east coast of Australia (27°28′03.54″S 153°01′39.59″E), is the capital of the Australian State of Queensland. Its climate, classified as humid subtropical, and among other factors, the spread of the city and its low population density contribute to low pollutant concentrations in the city [137, 144]. In ***Table 1*** information on meteoclimatic parameters during the experimental campaigns, obtained by the Meteorological Data Archives of the US National Weather Service's National Centers for Environmental Prediction (http://ready.arl.noaa.gov/archives.php), is reported for the five cities investigated. From the inspection of the data it can be concluded that a higher reduction of the exposure in outdoor environments (due to both ventilation and rain) is expected in Lund and Brisbane when compared to Cassino and Barcelona.

Table 1 *Data of the main meteoclimatic parameters during the experimental campaigns for the five cities investigated, as reported by the US National Weather Service's National Centers for Environmental Prediction. Temperature, relative humidity, and wind speed data are reported as median values.*

City		Barcelona (Spain)	Cassino (Italy)	Guilford (UK)	Lund (Sweden)	Brisbane (Australia)
Measurement period		Oct-Dec 2015	Apr-June 2016	Aug-Nov 2016	Sept-Dec 2016	Jun-Aug 2016
Meteoclimatic parameters	Temperature (°C)	18	17	17	10	27
	Relative Humidity (%)	73	74	81	78	79
	Wind speed (m/s)	7	8	7	18	8
	Rainfall depth (mm)	127	111	83	272	284
	Number of rainy days (-)	17	25	49	44	27

Information on climate and location of the cities investigated is of importance since they do affect the outdoor particle concentration levels and the resulting contribution to the population daily dose. Still, a great contribution to the daily dose is expected to be due to indoor microenvironments where significant particle sources [145-147] and low building ventilation [92, 115, 148] contribute to high exposures and doses in people living/residing therein [70].

3.1.2 Study design

In order to estimate the daily dose of sub-micron airborne particles, expressed in terms of particle surface area received by the populations living in the five cities under investigation, the following procedure was applied:

a) identification of the typical time activity pattern characteristic to citizens living in each of the five cities,
b) measurements of the concentrations of Lung Deposited particle Surface Area (LDSA) to which citizens are exposed in different microenvironments,
c) estimation of the daily dose received by the typical population living in the five cities through a Monte Carlo method capable of combining both time activity pattern and exposure data.

Once again, it was a direct method, which was applied here to evaluate the dose received by population, by performing measurements at a personal scale (“direct exposure assessment approach”).

3.1.2.1 Time activity pattern of the population

The typical time activity patterns characteristic to citizens living in the five cities were obtain from national human activity pattern surveys performed by National Statistics Institutes and/or research studies taking into account people living both in urban areas and country sites [149-154].

3.1.2.2 Measurement of the exposure to particle surface area concentration

In order to evaluate the most probable value of SA dose received by the populations considered in the present study, LDSA concentration levels (sum of alveolar- and tracheobronchial-deposited contributions) were measured during different experimental campaigns performed in the five cities, through personal monitors.

The exposure to airborne particles in each microenvironment of the five cities was obtained by performing mobile measurements of particle number concentrations (PNC), average particle sizes and LDSA concentrations through direct measurements carried out with hand-held diffusion charger particle counters (a NanoTracer Philips and a DiscMini Testo). Exposure characterization was carried out in different periods summarized in **Table 1**: from October to December 2015 in Barcelona, from April to June 2016 in Cassino, from June to August 2016 in Brisbane, from August to November 2016 in Guilford, and from September to December 2016 in Lund.

The authors point out that, since a 1-year experimental campaign for each site would have been not workable for practical reasons, roughly three-four months for each site were considered: in particular, a period of the year representative of the average exposure was chosen for each site then avoiding extreme/critical meteorological situations likely leading to reduced ventilation of indoor environments or temperature inversion phenomena in outdoors. In order to obtain a significant amount of data for each microenvironment, 75 non-smoking volunteers (15 for each city) were selected. The volunteers, both males and females aged from 25 to 55 years old, lived and worked (non-industrial jobs) in the urban area of the city. 15 volunteers for each city were considered in order to have an adequate representativeness of the exposure level in each microenvironment/activity. As an example, different measurements in similar microenvironments allow to include effects of cooking practices (such as the type of

food, cooking and stove [155-158]) and transport microenvironment (different transport modes, i.e. metro, train, car [69, 159]) on the exposure levels. Personal, belt-mounted particle counters were worn by the volunteers for 3 days, then each volunteer performed continuous measurements for 3 days. When volunteers were at home/office (e.g. working, studying, sleeping, etc.) the instrument was left on a close desk. Moreover, the volunteers were asked to fill an activity diary to take note about place, time, and kind of activity in order to relate the particle exposure values to the activity and to the specific microenvironments.

On the basis of PNC and average particle size (D_p) measured through the Nanotracer (and corrected by calibration factors, please see "Instrumentation and quality assurance" section), the alveolar- and tracheobronchial-deposited particle SA concentration (S_{Alv} and S_{TB}, respectively) were calculated by means of the semi-empirical correlation (1) for a reference worker (dosimetry model developed by the International Commission on Radiological Protection [136]) then allowing to determine the overall LDSA concentration:

$$\boldsymbol{LDSA = S_{Alv} + S_{TB} = (4.7 \cdot 10^{-5} + 0.95 \cdot 10^{-5}) \cdot PNC \cdot D_p} \quad (1)$$

As regards DiscMini measurements, the lung deposited surface area concentrations provided by the instrument was used since the accuracy of the DiscMini was recognized to be better for the lung deposited surface area than for PNC [160].

In order to obtain a statistical analysis of the concentration levels for each microenvironment a preliminary normality test (Shapiro-Wilk test) was performed to check the statistical distribution of data. Since the data did not meet a Gaussian distribution, a non-parametric test and a further post-hoc test (Kruskal-Wallis test; [161]) was considered in the analysis; further details are reported in Rizza, et al. [60].

3.1.2.3 Daily dose of the population

Doses of submicron particles were calculated on the basis of the data concerning the typical exposure to lung deposited particle surface area concentrations and time activity patterns. In particular, the total surface area dose (δ_{SA}) for each population was obtained as reported in Buonanno, et al. [137]:

$$\boldsymbol{\delta_{SA} = \sum_{j=1}^{n} \{ IR_{activity} \cdot LDSA \cdot T_j \}} \quad (2)$$

where $IR_{activity}$ ($m^3\ h^{-1}$) is the inhalation rate (which depends on age and activity [137]), and T_j is time spent on each activity (as a function of the age and gender) reported in the abovementioned statistical surveys for each population (please see "Time activity pattern of the population" section). The authors point out that the information on time activity patterns obtained from the activity diary were not used to calculate the dose since they were specific of the volunteers under investigation. Once again, time activity diary was just used to relate the particle exposure values to the microenvironments. The activities performed by the population, obtained on the basis of the typical time activity patterns, were grouped in seven main microenvironments as reported in ***Table 2*** [137].

Table 2 *Classification of the activities performed by the citizens in seven main microenvironments.*

Microenvironment	Activities
Transportation	Trip and use of time not specified, round-trip to work
Working	Non-industrial workplaces, Profitable work, Main and secondary job, Working-connected activities, Studying, School, Institute or University, Voluntary job and meetings, Voluntary work in an organization
Eating	Eating and drinking (including home and restaurant)
Cooking	Cooking
Outdoor day	Gardening and animal care, Construction and restoration, Sport and outdoor activities, Physical workout, Productive exercise, Sports-connected activities
Indoor day	Personal care, Other personal care, Studying not specified, Studying in the free time, Activities for home and family not specified, Housework, Clothes care and folding, Purchasing goods and services, Home maintenance, Baby care, Helping adult family members, Helping other family members, Active Activities, Social Activities and entertainment, Social life, Entertainment and culture, Inactivity, Hobbies and computer science, Art and hobbies, Computing, Playing, Media, Reading, Watching TV, DVD or videos, Listening to the radio or recording
Indoor evening and night	Sleeping

Data of particle concentrations and time activity pattern were combined through a Monte Carlo method to obtain the probability distribution function of the daily dose of each population then allowing to recognize the most probable daily dose. To this end, mean and standard deviation values of time spent in each activity were used for Italian, Spanish, Swedish and Australian people, whereas minimum and maximum values were considered for U.K. people (such range is due to the fact that both Irish

and English time activity patterns were available). Moreover, since the of particle SA exposure data were not Gaussian, probability distribution function was calculated from the measured data, considering 10 equally-spaced concentration ranges. Finally, fixed values of inhalation rate, specific of each activity were applied [137]).
In order to compare the dose in different microenvironments, the dose intensity ratio, i.e. the ratio between the daily dose fraction and the daily time fraction characteristics of each activity, was also evaluated [133].

3.1.2.4 Instrumentation and quality assurance

PNC and average particle sizes were measured trough two diffusion charger particle counters:

i) an Aerasense NanoTracer XP (Oxility, partner of Royal Philips Electronics), which measures PNC and the average particle size in the range 10-300 nm, with 10 seconds sampling time when used in "Advanced Mode". The NanoTracer was used in the experimental analyses performed in Barcelona, Lund and Brisbane.
ii) a DiscMini (Testo) measuring PNC and the average particle size in the range 10-700 nm with 1 second sampling time. The DiscMini was used in the experimental analyses performed in Cassino and Guilford.

The operating principles of these instruments is based on the diffusion charging technique. In particular, the sampled aerosol is charged in a positive unipolar diffusion charger imparting an average known charge on the particles, that is approximately proportional to the particle diameter of the aerosol. The number of charges, and thus the number of particles, is then detected by an electrometer [162-164]. Since over 99% of total PNC in urban environments are contributed by the particles below 300 nm in diameter [165, 166], both instruments were able to measure total PNC despite their different upper sampling cut-off point for particle diameters.

3.1.2.5 Instrument intercomparison

The devices were calibrated before and after the experimental campaigns. To this end, both a CPC (model 3775, TSI Inc.) and SMPS system (model 3936, TSI Inc.) were used to compare the NanoTracer and DiscMini in terms of number concentration and particle size, respectively. The SMPS consisted of an Electrostatic Classifier (model

3080, TSI Inc.), a Differential Mobility Analyzer (model DMA3081, TSI Inc.) and a CPC 3775. The SMPS 3936 was used, with aerosol/sheath flow ratio of 0.3/3.0 L min^{-1}, thus measuring particle number distributions in the range 14-700 nm. Calibrations were performed at the European Accredited Laboratory of Industrial Measurements (LaMI) of the University of Cassino and Southern Lazio (Italy) located in a 150 m^3 room, with an ordinary mechanical ventilation system guaranteeing constant thermo-hygrometric conditions (20±2 °C and 50±5% RH). Moreover, the DiscMini was also compared in terms of LDSA concentrations to the SMPS through the methodology reported in [167]. Comparisons were performed for two different aerosols: aged indoor aerosol and fresh emitted aerosol produced by incense burning. Tests were performed during 2 h co-located measurements of the diffusion charger monitor (Nanotracer or DiscMini), CPC 3775 and SMPS 3936. To this end CPC sampling time was 1-s, while SMPS scans were 135-s. SMPS measurements were corrected for multiple charge and diffusion losses. The average correction factors in terms of PNC, obtained by averaging the two aerosols investigated before and after the experimental campaign, were applied as correction factors for the entire campaigns: correction factors equal to 1.08 and 1.03 in terms of PNC were estimated for NanoTracer and DiscMini, respectively, whereas a correction of 0.98 in terms of LDSA concentration was applied for DiscMini. Moreover, the CPC and SMPS were also calibrated in the European Accredited Laboratory at the University of Cassino and Southern Lazio by comparison with a TSI 3068B Aerosol Electrometer, using NaCl particles generated through a Submicrometer Aerosol Generator (TSI 3940) [168].

3.2 Results

3.2.1 Time activity pattern

In ***Table 3*** data on time activity patterns of the populations under investigation, obtained from the national statistics institutes and/or research studies, as a function of the age, are reported. The data clearly demonstrate that, whatever the population and the gender, people spend the largest time fraction in indoors: from 88% for the Swedish population to 95% for Australian population. Cooking and eating, recognized as the most significant activities in terms of exposure [169], present jointly a contribution

ranging from 13% to 26%. On average, the Swedish people spent less time than other population in cooking and eating activities, whereas Spanish citizens devote the highest time fraction to these activities. Apart from the Swedish population, the contribution of cooking and eating activities increases as a function of age. Cooking activities by themselves account for a maximum contribution equal to 6% with higher exposure time values for females than males. A further microenvironment recognized as critical in terms of people exposure [77, 170] is the transport, however the exposure time in such microenvironments is limited, since its daily time contribution range from <1% (Australian citizens older than 65) to about 6% (for Spanish people younger than 65). Whatever the age, the Australian population spends a smaller fraction of time in the transport microenvironment. Further, in general, the time spent in transport decreases as the age increases for all the populations under investigation. Sleeping and resting activities, as expected, account for a third of the day: in particular, time fraction averaged across all the age groups, ranges from roughly 30% (Italian and Australian) to roughly 37% (Spanish, UK and Swedish). ‘Other indoor day’ activities, averaged across all the age groups, account for about 30% of the time, except for the Australian population, which spends 45% of their day in such activities. Finally, ‘other outdoor’ activities, averaged across all the age groups, engage for about 4-8% of the day.

Table 3 *Time activity pattern data (daily time spent, in minutes, for each main microenvironment) of the typical population investigated, as function of age and gender, as obtained from the national statistics institutes and/or research studies. Time activity data are reported as mean ± standard deviation for Italian, Spanish, Swedish and Australian people, whereas minimum and maximum values were considered for U.K. people.*

	Barcelona (Spain)		**Cassino (Italy)**		**Guilford (UK)**		**Lund (Sweden)**		**Brisbane (Australia)**	
Microenvironment	**Female 19-40**	**Male 19-40**	**Female 19-40**	**Male 19-40**	**Female 19-40**	**Male 19-40**	**Female 19-40**	**Male 19-40**	**Female 19-40**	**Male 19-40**
Sleeping	523±43	527±47	436 ±36	433±38	504-543	497-523	544±69	532±53	403±16	434±12
Indoor Day	437±153	372±129	429±150	411±143	444-583	391-446	385±284	356±259	729±81	572±57
Outdoor Day	37±14	68±29	79±30	84±36	35-46	64-76	106±111	101±88	42±23	45±23
Transport	81±2	94±2	68±2	70±1	55-91	72-97	60±63	59±51	14±0	28±1
Working	187±50	256±76	310±82	340±101	72-204	73-267	229±185	290±127	130±7	264±9
Eating	110±3	116±3	64±1	67±2	73-143	76 262	81±37	76±26	72±3	72±2
Cooking	61±21	3±1	47±16	35±10	34-46	12-20	33±20	25±13	46±2	20±1
Microenvironment	**Female 41-64**	**Male 41-64**	**Female 41-64**	**Male 41-64**	**Female 41-64**	**Male 41-64**	**Female 41-64**	**Male 41-64**	**Female 41-64**	**Male 41-64**
Sleeping	501±39	505±44	446±35	456±40	510-533	503-518	528±64	513±42	409±21	436±13
Indoor Day	467±133	402±126	480±137	434±136	487-616	407-479	402±226	378±215	677±86	558±52
Outdoor Day	51±21	82±36	76±31	83±37	37-45	60-75	97±100	93±76	56±25	57±25
Transport	75±5	88±8	55±4	62±5	50-84	67-95	51±46	53±38	13±0	24±1
Working	131±50	199±74	226±87	275±103	72-162	73-245	232±167	292±114	129±8	244±8
Eating	117±7	122±11	67±4	74±6	81-86	87-205	88±38	82±21	90±5	91±3
Cooking	95±26	38±9	87±24	49±11	54-58	27-35	39±20	27±11	64±4	26±1
Microenvironment	**Female >65**	**Male >65**	**Female >65**	**Male >65**	**Female >65**	**Male >65**	**Female >65**	**Male >65**	**Female >65**	**Male >65**
Sleeping	548±45	585±55	493±40	477±44	532-559	551-573	560±47	550±47	456±27	488±22
Indoor Day	540±122	507±128	612±138	531±134	636-676	540 571	494±230	483±230	717±97	664±76
Outdoor Day	71±23	106±44	71±23	114±47	54-56	81-88	146±85	137±85	74±30	98±35
Transport	26±0	42±3	59±1	57±4	28-40	47-76	54±48	67±48	0±0	4±0
Working	41±28	26±10	27±18	116±47	58-75	30-62	8±58	49±58	3±2	19±12
Eating	113±2	126±11	78±1	81±7	19-32	85-102	119±25	122±25	113±7	119±6
Cooking	97±26	45±13	96±26	59±17	54-54	34-36	58±11	30±11	78±5	49±2

3.2.2 Concentration levels of sub-micron particles in the investigated cities

In ***Figure 1*** and ***Table 4*** statistics of the levels of sub-micron particles in terms of particle number concentration, lung-deposited surface area concentration and average particle size are reported as a function of the microenvironment, age, gender and population nationality under investigation.

Data clearly show that the maximum concentrations of sub-micron particles, which the residents of the five populations/cities are exposed, are related to cooking and eating microenvironments. As regards to cooking activities, Cassino and Guilford display the statistically highest concentration levels: PNC/LDSA median concentrations measured in the two cities were equal to 5.14×10^5 particles cm^{-3}/856 μm^2 cm^{-3} and 4.36×10^5 particles cm^{-3}/1362 μm^2 cm^{-3}, respectively. The lowest concentration range was measured in Lund (Sweden) where the median level is equal to 4.46×10^4 particles cm^{-3}/94.3 μm^2 cm^{-3}. Similar results are for eating activities: citizens living in Cassino and Guilford are exposed to the highest concentrations (median values of 2.28×10^5 particles cm^{-3}/559 μm^2 cm^{-3} and 6.01×10^4 particles cm^{-3}/185 μm^2 cm^{-3}, respectively). Other indoor day activities cannot be considered negligible in terms of people exposure too: indeed, apart from Lund, whose citizens are exposed to median concentrations lower than 1×10^3 particles cm^{-3}, the median concentration in such a microenvironment is higher than 1×10^4 part. cm^{-3}/10 μm^2 cm^{-3} for all the cities investigated. Generally, sleeping activities shown the lowest concentrations since no indoor sources were typically used during the night, therefore the indoor concentrations in this microenvironments are mainly affected by outdoor concentration levels, with the exception of Cassino whose citizens during the night were exposed to concentration levels statistically larger than outdoor day ones: this aspect is worthy of further investigation and could be related to the high concentrations due to the previous cooking activities (slow decay of concentration). Transport and outdoor, considered as the main microenvironments in terms of people exposures show concentration much lower than cooking and eating activities. Indeed, the highest concentration level for transport microenvironments was measured in Barcelona (2.79×10^4 part. cm^{-3}/112 μm^2 cm^{-3}) maybe due to the high vehicle density in the city and the presence of exposure hot-spots [69]: here the exposure to transport and eating activities resulted statistically not different. Also, working microenvironments, were characterized by lower exposures: median values lower than 1×10^4 part. cm^{-3} were measured for all the cities except for Barcelona, whose population is exposed to some median PNC of 1.42×10^4 part. cm^{-3}. We hypothesize that lower concentrations in indoor environments in Lund, also recognized in previous papers [142, 171], can be

the result of widespread use of mechanical ventilation systems, likely reducing the impact of the main indoor particle sources (e.g. cooking activities) through an increased air exchange rate and the simultaneous low outdoor concentration (built-up environment effect).

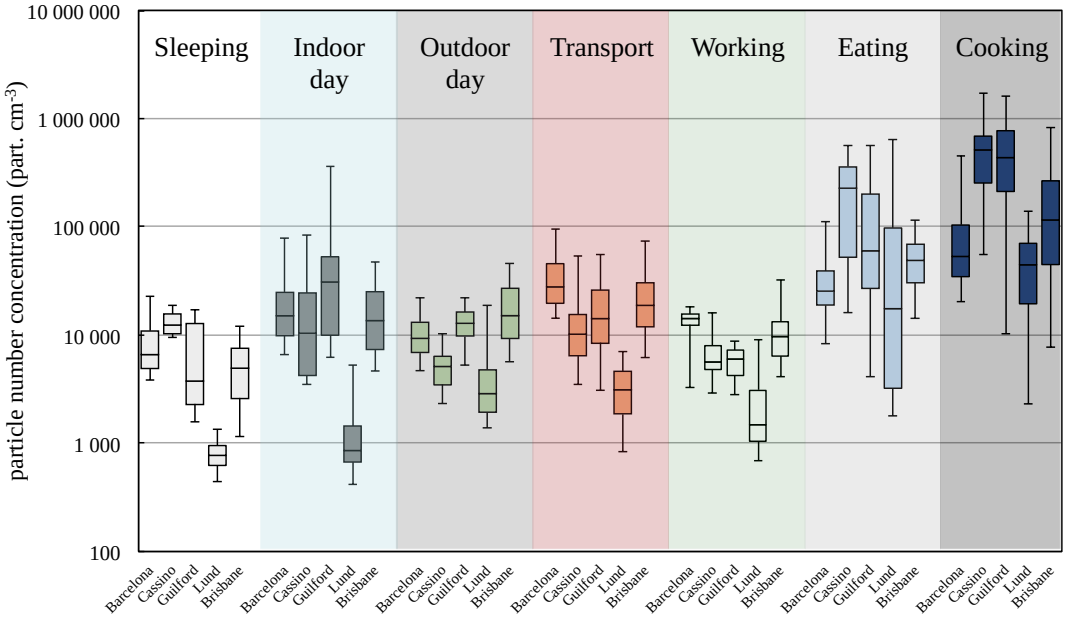

Figure 1 *Box plot of particles number concentrations in the investigated cities as a function of the microenvironments.*

Table 4 *Median values of particle number concentration, particle average size and lung deposited surface area dose calculated for the populations under investigation as a function of the microenvironment.*

		Sleeping	Indoor Day	Outdoor Day	Transport	Working	Eating	Cooking
Barcelona (Spain)	PNC (part cm^{-3})	6.60×10^{3}	1.51×10^{4}	9.32×10^{3}	2.79×10^{4}	1.42×10^{4}	2.54×10^{4}	5.32×10^{4}
	D_p (nm)	50	48	59	65	49	45	42
	S_{alv+TB} (μm^2 cm^{-3})	17.0	41.0	30.5	112	38.7	63.3	126
Cassino (Italy)	PNC (part cm^{-3})	1.24×10^{4}	1.04×10^{4}	5.13×10^{3}	1.02×10^{4}	5.72×10^{3}	2.28×10^{5}	5.14×10^{5}
	D_p (nm)	61	62	110	88.3	97.0	63.6	31.5
	S_{alv+TB} (μm^2 cm^{-3})	43.9	34.9	31.6	52.9	29.6	570	873
Guilford (UK)	PNC (part cm^{-3})	3.76×10^{3}	3.09×10^{4}	1.29×10^{4}	1.42×10^{4}	6.05×10^{3}	6.01×10^{4}	4.36×10^{5}
	D_p (nm)	82	54	63	56	85	73	61
	S_{alv+TB} (μm^2 cm^{-3})	15.4	94.4	44.7	43.3	25.5	189	1390
Sweden (Lund)	PNC (part cm^{-3})	7.74×10^{2}	8.58×10^{2}	2.88×10^{3}	3.13×10^{3}	1.48×10^{3}	1.43×10^{4}	4.46×10^{4}
	D_p (nm)	72	62	47	55	58	33	41
	S_{alv+TB} (μm^2 cm^{-3})	3.16	3.26	7.87	9.82	4.73	27.5	94.3
Australia (Brisbane)	PNC (part cm^{-3})	4.94×10^{3}	1.36×10^{4}	1.51×10^{4}	1.88×10^{4}	9.70×10^{3}	4.89×10^{4}	1.16×10^{5}
	D_p (nm)	59	43	38	40	54	77	44
	S_{alv+TB} (μm^2 cm^{-3})	13.5	31.4	31.4	44.9	26.8	212	258

3.2.3 Total daily dose received by population

In **Table 5** the most probable values of particle surface area doses received by the populations of the cities investigated, as obtained from the Monte Carlo simulation, combining (i) particle concentration data (summarized in the "Concentration levels of sub-micron particles in the investigated cities" section, whose related probability distribution function were evaluated), (ii) time activity patterns of the typical

population, and (iii) inhalation rates characteristics of the age and activity. In particular, in **Table 5** the particle surface area doses were reported as a function of population age, gender and nationality as well as of the seven main microenvironments. Moreover, the percentage contributions to the daily dose and dose intensity ratios (mm^2 min^{-1}) for each microenvironment are also reported.

The total dose received by Lund citizens is, by far, the lowest amongst the populations investigated, with values ranging from about 90 mm^2, for people aged up to 40 years old, to about 130 mm^2, for people older than 65. The main contribution to such dose values is due to the cooking and 'indoor day' activity, nonetheless the exposure in such microenvironments is significantly lower than that experienced by other populations investigated; in fact, the dose intensity ratios are the lowest amongst the cities under analysis whatever the age, gender or microenvironment. This cannot be related to the time activity patterns but likely to the presence of the abovementioned mechanical ventilation systems, typically used in homes which can reduce the impact of indoor sources, in particular cooking activities.

The highest doses amongst the populations under investigation are received by the Italian and UK populations. Cassino and Guilford citizens receive particle surface area dose ranging from 1000 to 1900 mm^2 and from 1000 to 1500 mm^2, respectively. These values represent very high concentrations when compared to the those in Lund (by an order of magnitude): such differences can be ascribed to the low concentrations measured both in outdoor and indoor microenvironments in Lund. Cooking, in particular for females, represents the main activity in terms of dose received by population living in Cassino, with dose intensity ratios up to 14. 'Indoor day' and eating activities account for about 20-25% of the total dose. Similar doses were received in Guilford, with a more pronounced contribution of the 'indoor day' activities, compared to eating.

The total daily dose received by the Barcelona and Brisbane was lower than by the Cassino and Guilford residents: most probable daily doses range between about 600 and 800 mm^2. The main contribution to such doses was once again the 'indoor day' activities (300-400 mm^2) whereas the contribution of cooking and eating activities was lower than that measured in Cassino and Guilford: in fact, the corresponding dose

intensity ratios were lower than 5. In Barcelona, a significant dose contribution was due, in particular for people aged <65, to the transport microenvironments (about 20%), which could be related to the higher abovementioned concentration levels. Apart from this, once again, the effect of outdoor day, transport and workplace environments can be considered very limited.

Summarizing, the total daily dose of the population is not highly affected by the outdoor air quality: even if the exposure in outdoor and transport microenvironments may differ amongst the cities, the contribution of such microenvironments to the overall daily dose is generally negligible for all the populations investigated. On the contrary, the lifestyle, in terms of both lifestyle and age, is a main parameter affecting the daily dose of the population: e.g. the time spent in indoor activities (including eating and cooking) leads to significant contribution to the daily dose received by populations. In fact, for all the populations under investigation, mainly females (cultural/lifestyle aspect) are involved in cooking activities, thus receiving higher doses than males. The effect of the lifestyle can also be recognized when doses received by different age groups are considered (age effect): in general, older people spend more time indoors than younger ones, therefore receiving, on average, higher daily doses. Nonetheless, the results shown here demonstrate that paying more attention to air quality indoors is likely to significantly reduce the dose received by populations: the presence of mechanical ventilation systems typically used indoors in Lund reduce the exposure and the corresponding dose received during the indoor activities.

We would like to highlight that the total daily doses for Italian and Australian populations were estimated in a previous study, by an indirect exposure assessment: doses values equal to about 2000 mm^2 and 450 mm^2 were estimated for Southern Italian and Australian populations, respectively [137]. The results of that studies are likely comparable to the results of the present study. In fact, since the same activity patterns were considered in the two studies, the difference in dose values calculated with the two approaches can be just ascribed to the exposure assessment approach itself: the indirect approach can be performed utilizing instrumentation of better accuracy, but they cannot provide the exposure at a personal scale.

Table 5 *Dose, dose intensity and contribution to the daily dose as function of the population, age, gender (female/male, F/M) and microenvironment. Data represent the most probable values as obtained from the Monte Carlo simulation.*

		age	Sleeping (F/M)	Indoor Day (F/M)	Outdoor Day (F/M)	Transport (F/M)	Working (F/M)	Eating (F/M)	Cooking (F/M)	Total daily Dose (F/M)
Barcelona (Spain)	Dose, δ_{Alv+TB} (mm^2)	19-40	57/57	313/265	19/34	99/115	54/73	55/57	68/4	664/606
		41-64	62/64	361/314	28/45	95/112	40/62	65/69	113/45	763/711
		>65	67/73	411/391	38/57	34/53	12/8	60/71	114/54	736/707
	Dose intensity ratio (mm^2 min^{-1})	19-40	0.11/0.11	0.72/0.71	0.5/0.5	1.22/1.21	0.29/0.28	0.5/0.49	1.1/1.09	
		41-64	0.12/0.13	0.97/0.78	0.41/0.55	1/1.27	0.16/0.31	0.56/0.57	2.96/1.18	
		>65	0.12/0.12	0.76/0.77	0.54/0.54	1.28/1.26	0.28/0.3	0.53/0.56	1.17/1.18	
	Contribution to the daily dose (%)	19-40	9/9	47/44	3/6	15/19	8/12	8/9	10/1	
		41-64	8/9	47/44	4/6	12/ 16	5/9	9/10	15/6	
		>65	9/10	56/55	5/8	5/7	2/1	8/10	16/8	
Cassino (Italy)	Dose, δ_{Alv+TB} (mm^2)	19-40	118/114	247/230	38/39	38/38	77/83	273/274	323/237	1114/1015
		41-64	144/138	307/262	41/42	32/34	65/74	317/327	694/371	1600/1249
		>65	168/143	406/312	41/58	39/31	8/31	401/351	809/436	1873/1361
	Dose intensity ratio (mm^2 min^{-1})	19-40	0.27/0.26	0.57/0.56	0.48/0.47	0.55/0.54	0.25/0.24	4.21/4.09	6.88/6.78	
		41-64	0.33/0.3	0.75/0.6	0.49/0.51	0.46/0.54	0.19/0.27	4.73/4.37	14.17/7.56	
		>65	0.34/0.3	0.66/0.59	0.57/0.5	0.65/0.54	0.31/0.27	5.08/4.33	8.43/7.38	
	Contribution to the daily dose (%)	19-40	11/11	22 /23	3/4	3/4	7/8	25 /27	29/23	
		41-64	9/11	19/21	3/3	2/ 3	4/6	20/ 26	43/30	
		>65	9/10	22/23	2/4	2/2	<1/2	21/26	43/32	
Guilford (UK)	Dose, δ_{Alv+TB} (mm^2)	19-40	63/61	590/455	28/47	32/38	27/32	156/259	487/191	1384/1083
		41-64	62/60	615/477	28/45	29/35	23/30	97/210	668/364	1521/1221
		>65	57/72	598/638	31/61	15/29	5/10	81/123	558/450	1346/1382
	Dose intensity ratio (mm^2 min^{-1})	19-40	0.12/0.12	1.15/1.09	0.68/0.67	0.44/0.44	0.2/0.19	1.44/1.52	11.94/11.79	
		41-64	0.12/0.12	1.47/1.08	0.4/0.66	0.34/0.43	0.13/0.19	0.57/1.44	21.1/11.49	
		>65	0.11/0.13	0.91/1.15	0.56/0.71	0.43/0.46	0.08/0.21	3.15/1.32	10.29/12.75	
	Contribution to the daily dose (%)	19-40	5/6	43/42	2/4	2 /3	2/3	11 /24	35/18	
		41-64	4/5	40/39	2/4	2/ 3	2/ 2	6/17	44/30	
		>65	4/5	44/46	2/ 4	1/ 2	<1/1	6 /9	41/33	
Sweden (Lund)	Dose, δ_{Alv+TB} (mm^2)	19-40	10/10	21/20	14/13	6/5	9/11	12/11	24/19	96/87
		41-64	11/11	24/22	14/12	5/5	9/12	14/12	31/22	108/96
		>65	12/12	29/28	19/18	5/6	0/2	16/17	51/25	132/109
	Dose intensity ratio (mm^2 min^{-1})	19-40	0.02/0.02	0.06/0.05	0.13/0.12	0.09/0.09	0.04/0.04	0.15/0.14	0.72/0.74	
		41-64	0.02/0.02	0.07/0.06	0.13/0.13	0.08/0.09	0.03/0.04	0.19/0.15	1.15/0.82	
		>65	0.02/0.02	0.06/0.06	0.13/0.13	0.09/0.09	0.05/0.05	0.14/0.14	0.88/0.83	
	Contribution to the daily dose (%)	19-40	10/11	22/22	14/14	6/6	9/12	13/12	25/21	
		41-64	10/11	22/23	13/13	4/5	9/12	13/13	29/23	
		>65	9/11	22/26	14/16	4/6	<1/2	12/16	39/23	
Brisbane (Australia)	Dose, δ_{Alv+TB} (mm^2)	19-40	32/38	318/271	17/20	6/12	38/86	100/108	93/34	604/570
		41-64	38/45	331/294	25/28	6/11	42/89	140/154	114/50	696/671
		>65	43/52	352/366	33/50	0/2	1/6	177/209	140/97	745/782
	Dose intensity ratio (mm^2 min^{-1})	19-40	0.08/0.09	0.44/0.47	0.4/0.44	0.42/0.44	0.29/0.32	1.38/1.5	2.02/1.72	
		41-64	0.09/0.1	0.58/0.53	0.56/0.49	0.21/0.48	0.16/0.37	1.94/1.69	4.4/1.91	
		>65	0.09/0.11	0.49/0.55	0.45/0.51	0/0.51	0.27/0.31	1.56/1.76	1.79/1.98	
	Contribution to the daily dose (%)	19-40	5/7	53/48	3/3	1/2	6/15	16/ 19	15/6	
		41-64	6 /7	48/44	4/4	1/ 2	6/13	20/ 23	16/7	
		>65	6/7	47/47	4/6	<1/<1	<1/1	24/27	19/12	

4 VEHICLE INTERIOR AIR QUALITY CONDITIONS WHEN TRAVELLING BY TAXI

In this experimental campaign we turn our attention to variations in air quality experienced when travelling across Barcelona by taxi, a key transport mode used in the city and one that has been described as "bridging the gap between private and other public transport" [172].

The published literature on vehicular interior air quality (VIAQ) has already demonstrated that car commuters can be exposed to significantly enhanced levels of inhalable particles (PM_{10}, $PM_{2.5}$ and PM_1: particles in suspension with diameter less than 10, 2.5 and 1 μm respectively) and gases (CO, CO_2, NO_2, VOCs) (e.g. [68, 173-177]). Taxi drivers offer a special case in that they are chronically exposed to Traffic-Related Air Pollutants (TRAPs) as an occupational hazard, and this transport mode is additionally interesting in that current taxi fleets utilise various fuel options that include both hybrid and electric vehicles, which generate different patterns of pollutant emissions. While most city taxi fleets are still dominated by traditional gasoline- or diesel-powered engines, this is changing rapidly. In 2017 for example already one third of the 10,523 taxis operating in the city of Barcelona use alternative fuels, with the fleet composition being 67% diesel, 26% hybrid, 6% liquefied gas (LPG, mainly propane and butane), 0.4% compressed natural gas (CNG, methane and ethane) and 0.3% electric. Our study of VIAQ inside taxis included all these vehicle types and involved simultaneous collection (tracked by GPS) of air quality data on inhalable particle mass, number, and chemistry, as well as gaseous contaminants (CO, CO_2 and VOCs). The data recorded everyday VIAQ conditions breathed by taxi drivers and passengers during 6-hours of a working day (10.00-16.00) and involved the co-

operation of taxi drivers who consented to collect the equipment in the morning and carry it in the car with them as they went about their business.

4.1 Methodology

The study was carried out in the metropolitan area of Barcelona with the collaboration of the Barcelona Metropolitan Taxi Institute (IMET) which gave permission and helped with the logistics of organising the sampling campaign that lasted from 4th-31st of October 2017 (weekdays only). On each day two taxis carried an identical set of measuring equipment, one vehicle always being diesel, and the other non-diesel (hybrid, LPG, CNG or electric). The equipment was carried all together, usually in the boot (trunk) kept with roof open to the taxi interior. Both taxis started their journey together at the IDAEA-CSIC institute at 10.00 am avoiding the height of the rush hour (although the city is by then extremely busy), and returned the equipment to the same location six hours later after working normally in the city. Note was taken of mileages covered plus any special variables such as the use of air conditioning, air fresheners, and whether the windows were open or closed. The range of taxi models and engine types that participated in the study are listed in ***Table 6***.

Table 6 *List of vehicles that participated in the Barcelona Taxi Air Quality Monitoring Campaign. For hybrid, CNG and electric the same taxi was used for repeated experiments.*

Model (number vehicles)	Km on odometer	Year of purchase	Fuel type	Euro stage
Skoda Octavia (8)	690,000 575,000 780,000 650,000 560,000 550,000 256,000 255,000	2006 2009 2010 2010 2010 2010 2010 2014	Diesel	E4 E5 E5 E6
Seat Toledo (2)	300,000 150,00	2014 2016	Diesel	E5 E6
Seat Altea (5)	737,000 572,000 614,000 575,000 542,000	2010 2010 2011 2011 2011	Diesel	E5 E6
Toyota Prius (4)	387,000	2012	Hybrid (petrol)	E6
Citroen C-Elysée (4)	165,000 153,000	2016 (1) 2016 (3)	LPG	E5
Volkswagen Caddy (3)	47,000	2017	CNG	E6
Nissan Evalia (4)	160,000	2014	Electric	E6

Air quality measurements were registered every 10 seconds with the following equipments:

- Personal Environmental Monitor (PEM) to collect PM_{10} with a flow rate of 10 L/min on previously weighed 63 mm quartz microfiber filters, this allowing both measurement of average PM concentration and also a full chemical analysis of the particles being breathed.
- Mini-aethalometer (Magee Scientific) to measure black carbon (BC) (only in the diesel taxis).

- DiSCmini (Matter Aerosol AG, Wohlen AG, Swiss) to monitor particle number concentrations (PNC, expressed in # /cm^3) and size mode in the size range of 10-700 nm, as well as lung deposited surface area (LDSA μm^2/cm^3).
- IAQ-track (Model 7545, TSI) to analyse levels of CO_2, CO, temperature and humidity.
- Low-volume VOC detectors for later analysis using gas chromatography.
- GPS to monitor the routes taken by each taxi during the working day.

Given that the data were collected over a period of 4 weeks, they were deseasonalised to remove temporal fluctuations when comparing the levels of pollutants between the taxis. This was done with reference to the "Palau Reial" Urban Background station (termed UB-PR), where the same pollutants were monitored throughout the sampling period [83]. This station is located in the garden of the IDAEA-CSIC building (41°23′14″ N, 02°06′56″E, 78 m.a.s.l) and is exposed to road traffic emissions from the Diagonal Avenue (200 m away), one of the largest thoroughfares in Barcelona (100,000 cars/day). The adjusted concentration $(C_i^j)_k$* of the ith pollutant for the kth day at the taxi jth was calculated as shown in Eq. (3):

$$(\boldsymbol{C_i^j})_{\boldsymbol{k}}^{*} = (\boldsymbol{C_i^j})_{\boldsymbol{k}} / \left[(\boldsymbol{C_i^{PR}})_{\boldsymbol{k}} / (\overline{\boldsymbol{C_i^{PR}}})\right] \quad (3)$$

where $(C_i^j)_k$ is the concentration measured at the taxi, $(C_i^{PR})_k$ and $\left(\overline{C_i^{PR}}\right)$ are the 6h average corresponding to day kth and campaign averages at UB-PR, respectively.

A total of 30 PM_{10} gravimetric samples collected using the PEM were chemically analysed using ICP-AES and ICP-MS for major and trace elements respectively. After sampling, filters were dried for 24 h at room temperature, (20–25°C and 25% humidity), before being chemically analysed. SiO_2 and CO_3^{2-} were indirectly determined on the basis of empirical factors (Al x 1.89=Al_2O_3, 3 x Al_2O_3=SiO_2 and (1.5 x Ca)+(2.5 x Mg)=CO_3^{2-}, see Querol et al., 2001). A portion of each filter was digested in acidic environment (5 ml HF, 2.5 ml HNO_3, 2.5 ml $HClO_4$) for the determination of major and trace elements. A sub-sample measuring 1.5 cm^2 was taken from each filter to allow the determination of Organic Carbon (OC) and Elemental Carbon (EC) content by thermo-optical transmission using a Sunset Laboratory OCEC Analyzer. Blank filters were used for every stock purchased for sampling (one blank

filter for each 12-filter stock). A few milligrams of the NIST 1633b reference material were added to blank filters to check the precision of the data obtained. Regarding the precision of the analyses, most of the elements showed an analytical error <10%, except for P and K which had a 15% error.

Volatile organic compounds (VOC) in air samples were collected using stainless steel cartridges (89 mm length x 6.4 mm O.D. x 5 mm I.D, Markes International Ltd., Llantrisant, UK) custom packed with three successive sections of activated graphitized BC adsorbents, 150 mg Carbotrap C 20-40 mesh, 150 mg of Carbotrap 20-40 mesh and 150 mg of Carbotrap X 40-60 mesh (Supelco, Sigma-Aldrich, St. Louis, USA). The cartridges were pre-conditioned at 320°C with helium (5N quality) flow at 100 mL/min for 2 hours and conditioned before each sampling at 335°C with same helium flow for 30 min. The clean cartridges were capped with ¼ inch brass long-term storage caps with ¼ PTFE ferrules and storage in free-VOC ambient until its use. For active sampling the cartridges were coupled to a low-flow pump through a single air inlet port of Pocket Pump Air (SKC Ltd., Blandford Forum, UK) with constant flow compensation at 20 mL/min for 6 hours. The pump was calibrated before and after each air intake with the Defender 510-L primary flow calibrator (Bios Drycal, NJ, USA). The VOC trapped in the cartridges were analyzed by the thermal desorption equipment Ultra 50:50 Multi-tube Auto-sampler/Thermal Desorber Unity Series 2 (Markes International Ltd, Llantrisant, UK) coupled to a gas chromatograph with mass spectrometry detector. External calibration method was used for quantification of target VOC using multi-point reference stock solutions at different concentration in the range of 0.25 and 200 µg/mL in methanol from different commercial solutions: FIA Paraffin Standard (Accustandard Inc., New Haven, USA), Special Mix 6 compounds (CPAchem Ltd., Bulgaria), 8260B Calibration Mix #1 (Restek Corporation, Bellefonte, USA) and Cannabis Terpenes Standard #1 (Restek Corporation, Bellefonte, USA). 1 µL reference stock solution was injected onto clean cartridge through the injector port of Calibration Solution Loading Ring (CSLR, Markes International Ltd, Llantrisant, UK) using a standard syringe and purged for 3 min with helium (5N quality) at 50 mL/min to remove the solvent. Carbon disulfide, ethyl methacrylate, iodomethane, methyl acrylate, 2-nitropropane, methylene chloride,

acetonitrile, 2-chloroethanol, (-)-alpha-bisabolol, linalool and geraniol from commercial solution could not be determined. Calibration for most these targets showed excellent linearity (R2 ≥ 0.99). Clean cartridges were spiked at low different concentration levels to determine the limit of detection, ranged 0.03 to 1.5 ng/cartridge. For the PM_{10} source apportionment, the Positive Matrix Factorization (PMF, Paatero and Tapper [178]) model was run by means of the EPA PMF v5 software. The input data uncertainty estimates were based on the approach of Amato, et al. [179] and provided a criterion to separate the 22 species which retain a significant signal from the remaining ones with higher noise. This criterion is based on the signal-to-noise S/N ratio defined by Paatero and Hopke [180]. As an additional criterion, we used the percentage of data above detection limit. The combination of both criteria permitted to select for the PMF analysis 21 strong species and 1 weak species (Cr). Given the low number (30) of PM_{10} samples obtained in the taxis, the PMF was run to an extended matrix where we added 90 additional ambient air PM samples collected at the urban background monitoring site "Palau Reial" (41°23′14″ N, 02°06′56″E, 78 m.a.s.l). This data assembling showed the most satisfactory results for factor profiles since it allowed exploring a larger area of the N-dimensional source contributions space. The data matrix was uncensored, i.e. negative, zero and below detection limit (BDL) values were included as such in the analyses to avoid a bias in the results Paaetro [181]. Given that samplings in different taxi engine types were performed in different days, resolved source contributions were deseasonalized using simultaneous data from the continuously running "Palau Reial" monitoring station, following the method of Rivas, et al. [83].

4.2 Results

4.2.1 Physical measurements

Concentration ranges and median values for pollutant concentrations are presented in ***Table 7*** and demonstrate considerable variation in VIAQ. Diesel and LPG vehicle interiors registered highest median values of PM_{10} (75-81 μg/m^3), OC (26 μg/m^3), and EC (9-11 μg/m^3). Diesel cars also recorded the highest median levels of CO (2.1 ppm) and LDSA (104 μm^2/cm^3) and largest sizes (46 nm) of UFP, but registered lower

concentrations of particle numbers (median PNC <33000 #/cm^3) than hybrid, natural gas or LPG car interiors (39-46000 #/cm^3). In contrast, electric and hybrid operated taxis recorded the lowest interior PM_{10} values (50 µg/m^3). The interiors of electric powered taxis driven with closed windows showed the lowest median values in EC (4.6 µg/m^3), number of UFP (PNC= 10614 #/cm^3), LDSA (12 µm^2/cm^3), and CO (0.1 ppm). The CO_2 data demonstrate clearly that concentrations of this gas are is strongly influenced by whether windows are open for much of the day (<570 ppm) or kept closed (>1700 ppm): the electric taxi used in the study for example was driven all day with closed windows, producing median CO_2 values of 2395 ppm. A closer look at the data is presented below, focusing on individual 6-hour journeys and daily pairings, and emphasising the effects on VIAQ of driving with windows open or closed.

Table 7 *Median (MD), maximum (max) and minimum (min) values for selected parameters measured at different fuel-type taxis. n: number of taxis. LPG: liquid petroleum gas, CNG: compressed natural gas.*

	n	*PM_{10} (µg/m^3)*			*OC (µg/m^3)*			*EC (µg/m^3)*			*BC (µg/m^3)*		
		MD	max	min	MD	max	min	MD	max	min	MD	max	min
Diesel	14	75.2	106.3	41.8	25.6	40.3	10.8	9.4	28.2	3.2	6.5	17.2	2.22
Hybrid	4	49.6	61.2	43.8	18.6	21.0	14.9	7.4	10.9	5.5			
LPG	4	81.0	94.6	64.5	26.3	32.0	18.1	10.5	13.3	4.2			
CNG	3	51.0	54.2	47.8	15.0	15.18	15.0	8.3	9.4	7.3			
Electric	4	49.8	75.4	35.0	21.7	40.8	12.4	4.6	7.3	2.5			

	Number (#/cm^3)			*Size (nm)*			*LDSA (µm^2/cm^3)*			*CO (ppm)*			*CO_2 (ppm)*		
	MD	max	min	MD	max	min	MD	max	min	MD	max	min	MD	max	min
Diesel	32138	88257	7938	46	59	31	104	233	45	2.1	3.7	1.2	418	2052	364
Hybrid	48436	58153	31900	34	36	33	55	66	29	1.2	1.4	0.7	398	529	346
LPG	38614	65778	7017	38	46	35	53	91	17	1.5	2.4	1.1	410	2139	361
CNG	45701	46208	45194	32	33	31	46	47	45	1.0	1.1	0.8	391	424	358
Electric	10614	13214	7329	34	40	34	12	13	12	0.1	0.5	0.1	2395	3478	1724

Opening windows during road travel allows direct entry of outside traffic contaminants into the vehicle, whereas a closed system will encourage the build-up of internally-

generated pollutants. This contrast between interior and exterior contaminants is demonstrated by ***Figure 2*** which compares particle number concentrations (PNC: in the size range of 10-700 nm) with levels of carbon dioxide. Taxis circulating with windows closed recorded low PNC values across a limited range (7-13000 $\#\cdot cm^{-3}$), whereas those driving in the city with windows open showed median interior PNC levels always above 20000 $\#\cdot cm^{-3}$ and in extreme cases exceeding 80000 $\#\cdot cm^{-3}$. Conversely, open-window taxis record VIAQ ambient CO_2 concentrations similar to outdoor levels of around 400 ppm, whereas when the taxi interior becomes a closed system CO_2 concentration rise substantially, depending on the number of passengers being carried. The highest median CO_2 value recorded in the study (3478 ppm) was measured in a closed electric car, with peaks occasionally exceeding 4500 ppm during the 6-hour monitoring period.

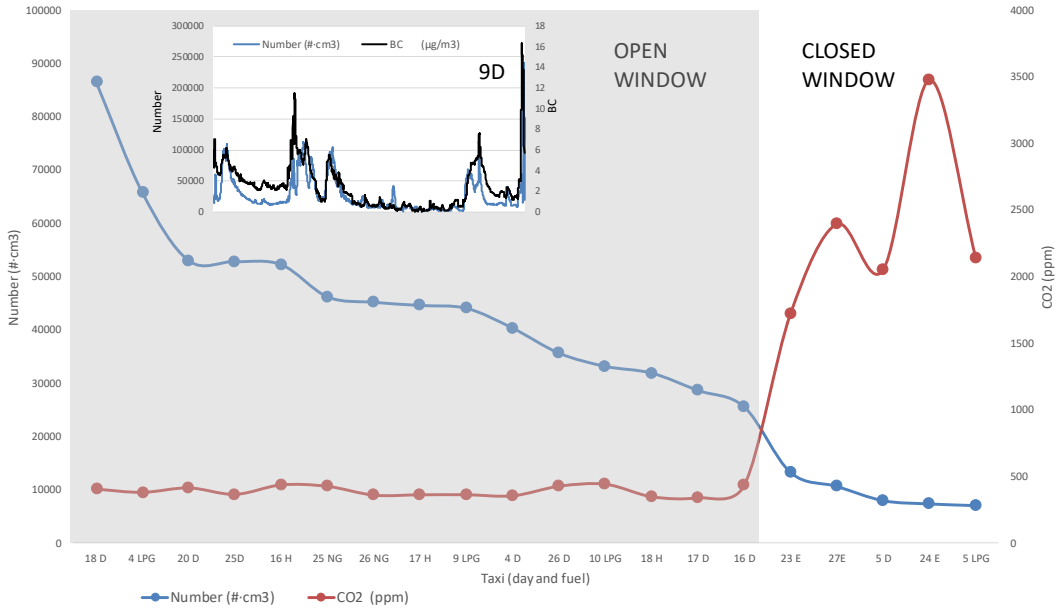

Figure 2 *Median values of particle numbers (PNC, in blue, expressed in #/cm^3 in the size range of 10-700 nm) measured inside taxis compared to CO_2 concentrations (in red) for conditions of either open (CO_2 = 330-440 ppm) or closed (CO_2 1700-3500 ppm) windows over 6-hour daytime period. Lowest values of N, and highest values of CO_2, were recorded when windows were closed. The number on the horizontal axis refers to the date in October 2017 (all dry days without precipitation), and the letter refers to the fuel type (D = diesel; E = electric; H = hybrid; LPG = liquid petroleum gas; NG = natural gas). Five taxis (9D, 10D, 23D, 27D, 20H: not shown on this figure) recorded CO_2 values between 450-600 ppm due to windows being opened occasionally, and in one taxi (31D) the CO_2 equipment malfunctioned. The inset shows an example of how PNC and black carbon peaks can be positively correlated (diesel taxi 9th October with windows open), as demonstrated in previous publications (e.g. Krecl, et al. [182]).*

Further comparison between VIAQ in taxis with windows open and closed is provided by the box plot on ***Figure 3***. The pattern of higher PNC with a much greater concentration range in open window vehicles is also shown by both PM_{10} and LDSA values. The results for both PNC and LDSA are strikingly lower in the closed taxi interiors, and contrast with median particle size values which show little variation irrespective of whether windows are open or closed (around 40 nm).

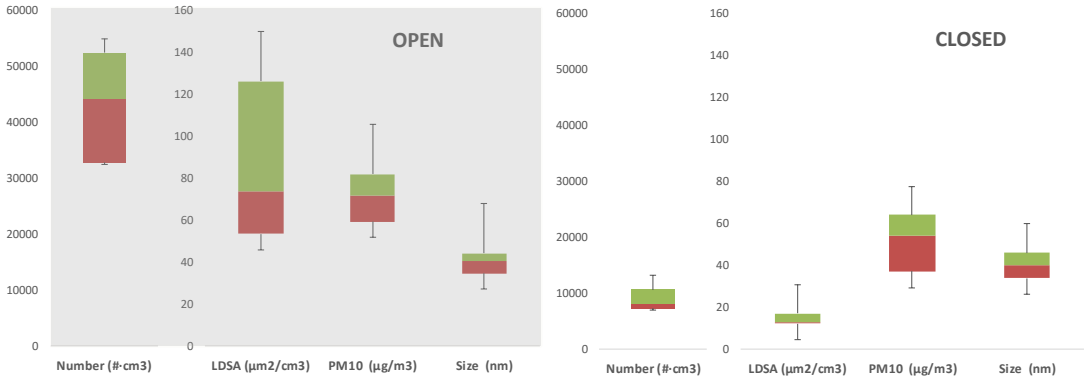

Figure 3 *Box plot comparing VIAQ parameters particle number, lung deposited surface area (LDSA), PM_{10} mass, and particle size inside taxis with windows open and closed (median values over 6-hour daytime period). The coloured box defines the interquartile range, and the median is represented by the horizontal line separating the two colours. Particulate number, LDSA and mass levels are lower and less variable in the protected environment of a taxi interior with closed windows.*

Ambient concentrations of carbon monoxide measured inside the taxis during this study were low, although there was considerable variation, with median values ranging between 0.1-3.7 ppm. ***Figure 4*** plots CO levels against kilometer age (thousands of km driven) and tax models employed in the study. It is apparent from the figure that, with one exception (4LPG), the highest interior CO values (>2 ppm) were reached in diesel vehicles, irrespective of whether the windows are open or closed. Of the different models used in this study the highest CO levels (2.5 ppm or above) were measured in Skoda Octavia taxis that had over 500000 km on the odometer. In contrast, median concentrations of CO inside the hybrid taxi used in the study (a Toyota Prius) remained below 1.5 ppm despite the car having nearly 400000 km on the odometer. The lowest CO concentrations measured in the study (0-0.5ppm) were recorded inside an electric powered Nissan Evalia (160000 km), this comparing with median CO levels of 2.2 ppm inside a Skoda Octavia (650000 km) even though both taxis were driven with windows closed and a/c on.

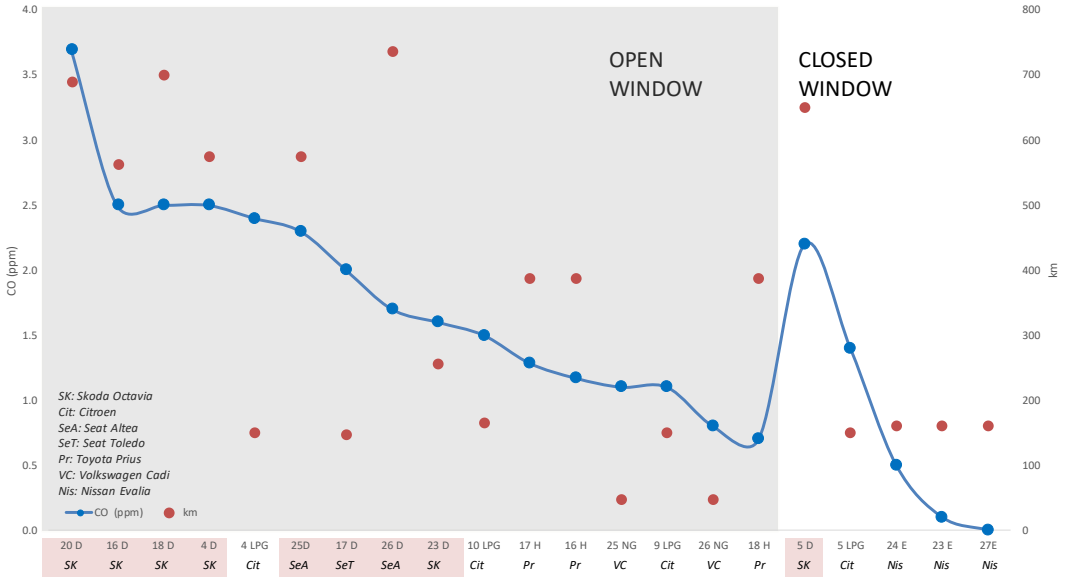

Figure 4 *Median 6-hour daytime values of carbon monoxide levels in taxi interiors with windows open (CO_2 = 330-570 ppm) and closed (CO_2 1700-3500 ppm). Higher levels of CO are mostly associated with diesel taxis (pink shading), notably the high-km Skoda Octavia. Lowest CO levels were recorded in electric-powered taxis driving with windows closed. Note the difference between closed-window diesel and electric vehicles. The number on the horizontal axis refers to the date in October 2017, and the letter refers to the fuel type (D = diesel (pink background); E = electric; H = hybrid; LPG = liquid petroleum gas; NG = natural gas). All diesel cars were different (this being the most common taxi type in Barcelona), whereas for other fuel types the same car was used more than once except in the case of LPG where two different vehicles were used.*

With regard to ultrafine particle size measured in the taxi interior, as previously mentioned **Table 7** demonstrates that those vehicles using diesel fuel registered larger median particle sizes than in the non-diesel vehicles. This difference is recorded in every daily pairing, irrespective of whether the non-diesel partner taxi was LPG, NG, hybrid or electric (***Figure 5***). Diesel interior median UFP sizes ranged from 31-59 nm (median 46 nm) as compared to 31-46 nm (median 34 nm) for non-diesels.

The GPS-Route data obtained during this study confirm the highly polluted nature of the Barcelona city centre road system, especially the grid plan area known as L'Eixample (the Enlargement) built to the west and north of the mainly pedestrianized medieval core. Taxis circulating with open windows through L'Eixample consistently show poor VIAQ ***(Figure 6a-b***). The routes illustrated by ***Figure 6a*** and ***Figure 6b***

for example compare concentrations of UFP numbers and black carbon (BC) breathed inside a Skoda Octavia diesel taxi with 700000 km on the odometer during a 6-hour daytime period mostly confined within L'Eixample and the equally congested central tourist route from Via Laetana to the sea front. The comparison not only graphically demonstrates the poor air quality (PNC >75000 #·cm^{-3}; BC > 12 µm^2/m^3 for much of the time) but also reaffirms the positive correlation between PNC and BC in the VIAQ of diesel taxis (***Figure 2***). In contrast ***Figure 6c*** and ***Figure 6d*** compare ultrafine particle numbers inside electric and diesel taxis driving with windows closed. Under these conditions the interior concentration of UFP is kept low (usually PNC<25000 #·cm^{-3} and for most of the time driving in the city centre, especially inside the electric vehicle, PNC<10000 #·cm^{-3}).

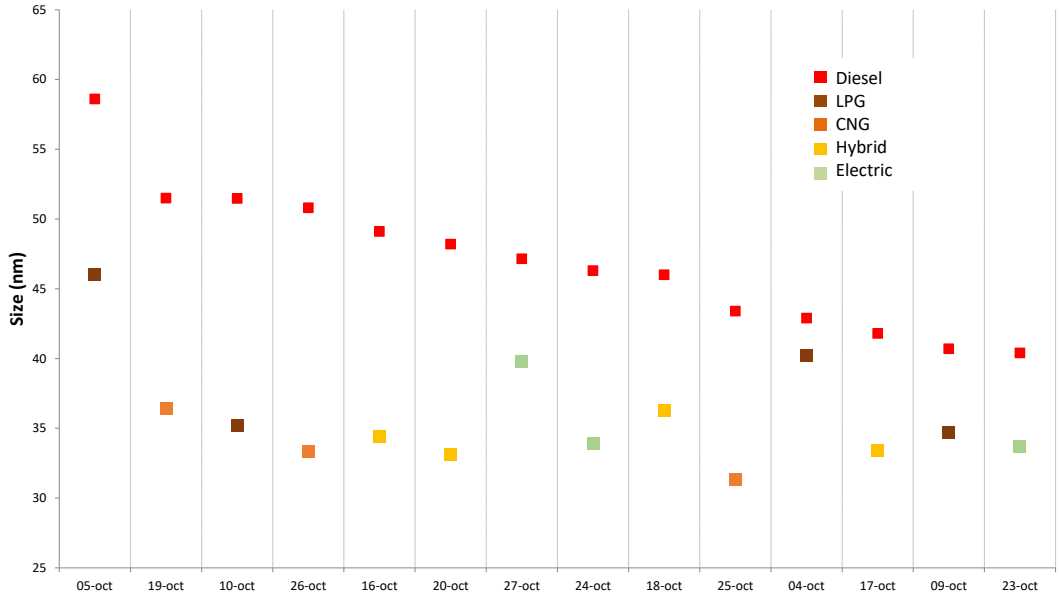

Figure 5 *Median ultrafine particle sizes (nm) inside taxi pairings over 6-hour daytime working period. Diesel taxi VIAQ consistently shows larger median particle sizes than other engine types.*

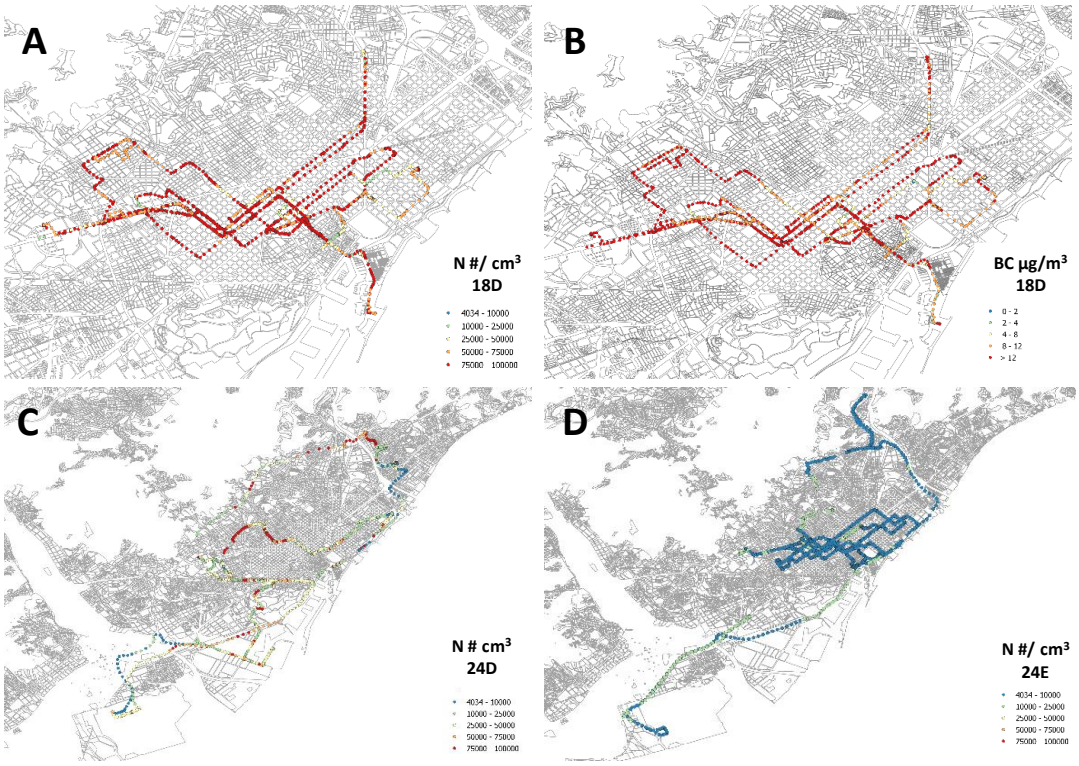

Figure 6 *Examples of pollutant concentrations inside taxis driving through the Barcelona area during the 6-hour daytime monitoring period (10.00-16.00). The route taken by the open-window diesel taxi on 18th October was restricted to the city centre, especially the traffic-choked grid-plan L'Eixample area, and records generally very high levels of both UFP number (N: 6a) and black carbon (BC: 6b). In contrast the two taxis represented in Figures 6c and 6d drove with windows closed and A/C on, spending much of the time in the city centre but also making excursions out of the city to the southwest and the northeast. Levels of UFP numbers inside the closed taxis remained very low except when the windows were opened briefly (see text for discussion).*

The routes driven by the electric and diesel taxis recorded in ***Figure 6c*** and ***Figure 6d*** include journeys away from the city centre, both to the airport (southwest of the city) and to the Besòs River estuary on the northeast side of the city, as well as use of the urban ring road system. Excursions such as those out to the airport involve motorway driving conditions, usually at higher speeds that favour the infiltration of outside contaminants even into cars driving with windows closed so that interior N rises above 10000 #·cm^{-3}. Thus both closed taxis 24E (***Figure 6c***) and 5D (***Figure 6d***) recorded lowest interior particulate levels when driving slowly in the city centre, but demonstrated increasing entry of external pollutants into the car when driven out to

the airport. A comparison between the VIAQ of these two taxis (24E and 6D) further reveals that whereas the driver of the electric taxi 24E ensured that windows were kept closed (with 6-hour median CO_2 levels consequently rising to 3478 ppm), this was not the case for taxi 5D which recorded two VIAQ pollution events (***Figure 7***). One of these was in the airport area and resulted in PNC rising to a peak around 200000 #·cm^{-3}, whereas the other occurred when driving along the extremely congested and canyon-like enclosed Gran Via 6-lane urban motorway leading northeast out of the city, when PNC levels suddenly spiked to 1000000 #·cm^{-3} (***Figure 6d*** and ***Figure 7***). Note also on ***Figure 7*** how peaks in PNC are accompanied by troughs in particle size.

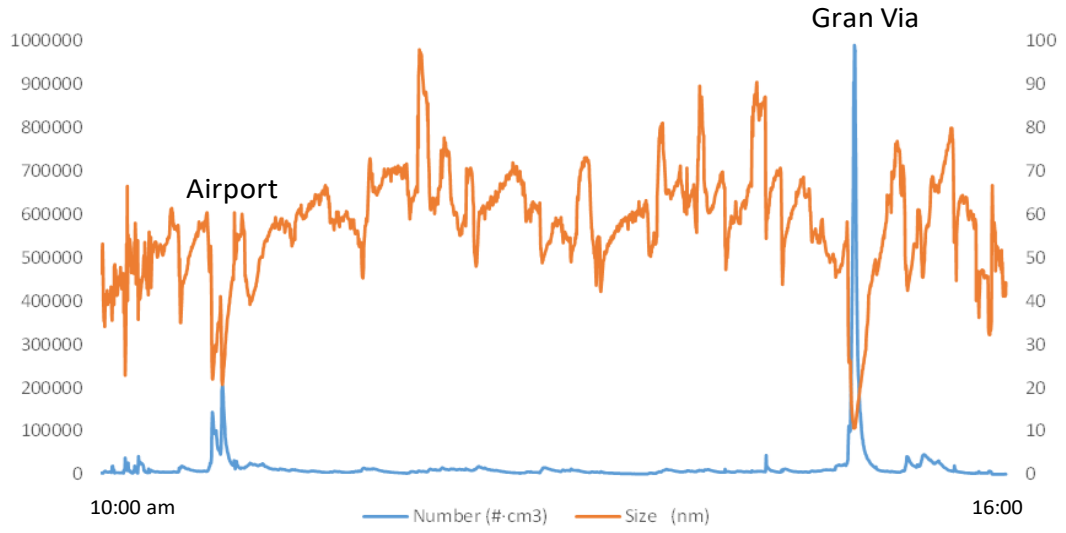

Figure 7 *Comparison of median UFP number (PNC) and particle size (nm) during the 6-hour monitoring period inside taxi 5D (Figure 6d). Generally low levels of PNC (<10000 #/cm^3) were maintained during the day by keeping windows closed, with the notable exception of two pollution events in the airport area and when driving along the congested Gran Via, when PNC rise rapidly and particle size decreased.*

4.2.2 Chemical measurements

Chemical data from the PM_{10} filter samples collected from vehicle interiors during the Barcelona taxi experiment are listed in **Table 8**. Average values for all taxis (28 samples) are accompanied by two subgroups selected to compare (1) taxis with open windows all day (as recorded by the driver and confirmed by median interior CO_2 levels below 450 ppm: 8 diesel and 8 non-diesel); (2) taxis with windows closed all or

most of the day (as recorded by the driver and confirmed by median CO_2 levels between 1700-3500 ppm: 1 diesel, 1 LPG; 4 electric). Levels of PM_{10} inside the taxis were on average around 3 times higher (67 µg/m^3) than urban background (22 µg/m^3), although once again there was considerable variation (35-106 µg/m^3). Elemental and organic carbon were the particle types most notably enriched inside all taxis, especially EC in vehicles with open windows, these registering concentrations >x10 urban background (***Table 8***). Interior levels of EC in open-window taxis (9-11 µg/m^3) were also notably higher than those with closed windows (3-5 µg/m^3), presumably reflecting the ingress of vehicle exhaust fumes from outside. In contrast, concentrations of OC in the closed electric vehicle were only slightly lower than those in openly ventilated diesel taxis (***Table 8***), implicating the greater influence of indoor sources, as will be discussed below.

Table 8 *Average values for chemical analysis of PM_{10} sampled from taxi interiors. In addition to all taxis (28 analyses) there are 5 subgroups depending on whether windows were kept open or closed, and on how the vehicle was powered.*

	ALL TAXIS	**OPEN WINDOWS (CO_2< 450ppm)**		**CLOSED WINDOWS**			**URBAN BACKGROUND**
µg/m³	(No.=28)	Diesel (8)	Non Diesel (8)	Diesel (1)	LPG (1)	Electric (4)	
PM_{10}	66.9	72.3	62.5	53.7	64.5	52.5	21.9
OC	21.7	25.6	20.8	14.6	18.1	24.2	2.5
EC	9.4	11.1	9.2	3.2	4.2	4.7	0.9
Al_2O_3	0.8	0.8	0.7	0.8	0.9	0.5	0.4
Ca	1.5	1.5	1.7	2.0	2.1	1.6	0.5
Fe	1.7	1.5	1.8	2.1	2.9	2.2	0.5
K	0.2	0.2	0.2	0.3	0.1	0.3	0.2
Na	0.5	0.5	0.8	0.7	1.1	0.7	0.6
Mg	0.1	0.1	0.3	0.3	0.3	0.2	0.1
P	0.1	0.1	0.1	0.1	0.2	0.1	<0.1
ng/m³							
Ti	23.6	28.6	27.9	23.6	8.3	16.1	14.4
Cr	14.7	16.3	15.3	<dl	<dl	<dl	4.8
Cu	90.0	88.8	106.5	40.7	90.0	53.5	17.9
Zn	63.7	59.2	79.3	58.9	69.4	36.9	25.3
Sr	4.1	4.5	5.5	3.1	4.7	1.5	2.2
Y	1.9	2.0	1.7	<dl	<dl	<dl	0.1
Zr	49.67	56.6	63.5	69.2	57.2	31.2	8.8
Nb	0.7	0.6	1.4	<dl	<dl	<dl	0.1
Sn	14.8	18.6	19.5	11.3	14.2	5.5	3.9
Sb	5.8	6.5	8.6	1.2	5.4	2.4	2.0
Hf	2.4	2.5	3.0	2.8	2.7	1.4	0.4
Pb	4.3	5.1	5.6	1.1	1.3	1.8	3.2
Th	0.3	0.3	0.3	<dl	<dl	<dl	0.1
U	1.0	1.0	0.8	<dl	<dl	<dl	0.1

The relative enrichment in urban air of carbonaceous particles and a range of traffic-emission-related trace metals such as Cu, Sn and Sb is demonstrated by the histograms on ***Figure 8*** which compares the taxi interior PM chemistry with that from the Barcelona outdoor urban background and a remote air monitoring site at Montsec in the Pyrenean Mountains 150 km NW from Barcelona. These metals, already noticeably enriched in background urban air, rise to concentrations commonly exceeding PM_{10}Cu 100 µg/m^3, PM_{10}Sn 15 µg/m^3, PM_{10}Sb 8 µg/m^3 within the taxi

interiors. Another metal showing notable enrichment is Zr, accompanied by other similarly enriched high field strength elements (HFSE) such as Hf, Nb, Y and U.

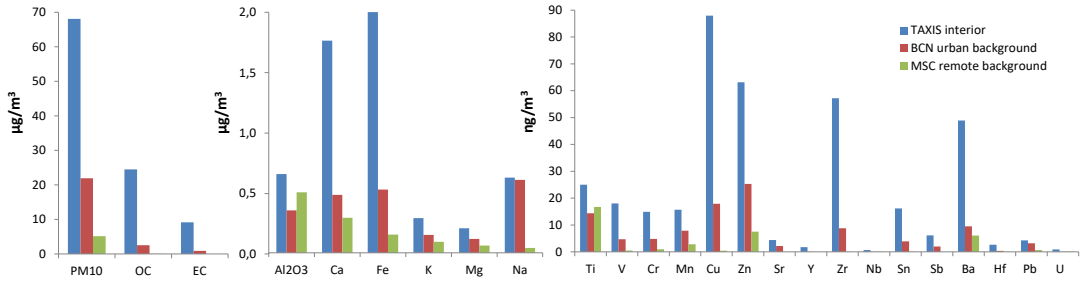

Figure 8 *Comparisons between the chemistry of PM_{10} measured inside taxis with data from the Barcelona urban background air monitoring site in Palau Reial, and from the European Monitoring and Evaluation Programme (EMEP) remote site at Montsec in the Catalan Pyrenees 150 km northwest of Barcelona (https://www.idaea.csic.es/egar/montsec/).*

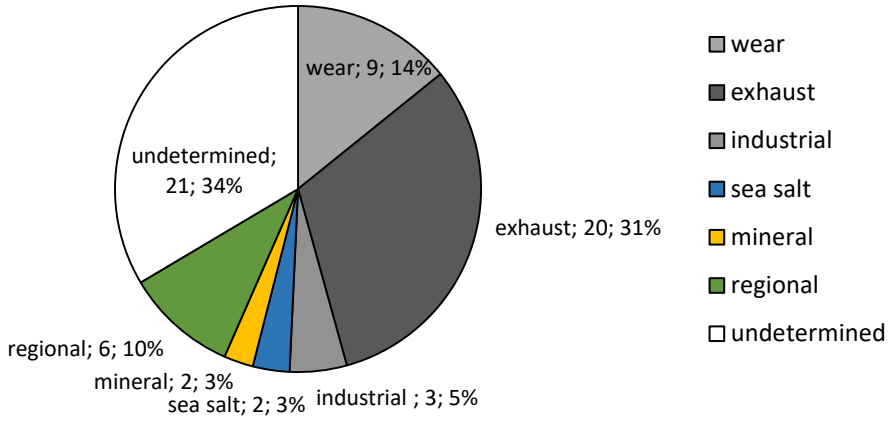

Figure 9 *Average mass contributions (in µg/m³ and %) of aerosol sources in the interior of the taxis determined by PMF.*

With regard to the source apportionment results, we identified six main sources of PM_{10} inside the taxis (***Figure 9***). The sum of the source contributions explained on average 66% of PM_{10} mass with the unexplained mass attributed mainly to a combination of ammonium nitrate particles and humidity. The six sources were labelled as vehicle wear, vehicle exhaust, industrial (mainly metallurgy), sea salt, mineral and regional (ammonium sulphate). On average the main impacting source was vehicle exhaust (31%, 20 µg/m^3), which resulted about twice the contribution from vehicle wear (14%, 9 µg/m^3) (***Figure 9*** and ***Figure 10***). This result is interpreted

as reflecting a relatively higher presence of submicron particles inside the taxi rather than super-micron particles. The third source by importance (excluding ammonium nitrate) was the regional source (10%, 6 μg/m^3), followed by industrial (5%, 3 μg/m^3), mineral and sea salt (both 3%, 2 μg/m^3). Given that about 80% of NOx emissions in the city have been calculated as due to road traffic (Querol et al., 2012), the total impact of traffic as a source for air pollutants breathed by taxi drivers and their passengers is estimated to be around 72%.

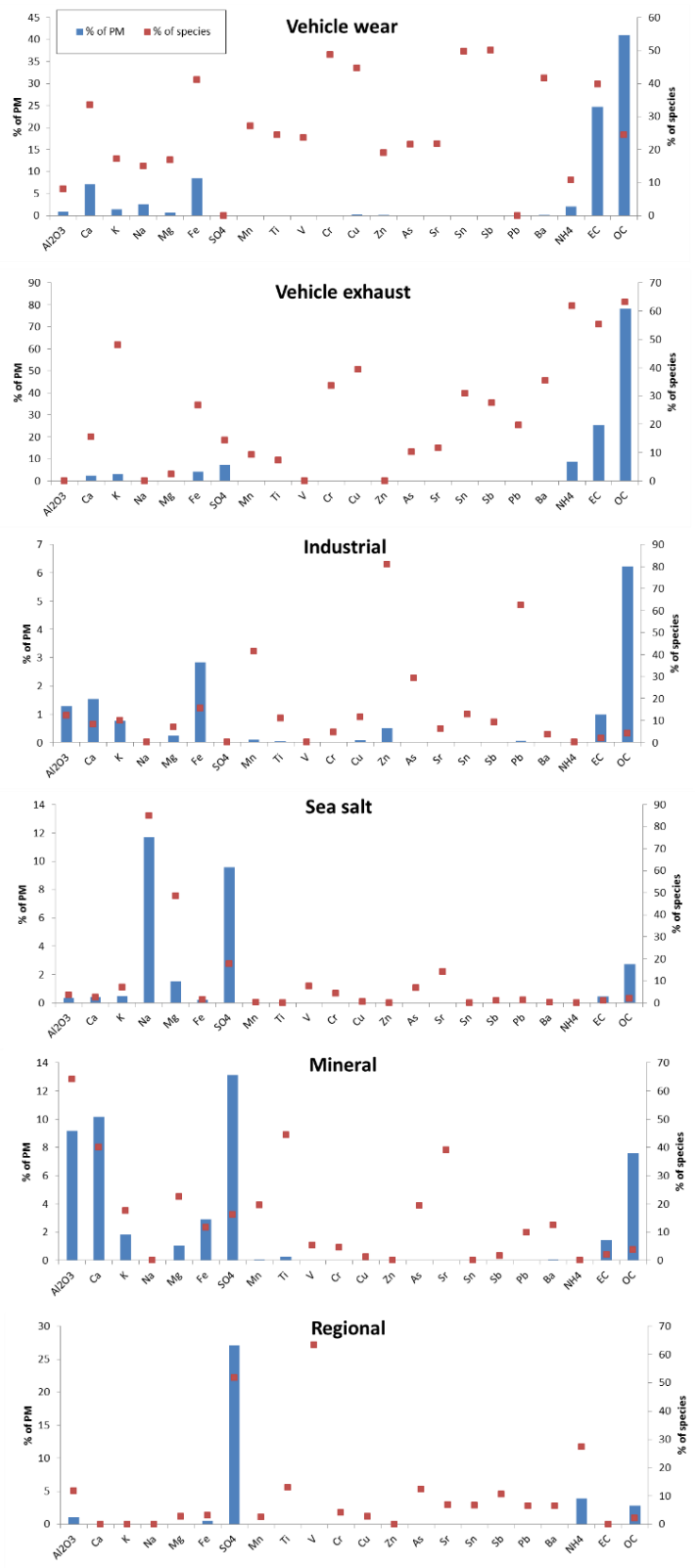

Figure 10 *Chemical profiles of the aerosol sources resolved by PMF.*

With regard to the analysis of Volatile Organic Compounds (VOCs) sampled in the taxi interiors, out of a total of 99 VOCs investigated 47 were detected and quantified (concentrations > 0.02 μg/m^3; ***Table 9***). These compounds included nine C_5-C_{10} alkanes and four C_5 alkenes (45-47% of total), thirteen C_6-C_{10} aromatic hydrocarbons (37-52%), eleven monoterpenes (0.7-15%), seven C_1-C_6 organochlorines (1-1.7%), two C_4 ethers and one C_5 ester (0.2-1.8%). In addition several compounds, such as 4-methyl-1-pentene naphthalene, isobutanol, 1,1,1-trichloroethane, 1,4-dioxane, dibromochloromethane, chlorobenzene, bromoform, α-terpinene, were found in some taxi vehicles but at the limit of detection. The VOCs not detected in the investigation were bromochloromethane, bromodichloromethane, dibromomethane, 1,1-dichloroethane, 1,2-dibromoethane, 1,1,2-trichloroethane, 1,1,1,2-tetrachloroethane, 1,1,2,2-tetrachloroethane, pentachloroethane, 1,1-dichloroethene, *trans*-1,2-dichloroethene, *cis*-1,2-dichloroethene, 1,2-dichloropropane, 1,3-dichloropropane, 3-chloropropene, 2,2-dichloropropane, 1,2,3-trichloropropane, 1,2-dibromo-3-chloropropane, 1,1-dichloropropene, *trans*-1,3-dichloropropene, *cis*-1,3-dichloropropene, *trans*-1,4-dichloro-2-butene, *cis*-1,4-dichloro-2-butene, 2-chloro-1,3-butadiene, hexachlorobutadiene 1,3-dichlorobenzene, 1,2-dichlorobenzene, 1,2,4-trichlorobenzene, 1,2,3-trichlorobenzene, bromobenzene, 2-chlorotoluene, 4-chlorotoluene, tert-butylbenzene, nitrobenzene, (-)-isopulegol, β-caryophyllene, α-humulene, *cis*-nerolidol, *trans*-nerolidol, (-)-guaiol, ethyl methacrylate, methacrylonitrile and propionitrile.

Table 9 *Concentrations of VOCs inside the studied taxi cars. LPG: liquefied petroleum gas; CNG: compressed natural gas. ND: not detected value. LOD: limit of detection*

	Concentration inside taxi (µg/m^3)				
***Group*/Compound**	**LP**	**Dies**	**Hyb**	**Elec**	**CN**
Alkanes/Alkenes					
n-Pentane	21	20	18	17	28
n-Heptane	5.9	4.9	2.9	6.0	7.5
n-Hexane	5.0	4.8	3.8	5.6	5.4
n-Octane	3.1	2.6	2.1	2.3	3.4
n-Decane	5.1	0.75	0.6	1.0	1.7
2-Methylbutane (i-pentane)	53	50	47	43	60
2,3-Dimethylpentane	2.2	2.0	1.6	2.3	2.4
Isooctane	0.32	0.74	0.46	2.2	1.3
Cyclohexane	2.2	2.1	1.6	2.6	3.2
Isoprene	11	4.1	2.0	31	5.7
1-Pentene	1.2	1.1	0.81	0.97	1.5
cis-Pentene	1.2	1.0	0.85	1.0	1.7
trans-2-Pentene	3.5	2.9	2.2	2.9	5.1
Total	***115***	***97***	***84***	***118***	***127***
Aromatics					
Benzene	8.6	6.8	6.8	5.3	10
Toluene	51	39	37	40	56
Ethylbenzene	10	8.0	6.5	7.1	11
m-Xylene	26	20	17	18	26
p-Xylene	9.9	7.8	6.5	6.8	11
o-Xylene	13	10	8.5	8.6	13
1,2,4-Trimethylbenzene	11	8.7	6.4	7.7	10
1,3,5-Trimethylbenzene	2.3	1.8	1.4	1.7	2.2
n-Propylbenzene	1.1	0.92	0.72	0.88	1.2
Styrene	1.0	0.67	0.80	0.50	1.0
Isopropylbenzene	0.40	0.33	0.26	0.29	0.43
n-Butylbenzene	0.29	0.22	0.18	ND	0.27
sec-Butylbenzene	0.09	0.07	0.08	ND	0.09
Total	***135***	***104***	***92***	***97***	***142***

Monoterpenes					
d-Limonene	4.5	0.80	0.86	30	4.4
Camphene	0.62	ND	ND	0.10	0.04
α-Pinene	0.43	0.21	0.26	1.8	0.56
(-)-β-Pinene/β-Myrcene	0.45	0.09	0.14	1.8	0.19
p-Cymene	0.58	0.25	0.23	0.64	0.37
δ-Terpinene	0.28	ND	ND	0.44	0.06
β-Ocimene	0.38	0.06	0.11	1.21	0.07
α-Ocimene	0.18	0.03	0.05	0.61	0.03
γ-Terpinene	0.14	ND	ND	1.31	0.10
δ3-Carene	0.12	0.05	0.06	0.25	0.09
Total	***7.7***	***1.5***	***1.7***	***38***	***6***
Organochlorines					
Tetrachloroethylene	0.78	0.83	0.95	0.54	2.3
1,2,2-Trichlorotrifluoroethane	0.70	0.71	0.73	0.65	0.79
Carbon Tetrachloride	0.57	0.59	0.60	0.58	0.61
Chloroform	0.37	0.18	0.39	0.11	0.33
1,2-Dichloroethane	0.21	0.23	0.23	0.52	0.24
Trichloroethylene	0.10	<LO	0.13	0.09	0.22
1,4-Dichlorbenzene	ND	0.06	ND	ND	0.14
Total	***2.7***	***2.6***	***3***	***2.5***	***4.6***
Others					
Methyl methacrylate	0.21	0.17	0.31	0.53	0.48
Tetrahydrofuran	0.17	0.19	0.20	0.29	0.49
Diethyl ether	0.06	0.12	0.13	3.9	0.06
Total	***0.44***	***0.48***	***0.64***	***4.7***	***1***

The most abundant compound of the alkane/alkene group was 2-methylbutane (43-60 µg/m^3) followed by n-pentane (17-28 µg/m^3) in all taxi models, whereas in the aromatic hydrocarbon group toluene was the most abundant compound (37-56 µg/m^3). All three of these VOCs are well documented as products of hydrocarbon fuel emissions. Other abundant VOCs were m-xylene, o-xylene, 1,2,4-trimethylbenzene, ethylbenzene, p-xylene, benzene, and 1,3,5-trimethylbenzene, all of which are also products of hydrocarbon fuel emissions (e.g. [183-186]). Several of these compounds are also known to be emitted by off-gassing of interior vehicle components (e.g. Brodzik, et al. [187]). The dominance of aliphatic and aromatic hydrocarbons conforms to what is known from other studies of VOCs inside passenger cars (Faber and Brodzik [188]).

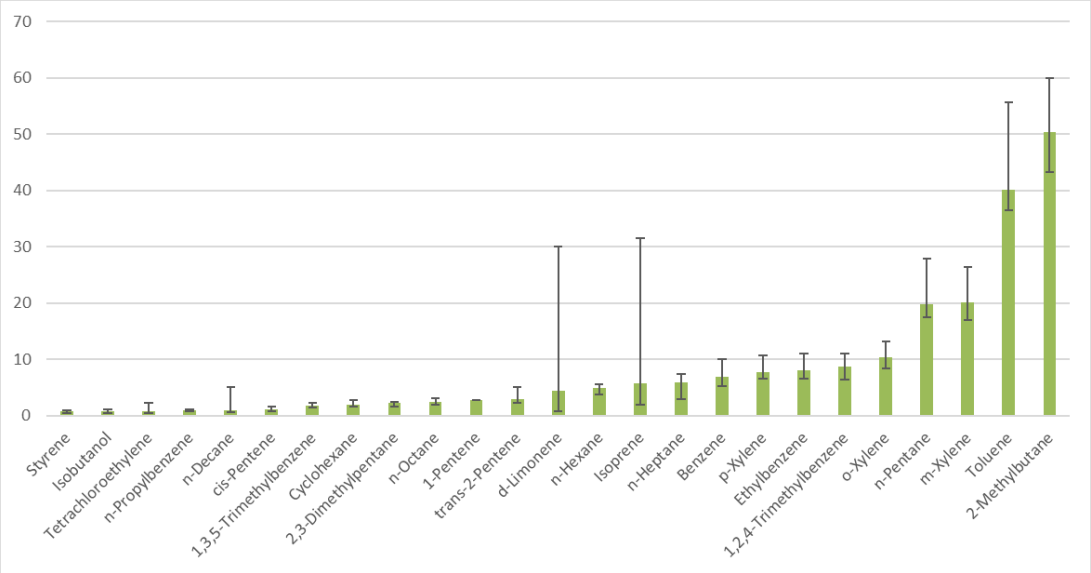

Figure 11 *Histograms ranking the relative abundances of VOCs measured inside taxis.*

The concentrations of benzene found in the taxi vehicles of the present study, 5.3-10 μg/m^3, were lower than those found in taxis of Guangzhou, 34 μg/m^3 [189] and those found in the inner atmospheres of patrol cars from North Carolina, 13 μg/m^3 [190]. The concentrations of toluene in the taxis of the present study, 37-56 μg/m^3, were lower than those found in the taxis of Guangzhou, 110 μg/m^3 [189] and similar to those found in the patrol cars of North Carolina, 39 μg/m^3 [190]. The taxis of Guangzhou also have higher concentrations of ethylbenzene, 20 μg/m^3, than those observed in the taxis of the present study, 6.5-11 μg/m^3. However, the concentrations of xylenes, m/p-xylenes and o-xylene in Guangzhou, 20 μg/m^3 and 17 μg/m^3, respectively, are similar to those of the present study, 23-37 μg/m^3 and 8.5-13 μg/m^3, respectively. In contrast, a study of VIAQ in Hong Kong taxis fuelled by LPG recorded much lower levels of aromatic hydrocarbons [191].

Normality testing of the concentration of these compounds inside each taxi under different fuel-engine models using the Shapiro-Wilk test showed non-normal distribution ($p < 0.001$). The Kruskal-Wallis test for non-parametric ANOVA indicated that the indoor taxi VOC concentrations of the different powered models were not significantly different for the compounds related with fuel emissions ($p = 0.322$). High correlations between the concentrations of alkanes/alkenes and aromatics

in the air of each taxi model were observed showing a predominance of the same emission sources.

Four of the five taxis used to sample VOCs were driven with windows open and therefore exposed to traffic pollutants infiltrating from outside. The only taxi driven with windows closed was the electric vehicle which recorded the lowest concentrations of n-pentane, 2-methybutane (both strongly associated with hydrocarbon fuel emissions) but the highest concentrations of isoprene and most monoterpenes. In particular, isoprene recorded concentrations of 31 $\mu g/m^3$ in the electric vehicle whereas in the others it ranged between 2 and 11 $\mu g/m^3$. A similar difference was observed for all monoterpenes (except camphene) which were found in higher concentration in the electric vehicle, e.g. δ-limonene, 30 $\mu g/m^3$, whereas in the atmospheres of the other cars it ranged between 0.8 and 4.5 $\mu g/m^3$ (***Table 9***). An obvious cause for this difference is the use of an air freshener in this vehicle. The high concentration of diethyl ether in the electric taxi model is probably also due to the use of the air freshener under closed window conditions.

Another factor proven to influence the VOC content of car interior air is the age of the vehicle [192, 193]. The youngest vehicle used in this study was that powered by natural gas (1-year old; <50000km on the odometer). The sample analysed from this vehicle showed the highest overall concentrations of alkanes/alkenes, aromatics, and organochlorines (***Table 9***), which we attribute to an extra VOC contribution by continued in-cabin degassing from a relatively young vehicle.

4.3 Discussion

The results summarised above offer insight into the controls on VIAQ inside a taxi driven through a busy city. They confirm the importance of air exchange rates (AER), the dominant influence of which has been noted by other publications dealing with VIAQ (e.g. [177, 194, 195]). The concentration of UFP provides a sensitive indicator of AER inside a road vehicle, rapidly responding to variations in ventilation, traffic conditions, car speed, and cabin pressure which together influence particle infiltration from outside (e.g. [67, 196]). Our data indicate that in taxis driven with windows and air circulation systems closed to outside air, the UFP number concentration can be

expected to be limited to relatively small variations above and below median values of 10000 #·cm^{-3} during the working day. In contrast, driving the vehicle through the city with windows open exposes the occupants to substantial and highly erratic increases in UFP numbers, with median values ranging from 20-90000 #·cm^{-3}, and with transient peak concentrations at times exceeding one million #·cm^{-3}.

Most of the UFP infiltrating the taxi cabin from outdoors will derive from the burning of hydrocarbon fuels, a process that produces nucleation mode particles that most commonly lie in the size range 10-20 nm. The rapid transformation of these fresh emissions to coarser accumulation mode particles by processes such as coagulation, especially in the confined microenvironment of a vehicle interior where dilution effects are impeded, is reflected by median UFP size values of 30-60 nm in our data. Our observation that median UFP size is always larger (usually by 10-15 nm) inside diesel vehicles as compared to taxis powered by other fuel systems suggests the influence of self-pollution inside the diesel cars, given the fact that PM emitted from diesel engines lie in a broader size range (20-130 nm) than those from gasoline engines (20-60 nm) (Morawska, et al. [197] and references therein). This suggestion is reinforced by data on black carbon (BC) concentrations measured in a taxi pair (diesel v. hybrid: this was only done on one day). The results from this pair recorded almost twice as much BC inside the diesel vehicle (16 October, diesel BC 17 μg/m^3/CO_2 433 ppm v. hybrid BC 9 μg/m^3/CO_2 435 ppm) even though both were driven around the city with open windows and with the equipment placed in the open boot (trunk). Similarly, in all cases where CO was measured simultaneously in taxi pairs, concentrations of this gas were higher in the diesel (average 2.1 ppm) as opposed to the non-diesel (0.1-1.5 ppm) vehicle, again indicating a component of self-pollution.

Median concentrations of LDSA measured in our study were highly variable (12-233 μg^2/cm^3), although once again diesel vehicles recorded generally higher levels than in non-diesel taxis (with two exceptions, in LPG taxis, which were similar to their diesel pair). All median values >100 μg^2/cm^3 were recorded only in diesel vehicles whereas, at the other extreme, LDSA values in the closed electric vehicle lay in the range 12-13 μg^2/cm^3. Lung deposited surface area values (for particles in the size range 20-400 nm) are likely to be a better predictor for pulmonary inflammation than number

concentration and, especially, PM mass [198, 199]. Our data confirm how LDSA concentrations present inside the cabin of a road vehicle are very sensitive to influxes of traffic pollutants from outside (see also Geiss, et al. [200]). In the transient peak example described previously (taxi 5D, ***Figure 6d*** and ***Figure 7***), for example, the dramatic increase in UFP numbers from 10491 #·cm^{-3} to 973696 #·cm^{-3} was matched by a rise in LDSA over the same 3-minute period from 132 µg^2/cm^3 to 1052 µg^2/cm^3, whilst simultaneously median particle size dropped from 54 nm to 11 nm in response to the entry of fresh traffic emissions.

Most studies of inhalable particle mass inside road vehicles have reported on concentrations of $PM_{2.5}$ rather than PM_{10}, placing emphasis on the dominant numbers of fine and ultrafine exhaust-generated particles in traffic emissions (e.g. [174, 201, 202]). In contrast we chose to measure PM_{10} on the basis of the fact that a large percentage of inhalable traffic-related particles derive from non-exhaust sources and are therefore abundantly present in the $PM_{2.5\text{-}10}$ size fraction. It has been shown for example that although particles emitted from brake wear range down to nanometric sizes [203], they commonly measure 2-6 µm and can contribute over 50% to the mass of traffic-related PM_{10} [204, 205]. Our data demonstrate that PM_{10} concentrations inside Barcelona taxis were variable but averaged 67 µg/m^3, which is more than treble the urban background for the same period (***Table 8***). Much of this difference in PM mass is attributable to increased levels of organic and elemental carbon, both of which are around x10 urban background inside taxi driven with windows open (***Table 8***) and source from both exhaust and non-exhaust traffic emissions. Our source apportionment data indicate the main impacting source of PM_{10} measured inside the taxis was vehicle exhaust (31%), with about half this value apportioned to vehicle wear (14%) (***Figure 9*** and ***Figure 10***).

The enrichment by a factor of x3 to x7 shown by a range of trace metals (Cr, Cu, Sn, Sb) in taxi interior air as compared to urban background is attributed mainly to the presence of particles abraded from brakes. The metalliferous nature of brake particles (which also contribute OC to traffic-contaminated air) has been well documented, with Cu and Sb being perhaps the most quoted classic markers of this source [205, 206]. To this list however we would add an "HSFE group" comprising mainly Zr and the

associated High Field Strength Elements of Hf, Nb, Y and U. The likely origin for these HFSE enrichment anomalies in traffic-contaminated air is their concentration in the mineral zircon ($ZrSiO_4$) used as an abrasive in road vehicle brakes. Such abrasive minerals can comprise up to 10% of the brake lining and are employed to increase friction and limit the build-up of transfer films [205, 207].

The unusual trace metal signature of brake-particle contaminated aerosol loadings breathed at roadsides and inside vehicles is graphically displayed in the ternary plot of ***Figure 12*** and introduced in a previous publication [69]. This triangular diagram uses Mn, Ti and Sbx10 to contrast the composition of particles produced by frictional movement of steel wheels and rails (subway), silicate-rich crustal (or "geological") particles (walking and street works), and those produced by Sb-rich brake emissions and breathed inside buses. Plotting our taxi data on this diagram demonstrates a clear affinity for the brake-contaminated apex, moving progressively away from a more crustal signature. For comparison the composition of Barcelona urban background for October 2018 is also plotted (blue star).

Our VIAQ data on VOCs inside taxi vehicles reveal a mix of compounds which reflects the complexity of traffic-related organic carbon emissions. The observation that the C_4-C_5 alkanes 2-methylbutane and n-pentane together comprise over half of the VOCs measured implicates the strong presence of light-hydrocarbon fuel emissions (gasoline, natural gas) [208, 209]. Given the fact that purely gasoline vehicles were not used in our study we can assume that most of these alkanes are infiltrating the taxi from outside, although note the content of n-pentane recorded inside the compressed natural gas vehicle (28 $\mu g/m^3$) was 7-11 $\mu g/m^3$ higher than all other vehicle types, suggesting an additional component of self-pollution. Over half the cars currently driven in Barcelona have diesel engines, so it is likely that many of the VOCs measured derive from diesel combustion. Separating diesel from gasoline emissions however is not simple as they share several species and fuels vary in composition, although it is likely that compounds such as m-xylene, trimethylbenzene and toluene derive at least in part from diesel engines [185]. Another complicating factor involves the well-documented effect of VOC off-gassing from interior materials, an influence that is most obvious in newer cars [184, 187, 192, 210]. This

may explain why the youngest car (1-year old and with the lowest km: Volkswagen Caddy CNG) recorded the highest concentrations of a majority of alkane/alkene and aromatic compounds (***Table 9***). Finally, the influence on VIAQ of introducing VOC-emitters such as air-fresheners can be dramatic. Our case of δ-limonene reaching median values of 30 µg/m^3 inside a closed electric taxi provides a good example, although it is eclipsed by the study of Fedoruk and Kerger [211] who recorded nearly 600 µg/m^3 of 2-butoxyethanol released by a deodoriser inside a used Ford Taurus.

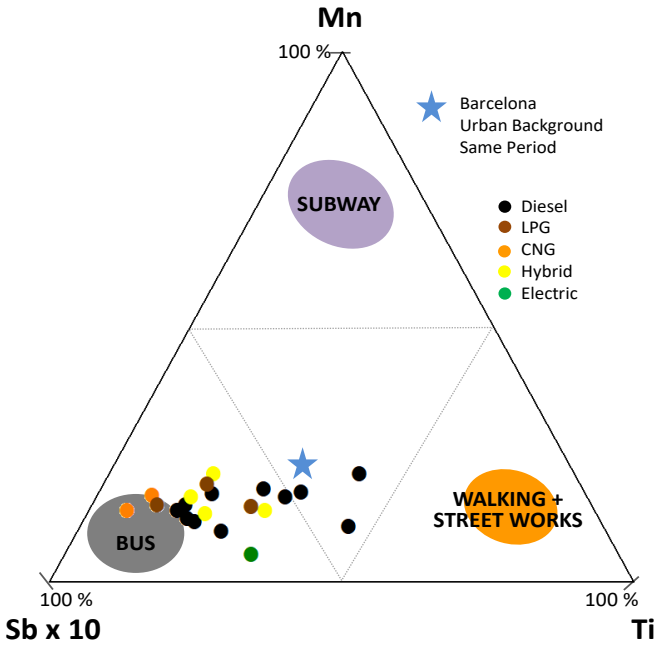

Figure 12 *Ternary plot comparing PM_{10} measured inside Barcelona taxis with the compositions of $PM_{2.5}$ collected from bus, subway and outdoor roadside microenvironments (see Moreno et al., 2015). The relative enrichment in Sb is attributed to brake particle emissions. The blue star marks the composition of Barcelona urban background during the October 2018 VIAQ taxi measurement campaign.*

Another result of operating taxis under closed ventilation conditions will be a rise in CO_2 concentrations. The maximum CO_2 level recorded in our study was 4600 ppm, reached inside a closed electric vehicle (24E). The taxi began work that day recording interior CO_2 concentrations of 400ppm, this rising to 3000 ppm in 45 minutes and staying above this level for over 4 hours before a sudden drop (over 3 minutes) to 2000ppm when the car was ventilated. This brief ventilation episode was accompanied

by a jump in N from 10000 to 20000 #·cm^{-3} and in LDSA from 10 to 20 µg^2/cm^{-3}, before closed conditions were re-established and CO_2 rose again. The rapidity (less than 1 hour to reach several thousand ppm) with which CO_2 concentrations can climb inside a taxi is a cause for concern. Although CO_2 is listed as a toxic contaminant workplace exposure to which should be kept below a 8-hour time-weighted average of 5000 ppm, various studies have demonstrated that concentrations lower than this, and certainly within the range of the example given above, can have a detectable effect on both mental performance and physical condition [212, 213]. A recent exercise in modelling CO_2 accumulation inside vehicles has emphasised the sagacity of ventilating the vehicle when CO_2 levels reach 2500 ppm, a threshold considered to be "consistently linked to detrimental cognitive effects" [175]. In the Barcelona electric taxi example described above this threshold of 2500 ppm CO_2 was exceeded for 4.5 hours of the 6-hour monitoring period.

Taxi drivers work at the coalface of modern transport-related urban air pollution. During their working day they are continuously exposed to enhanced mass and number concentrations of particles derived from vehicle exhaust and non-exhaust sources. Yet there seems to be only limited awareness of the risks associated with breathing poor quality air, as demonstrated by the fact that a majority of the taxi drivers in our study chose to drive through the busy city with open windows, thus unwittingly breathing UFP concentrations that, during extreme transient peaks, can exceed one million #/cm^3. A recent survey of taxi drivers in New York reflected this lack of awareness with 74% of respondents claiming they were not very worried about being exposed to air pollution while driving [214]. Presumably this situation applies not just to the hazard of pollutants infiltrating from outside but also to the problem of contaminants such as CO_2 that are generated within the taxi interior and need to be briefly but regularly ventilated, preferably in relatively clean air outside conditions. The taxi driver community would clearly benefit from awareness initiatives designed to help them better understand the value of good practice regarding VIAQ, and thus encourage them to take measures to reduce air pollutant exposure to themselves and their passengers.

5 LUNG CANCER RISK ASSESSMENT DUE TO TRAFFIC-GENERATED PARTICLES EXPOSURE IN URBAN STREET CANYONS: A NUMERICAL MODELLING APPROACH

In this experimental campaign, an innovative approach for the evaluation of the lung cancer risk of people exposed to traffic-generated particles inside street canyons was proposed. In particular, a modified risk-assessment model was used to estimate the Excess Lifetime Cancer Risk (ELCR, extra risk of develop cancer in a population of individuals, for a specific lifetime exposure and dose-response data) contribution of both ultrafine and coarse particles from light duty and heavy duty vehicles in urban area through the risk model developed by Sze-To, et al. [57] which was recently applied in estimating the lung cancer risk for the Italian population [215], and smokers [139], and for people living nearby an incinerator plant [216]. The proposed approach consists in the evaluation of the ELCR in emission from the tailpipe of vehicles applying the above-mentioned risk assessment model, using data of PAHs, heavy metals (As, Cd, Ni) and PCDD/Fs, available in literature. The calculated ELCR at the tailpipe is then used as input data in a numerical CFD (Computational Fluid Dynamics) scheme, based on the Spalart-Allmaras turbulence model and already used in previous work [76] in order to evaluate the lung cancer risk in every point of interest inside the street canyon, and analyse the influence of wind speed and canyon geometry on the ELCR at street level. Simulating the dispersion of the ELCR allows to consider the dispersion of both particles and relative toxicity, which represent a novel aspect of the proposed approach.

5.1 MATERIALS AND METHODS

5.1.1 ELCR model implementation

The risk model adopted in the present paper, originally developed by Sze-To, et al. [57], allows to estimate the lung cancer risk due to the exposure to the IARC Group 1 (carcinogenic to humans) agents deposited on inhalable airborne particles. The model accounts for the contribution of both ultrafine particles (UFPs) and super-micron particles. The contribution of UFPs is relative to the particle surface area, introducing a coefficient (c_f) to correlate the particle surface area-based cancer potency of the pollutant to the mass-based cancer potency of the pollutant itself (see Sze-To et al.[57] for major details). The equation for the risk characterization, for each pollutant, is:

$$\boldsymbol{ELCR_i = \frac{SF_i}{BW}\frac{m_i}{PM_{10}}\left(c_f \cdot \delta_S + \delta_{PM10}\right)} \quad (4)$$

Where, for each *i-th* pollutant, $ELCR_i$ is the excess lifetime cancer risk, SF_i is the inhalation slope factor, representing the increase of the risk of getting cancer associated with exposure to the specific dose of a chemical every day for a lifetime, and then it is used as the relationship between dose and response, *BW* is the body weight of the exposed individual (assumed as 70 kg), m_i is the mass concentration of the pollutant present on the PM_{10} mass (mg/m^3), δ_S (nm^2) and δ_{PM10} (mg) are the particle surface area (S) and mass (PM_{10}) deposited doses. The conversion coefficient c_f, that correlates the particle surface area-based cancer potency of the pollutant to the mass-based cancer potency of the pollutant itself, has the value of 6.60×10^{-13} mg/nm^2, experimentally obtained by Sze-To, et al. [57]. It is assumed by these authors that the c_f coefficient depends on physical characteristics rather than the chemical composition of the particles, and then we adopted the original value of the coefficient since the particle size distributions considered in this study are similar to those used in the original paper of Sze-To et al. The *SF* for the IARC Group 1 carcinogenic chemicals used in the risk assessment model were obtained from the Office of Environmental Health Hazard Assessment[217], and are reported in ***Table 10***. Further details about the ELCR model can be found in some recent papers of the authors[139, 215, 216].

Table 10 *Inhalation cancer slope factor (SF) for the considered IARC Group 1 carcinogenic compounds, as provided by Office of Environmental Health Hazard Assessment.[217]*

IARC Group 1 agent	***SF (kg d/mg)***
Benzo[α]pyrene (B[α]p)	3.85×10^{0}
Arsenic (As)	1.51×10^{1}
Cadmium (Cd)	6.30×10^{0}
Nickel (Ni)	9.10×10^{-1}
PCDD/F	1.16×10^{5}

Data on pollutant mass concentrations (Group 1 carcinogenic chemicals) and PM_{10} concentrations at the tailpipe were obtained from the inventory guidebook of European Environmental Agency [218]. In particular, the emission factors of all the considered Group 1 carcinogenic chemicals are summarized in ***Table 11***.

Table 11*. Emission factors of the considered emitted pollutants (literature data[218]).*

Pollutant agent	***LDV (g/km)***	***HDV (g/km)***
Benzo[α]pyrene (B[α]p)	1.10×10^{-6}	9.00×10^{-7}
Arsenic (As)	5.89×10^{-7}	2.63×10^{-6}
Cadmium (Cd)	8.96×10^{-7}	3.13×10^{-6}
Nickel (Ni)	2.63×10^{-6}	1.02×10^{-5}
PCDD/F	1.16×10^{-11}	2.17×10^{-4}
PM_{10}	3.74×10^{-2}	2.83×10^{-1}

Surface area dose (δ_S), considered as the sum of the tracheobronchial and alveolar depositions, was evaluated on the basis of an indirect exposure assessment approach[219] using the following equation:

$$\delta_S = IR_{activity} \cdot \tau \cdot \int \left[\varphi_{Alv+Tb}(IR_{activity}, D_p) \frac{dS}{dD_p} dD_p \right] \quad (5)$$

where S stands for particle surface area concentration, $IR_{activity}$ is the inhalation rate of the exposed population depending on their activity, φ_{Al} and φ_{Tb} are the alveolar and tracheobronchial fractional deposition depending on inhalation rate and particle diameter (D_p), $dS(D_p)/dD_p$ is the particle surface area distribution, and τ is the exposure time. In the present paper, an exposure time of 15 minutes per day was considered, as Buonanno, et al. [70] found that this is a time typically spent outdoors in urban areas for Italian population. An additional exposure time of 24 hours per day, representative of an extreme scenario, was taken into account for comparison.

Particle deposition fractions and inhalation rates were adapted from the International Commission on Radiological Protection [220]: in particular, fractional depositions in alveolar and tracheobronchial regions of the respiratory tract for subjects in light activity (average values amongst male and female normally breathing from the nose) were considered. The surface area was calculated on the basis of the available number distribution assuming spherical shape of the particles. PM_{10} dose was not considered because its contribution to the ELCR total value is orders of magnitude lower than that of UFPs[139, 216]. In the light of this, the δ_{PM10}, in equations (4) and (5) was ignored, as already done in recent papers of the authors[139, 215, 221]. It should be pointed out, anyway, that PM_{10}, causes other health concerns such as inflammatory effects or asthma[222].

5.1.2 Literature survey for particle size distributions

In order to correctly account for the contribution of the particle surface area to the ELCR, the physical characteristics of the particles emitted from the different typologies of vehicles should be carefully assessed. One of the biggest issue, in this regard, is relative to the wide variation of the size distribution and concentration of the emitted particles with the different real-life riding conditions (urban, extra-urban, idling, acceleration, deceleration etc.). There are also a lot of discrepancies between particle characteristics measurement for on-road or dynamometer tests as well as for measurements at the tailpipe or in a constant volume sampler (CSV). In addition, the

particle characteristics are different for the different engine technologies and after-treatment equipment installed on the vehicles. Summarizing, the available literature is characterized by inhomogeneous data since there are a lot of vehicles tested (with different engine technologies), measurements techniques (on road or at dynamometer, at the tailpipe or in CSV), and data presentation (emission factors or concentrations).

In the light of that, for the evaluation of the ELCR in street canyons (urban area) with the proposed methodology, the data for particle physical characteristics should be selected on the basis of two main aspects. The first one is relative to the need of consider only measurements made on the basis of vehicle urban cycles (limited velocity and frequent stops) and the second is relative to the choice of measurements made in CSV in order to account for the thermodynamic transformation of the freshly emitted particles, since the numerical model adopted for the present simulations does not account for these phenomena. In addition, in order to reproduce plausible emission scenarios, different kind of vehicles should be taken into account (light duty and heavy duty, diesel or gasoline fueled etc.).

In ***Table 12***, the particle physical characteristics are reported for the different typologies of vehicles considered (light duty and heavy duty, diesel and gasoline vehicles), together with the main vehicle/engine characteristics. All the reported data are relative to measurements made on chassis dynamometer, reproducing urban riding cycles, and sampling in CSVs. The authors point out that the choice of particle size distribution can be different if the model adopted for the simulations account for thermodynamic transformation (i.e. measurements made directly at the tailpipe).

***Table 12**. Particle physical characteristics emitted from the different typologies of vehicles considered (LDV: light duty vehicles, HDV: heavy duty vehicles), together with the main vehicle/engine characteristics (DPF: diesel particulate filter, EGR: exhaust gas recirculation, DOC: diesel oxidation catalyst, CDPF: catalyzed diesel particulate filter).*

Vehicle type	*PNC* *(#·cm^{-3})*	*Modes* *(nm)*	*Standard*	*Aftertreatment equipment*	*Reference*
LDV - gasoline	4.3×10^{4}	11/52	EU 6	3-way catalyst	Louis, et al. [223]
LDV - diesel	6.4×10^{5}	16/81	EU 4	DPF + EGR	Jung, et al. [224]
HDV – diesel (bus)	4.8×10^{3}	11/60	China-III	DOC + CDPF	Lou et al. [225]

5.1.3 ELCR calculation at the fleet-tailpipe

On the basis of (a) emission factor data reported in ***Table 11*** and (b) particle physical characteristics for each vehicle typology of ***Table 12***, the ELCR at the tailpipe for HDV, LDV diesel and LDV gasoline was evaluated on the basis of equation (4). Then, the final ELCR value was evaluated as weighted average of the considered fleet (5% HDV and 95% LDV[226], 60% of which gasoline and 40% diesel[227]). In particular, the m_i/PM_{10} and SF_i/BW ratios in equation (4) were obtained, for each compound, on the basis of the values reported in ***Table 10*** and ***Table 11*** and considering a body weight mean value of 70 kg. The surface area dose (δ_S) was calculated by means of equation (5) considering the surface area distribution calculated from the particle number distributions reported in ***Table 12*** for each vehicle typology.

5.1.4 CFD model details

The evaluation of the ELCR at street level in urban environment may be obtained by simulating the fluid flow evolution inside the street canyon. To this end, in the present work the commercial software Comsol Multiphysics® was used to solve the standard Spalart-Allmaras turbulence model and the conservation equation for species, as already done in previous papers of the authors[23, 76, 77, 216]. In these papers, the

model here adopted was validated against experimental data, showing good accuracy in reproducing particle dispersion.

The Group 1 substances are supposed to be deposited on the particle surface and their amount is directly related to the particle mass through the term (m_i/PM_{10}) of equation (4). The ELCR value is then directly related to the particle concentration; simulating the "dispersion" of ELCR (which is function of particle emission at the tailpipe) corresponds to the dispersion of particles in the street canyon for the evaluation of the ELCR in every point of interest of the domain, without calculating the dispersion of each pollutant and then the corresponding ELCR value in these points. In the present model, the dispersion of the particles was evaluated using an Eulerian approach, solving the following mass conservation equation with a *K*-closure method[228]:

$$\frac{\partial c}{\partial t} + \boldsymbol{U} \cdot \nabla \boldsymbol{c} = (\boldsymbol{D} + \boldsymbol{\nu_T})\nabla^2 \boldsymbol{c} \tag{6}$$

where c is the concentration and ν_T is the eddy viscosity, which is added to the molecular diffusion coefficient D in order to take into account the turbulent diffusion of the particles. UFPs were modelled as a gas phase, imposing their diameter by defining a corresponding diffusion coefficient as reported by Baron and Willeke [229]. The relation between diffusion coefficient and particle diameter is:

$$\boldsymbol{D} = \frac{\boldsymbol{kTC_C}}{\boldsymbol{3\pi\eta d_p}} \tag{7}$$

where D is the diffusion coefficient, k is the Boltzmann constant (1.38×10^{-23} N m/K), C_C is the Cunningham slip correction factor[230], η is the air viscosity and d_p the particle diameter. Even if heated surfaces within the street canyon can affect the air motion, and then the ELCR, thermal effects on particle diffusion were not taken into account for simplicity, even considering that for wind speed greater than 2 m/s turbulent transport and convection are predominant[231, 232], [232].

5.1.5 Computational domain and boundary conditions

The calculated value of the ELCR at the tailpipe, was used as input parameter in the above described CFD model in order to evaluate lung cancer risk in every point of interest inside the street canyon. In ***Figure 13*** the computational domain and the

boundary conditions employed are reported. Since a two-dimensional domain was considered for the simulations, it is assumed that the street canyon has an infinite length in the street direction. With this assumption a point source (square with side length equal to 0.1 m, at 0.1 m from ground approximating the vehicle exhaust pipe size), was used to simulate the dispersion of particles emitted by a single tailpipe having an emission calculated as weighted average of the fleet, as described above. A uniform velocity profile was imposed at the inlet section of the computational domain, while zero pressure condition, symmetry condition and zero velocity condition were imposed at the domain exit, domain top, and on the walls, respectively. The air physical properties were taken at 25 °C and atmospheric pressure.

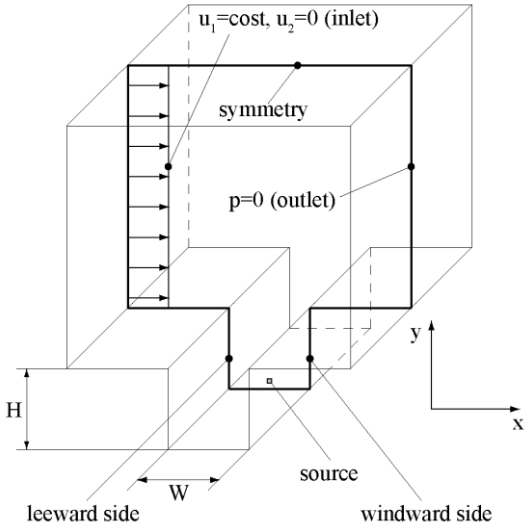

Figure 13 *Computational domain and boundary conditions used for the numerical simulations.*

ELCR was numerically obtained using different street canyon geometries and approaching wind speeds, in order to assess the influence of that parameters on the ELCR inside the canyon.

5.1.6 Parametric analysis

In order to evaluate the influential parameters on ELCR in urban environment, a parametric analysis was proposed, varying the street canyon geometry and the wind speed. The reference simulation condition is relative to an approaching wind velocity of 1 m/s and aspect ratio *H/W* equal to 1 (with height of building from street level *H*, and width of the street, *W* equal to 14 m). The background value of the ELCR was set

to zero for all the cases in order to evaluate only the effect of the vehicle emissions. Starting from the reference simulation case, two additional aspect ratios (*H/W*=2 and *H/W*=3) and two additional wind speeds (3 m/s and 5 m/s) were evaluated.

5.2 Results and discussions

The value of the ELCR at the tailpipe, calculated with the above described model, was found equal to 2.1×10^{-2}, which means 2 100 new lung cancer cases over a population of 100 000, hypothetically breathing directly at the tailpipe 24 hours per day for 70 years. In **Table 13** the *SF* of the mixture (SF_m, calculated as $SF_m = \sum_{i=1}^{n} SF_i \cdot \frac{m_i}{PM_{10}}$), and the contributions of the five pollutants to such SF_m were reported. SF_m values resulted one order of magnitude larger than those typical of cooking-generated particulate matters, estimated by Sze-To, et al. [57] on the basis of the data reported in He, et al. [233], whereas they resulted 1 – 2 orders of magnitude smaller to the SF_m evaluated for particles emitted from incinerator plants[216]. The main contribution to the SF_m was due to the metals: As (39 – 53%), Ni (11 – 12%) and Cd (25 – 26%), whereas a smaller contribution can be addressed to B[α]P and PCDD/F. The authors point out that the values reported in ***Table* 13** were only used to evaluate the contribution of each compound on the SF_m, (and then on the ELCR) and not for the calculation of the ELCR itself.

***Table 13**. Mass fractions of emitted carcinogenic compounds on PM_{10} (expressed as mg/mg) and corresponding SF of the mixture (SF_m). Data of SF for each compound obtained from Office of Environmental Health Hazard Assessment [217].*

	SF_m	m_i/PM_{10} (mg/mg)	Contribution to SF_m (%)
B[α]P	$6.01\times10^{-4} – 2.63\times10^{-4}$	$2.94\times10^{-5} – 3.18\times10^{-5}$	5 – 19
As		$1.57\times10^{-5} – 9.29\times10^{-6}$	39 – 53
Cd		$2.40\times10^{-5} – 1.11\times10^{-5}$	25 – 26
Ni		$7.03\times10^{-5} – 3.60\times10^{-5}$	11 – 12
PCDD/F		$3.10\times10^{-10} – 7.67\times10^{-11}$	3 – 6

In ***Figure 14*** the airflow fields and the corresponding ELCR distribution, calculated imposing the obtained value of ELCR at the tailpipe as input boundary condition, are reported for each aspect ratio of the street canyon, for a wind speed of 1 m s^{-1}, considering people exposed to traffic emissions 24 hours per day for 70 years. As can be seen, the air flow fields are different for the different aspect ratios analysed. For H/W=1, one main clockwise-rotating vortex was observed, while for H/W=2, two counter-rotating vortices are visible: the one below rotating counter clockwise and the one at the top rotating clockwise, in accordance with the free-stream wind direction. For the H/W=3 configuration, three vortices are generated in the street canyon, as depicted in ***Figure 14*** (c). The same flow configurations were observed also in other similar street canyon simulations of Scungio, et al. [77], and Scungio, et al. [76]. The corresponding ELCR distribution fields (reported at the right of each flow field in ***Figure 14***) are strictly related to the flow patterns. In particular, higher ELCR values can be observed at the bottom of each H/W configuration, since the interaction between the fluid flow inside the canyon with the free-stream wind is weaker at the base of the street canyon, as found in Scungio, et al. [77]. With the increasing of the

H/W ratio, this interaction becomes even more weaker at the bottom of the street canyon and then, as a consequence, the dispersion of pollutants emitted is limited in this point, leading to the increase of the ELCR value, that becomes maximum at the bottom of the H/W=3 street canyon configuration. In addition, looking at ***Figure 14***, since the variable direction of rotation of the vortex at the base of each H/W configuration (once clockwise and once counter-clockwise), the distribution of the ELCR varies. In particular, referring at the bottom of the street canyon, where people spend most of the time, higher ELCR values are observed on the leeward side for W/H=1 and W/H=3 (bottom vortex rotating clockwise), and on the windward side for H/W=2 (bottom vortex rotating counter-clockwise).

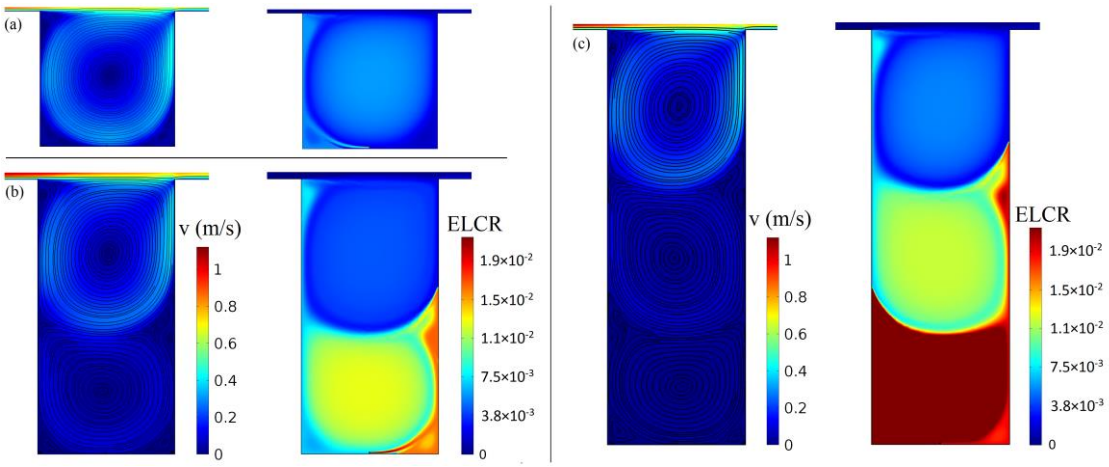

Figure 14 *Airflow fields and corresponding ELCR distribution for H/W=1 (a), H/W=2 (b) and H/W=3 (c), for a wind speed of 1 m/s, considering people exposed to traffic emissions 24 hours per day for 70 years.*

In **Figure 15** the ELCR calculated at a breathable height of 1.5 m on the leeward and windward sides of the street canyon is reported as a function of wind speed and aspect ratio H/W. In particular, on the top panel of ***Figure 15***, the ELCR is showed as function of the wind speed (1, 3 and 5 m/s) for the three analysed aspect ratios (1, 2 and 3), while on the bottom panel of ***Figure 15*** the ELCR is showed as function of the H/W ratio for the different wind speeds. The top panel of ***Figure 15*** confirms what stated above: the ELCR value at 1.5 m from the ground is higher on the leeward side for aspect ratios equal to 1 and 3, while for aspect ratio equal to 2 the ELCR is higher on the windward side, for all the three wind speeds analysed. As a general behaviour, with

the increasing of wind speed the ELCR becomes lower everywhere in the street canyon, due to the strengthened interaction between the free-stream flow and the flow inside the canyon. In addition, the effect of wind speed is more pronounced for wind speeds between 1 and 3 m/s than between 3 and 5 m/s, and this behaviour is more visible on the leeward side, for H/W=1 and 3, and on the windward side for H/W=2. As can be observed from the bottom panel of ***Figure 15***, the ELCR value at 1.5 m tends to increase with the increasing of the aspect ratio, with a different trend on the leeward and windward side of the street canyon: on the leeward side the ELCR tends to increase more than on the windward side, with the increasing of the aspect ratio, for all the three wind speeds analysed.

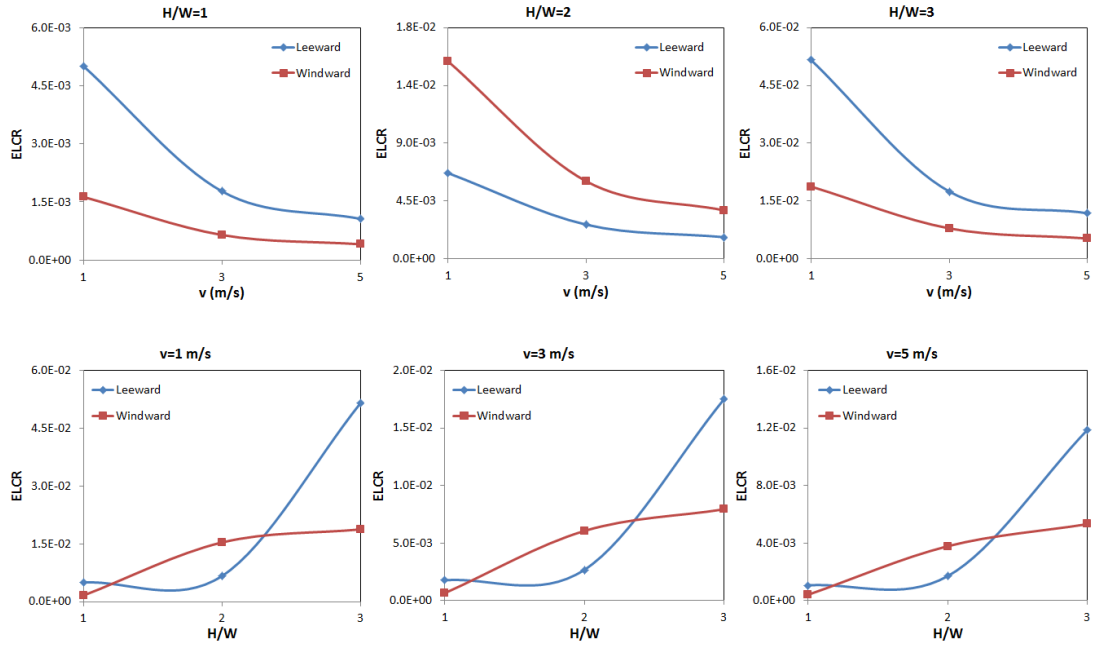

Figure 15 *ELCR calculated at a breathable height of 1.5 m from the street level on the leeward and windward sides of the street canyon as a function of wind speed (top panel) and aspect ratio H/W (bottom panel). People exposed 24 hours per day for 70 years.*

In **Table 14** and **Table 15** the calculated ELCR values are reported in details for all the aspect ratios and wind speeds considered, at a breathable height of 1.5 m, on the leeward and windward sides of the street canyon. The ELCR for the reference configuration are reported in bold. In particular, **Table 14** reports ELCR values for people ideally living 24 hours per day in the street canyon for 70 years, while **Table 15** reports ELCR values for a more realistic scenario of people spending 15 minutes

per day in the street canyon for 20 years. It should be stressed that the ELCR values reported in the tables are representative of the extra risk to develop cancer (new lung cancer cases) due to the exposure of pollution from urban traffic only, without considering the background pollution eventually present in the street canyon.

Table 14 *ELCR values calculated on the leeward and windward sides of the street canyon at a breathable height of 1.5 m, for people exposed 24 hours per day for 70 years. Reference simulation case in bold.*

	H/W=1		*H/W=2*		*H/W=3*	
v (m/s)	Leeward	Windward	Leeward	Windward	Leeward	Windward
1	5.0×10^{-3}	1.6×10^{-3}	6.7×10^{-3}	1.5×10^{-2}	5.2×10^{-2}	1.9×10^{-2}
3	1.8×10^{-3}	6.5×10^{-4}	2.7×10^{-3}	6.1×10^{-3}	1.7×10^{-2}	7.9×10^{-3}
5	1.1×10^{-3}	4.1×10^{-4}	1.7×10^{-3}	3.8×10^{-3}	1.2×10^{-2}	5.3×10^{-3}

Table 15*. ELCR values calculated on the leeward and windward sides of the street canyon at a breathable height of 1.5 m, for people exposed 15 minutes per day for 20 years. Reference simulation case in bold.*

	H/W=1		*H/W=2*		*H/W=3*	
v (m/s)	Leeward	Windward	Leeward	Windward	Leeward	Windward
1	1.5×10^{-5}	4.8×10^{-6}	2.0×10^{-5}	4.6×10^{-5}	1.5×10^{-4}	5.6×10^{-5}
3	5.3×10^{-6}	1.9×10^{-6}	8.0×10^{-6}	1.8×10^{-5}	5.2×10^{-5}	2.4×10^{-5}
5	3.2×10^{-6}	1.2×10^{-6}	5.1×10^{-6}	1.1×10^{-5}	3.5×10^{-5}	1.6×10^{-5}

As can be seen from **Table 14**, which reports an extreme scenario representative of worst possible condition, the maximum ELCR value found under the assumptions made in the methodology section, is equal to 5.2×10^{-2} on the leeward side of the H/W=3 street canyon configuration, with a wind speed of 1 m/s. This ELCR value means that on a population of 100 000 individuals, there will be 5 200 new lung cancer cases, according to the proposed model. In the same extreme scenario, the lower ELCR

value of 4.1×10^{-4} is relative to the windward side of the H/W=1 configuration, with wind speed of 5 m/s, meaning that 41 people will develop cancer over a population of 100 000. The reference configuration (H/W=1, wind speed of 1 m/s) presents ELCR values between 1.6×10^{-3} and 5.0×10^{-3} on the windward and leeward sides, respectively (160 and 500 new lung cancer cases over 100 000 peoples, respectively). For the scenario of people spending 15 minutes per day in the street canyon for 20 years,

Table 15 reports lower ELCR values, as expected. Again, the worst condition is observable on the leeward side of the H/W=3 configuration, with wind speed of 1 m/s (ELCR equal to 1.5×10^{-4} – 15 new lung cancer cases over 100 000 peoples), while the lower ELCR is relative to the windward side of the H/W=1 street canyon, with 5 m/s of wind speed (1.2×10^{-6} – 0.12 new lung cancer cases over 100 000 peoples). The reference configuration (H/W=1, wind speed of 1 m/s) presents ELCR values between 4.8×10^{-6} and 1.5×10^{-5} on the windward and leeward sides, respectively (0.48 and 1.5 new lung cancer cases over 100 000 peoples, respectively).

As a comparison with the data reported in the present paper in **Table 15** by applying the same risk model, Scungio, et al. [216] found ELCR values between 0.017 – 0.07×10^{-5} considering different scenarios of people living nearby a waste incineration plant in central-southern Italy exposed only to the particles emitted from the stack of the incinerator itself (without considering the background pollution), for the entire lifetime of the plant, supposed to be 20 years. Moreover, for typical Italian smokers the ELCR was found to be between 2 – 6×10^{-1} [139], considering typical smoking patterns, which is a value 3 – 4 orders of magnitude higher than that found in the present paper. In addition, the risk calculated in this work for the scenario depicted in **Table 14** results comparable to the ELCR target limit of 1×10^{-5} reported by WHO [234], and can be considered "safe" if compared to the EPA target risk range of 10^{-6} – 10^{-4} since, as EPA reports, ''even risks slightly greater than 1×10^{-4} may be considered adequately protective" under specific conditions[235].

6 PARTICLE-RELATED EXPOSURE, DOSE AND LUNG CANCER RISK OF PRIMARY SCHOOL CHILDREN IN TWO EUROPEAN COUNTRIES

A number of papers were published by the scientific community in terms of indoor concentration of PM_{10} and $PM_{2.5}$ at schools [96, 236-239], in particular, PM_{10} concentrations were found to exceed most of the time the WHO Air quality guidelines [240-243]. On the contrary, the scientific bibliography reporting the exposure to ultrafine particles (UFP) in schools is still scarce [104, 244, 245] [94, 246-252]. In particular, a lack of knowledge on (i) air-quality-based studies able to evaluate the actual exposure of children at schools [239, 242], (ii) corresponding airborne particle doses received by children [121, 199], (iii) correlation between children exposure to airborne particles and adverse health effects, (iv) evaluation of the lung cancer risk and the related effect of each particle-bounded carcinogenic compound was recognized.

To this purpose, the present study was conceived to provide results on children exposure to the different particle metrics (including the potentially promising metric of particle surface area) and to particle-bounded carcinogenic compounds in two European cities. Moreover, the daily dose in terms of lung deposited surface area (LDSA) received by children in classrooms was assessed as well as the estimate of the corresponding excess lung cancer risk associated with both surface area and particle mass doses.

6.1 Materials and methods

6.1.1 Study area and monitoring sites

The study was performed in two different Mediterranean cities, Barcelona (Spain) and Cassino (Italy). Barcelona is located on the northeast coast of Spain (41°23′N 2°11′E) between Mediterranean Sea and the Pyrenees mountains. It has a population of 1.6 million inhabitants and density vehicles of 5800 cars km^{-2} (data available at www.bcn.cat, Department de Estadistica, Ajuntament de Barcelona). Cassino is located in Central Italy (41°29′30″N 13°50′00″E), its population is equal to 39000 inhabitants and its vehicle density is roughly equal to 300 cars km^{-2} (data available at www.aci.it). Both these cities were characterized in terms of particle number concentration (PNC) in previous papers. Higher levels of airborne particles (both in terms of number and mass concentrations) were generally detected in Cassino likely due to the frequent temperature inversion phenomena in colder seasons [60, 133, 141, 253, 254].

The experimental analyses involved 39 primary schools in Barcelona covering roughly the cold and warm seasons (two experimental campaigns: from January 27th to June 22nd, 2012 and from September 14th, 2012 to February 22nd, 2013; [83]) and 3 schools in Cassino during wintertime (January, February and December 2011). All the schools under investigation were naturally ventilated buildings equipped with radiator heating systems (thus the typical air exchange rate is roughly equal to 0.1-0.2 h^{-1} as recognized by Stabile, et al. [91]). Measurements were performed simultaneously at different spatial scales: i) in classrooms (during school-time) to measure indoor air quality; ii) at school playgrounds as a proxy for outdoor air quality; iii) at background reference stations to measure the urban background concentrations of the two cities. In particular the background stations were located a) in the garden of the Instituto de Diagnóstico Ambiental y Estudios del Agua - CSIC (IDAEA-CISC) building in “Palau Reial” of Barcelona and b) on the rooftop of the University of Cassino and Southern Lazio for Cassino.

Indoor instruments were positioned on a shelf at a height between 0.7 to 1.5 m above the floor level to represent the height of pupils’ breathing zone. In order to avoid direct

exposure to chalk or blackboard emissions, the instruments were placed next to the wall, opposite from the blackboard, and away from the windows.

Particle number concentration, lung-deposited surface area (i.e. sum of particle surface area concentrations deposited in the alveolar and tracheobronchial regions of the lungs) and PM mass concentrations were monitored both in classrooms and school playgrounds. Similarly, PM samples were collected at school playgrounds of all the schools and in the classrooms in the 39 schools in Barcelona (no PM samples were collected in the three Italian schools). PM samples were then analysed to obtain the mass concentrations of Arsenic (As), Cadmium (Cd) and Nickel (Ni) and Polycyclic Aromatic Hydrocarbons (PAH), expressed as a Benzo-a-Pyrene (BaP).

6.1.2 Experimental apparatus and methodology

6.1.2.1 Experimental analysis in Barcelona

The following instruments were used in the experimental campaign performed in Barcelona (**Table 16**):

- 2 diffusion charger particle counters (DiscMini, Matter Aerosol AG), which are compact hand-held particle counters based on diffusion charging technique able to measure particle number concentration, average particle size, and lung-deposited surface area concentrations (sum of alveolar- and tracheobronchial-deposited particle surface area concentration, i.e. S_{Alv} and S_{TB}, respectively) in the 10-700 nm particle size range with 1-s sampling time [162, 163, 255];
- 2 hand-held laser photometers DustTrak™ DRX Aerosol Monitors (Model 8534, TSI Incorporated) to measure PM_1, $PM_{2.5}$, and PM_{10} on the basis of the light scattering technique with 1-s sampling time;

The DustTrak photometers were calibrated, in terms of $PM_{2.5}$, by comparison with the gravimetric method (which represents the reference method for particle mass concentration measurements [59, 256-258]) at the beginning of experimental campaigns. Similarly, the DiscMinis were compared and corrected by correlation to a DiSCmini of reference to minimize any measurement differences (prior and post each sampling campaign). Further details on the instrument calibration and data quality

assurance regarding the experimental campaign performed in Barcelona are reported in our previous paper [255].

39 schools in Barcelona were monitored during the school-time (from 9:00 to 17:00). The measurements were performed for four days on each of the sampling campaigns (from Monday morning to Friday morning).

Indoor and outdoor PM_1, $PM_{2.5}$, and PM_{10} concentrations were monitored in the 39 schools of Barcelona through two DustTrak photometers. Simultaneous school-time $PM_{2.5}$ samplings for post-hoc chemical analyses were performed daily in indoor and outdoor through the gravimetric technique (high-volume sampler MCV CAV-A/mb with a specific nozzle for $PM_{2.5}$). In particular, Pallflex quartz fibre filters (PALL 2500 QAT-UP 150 mm) were used to collected $PM_{2.5}$ samples; consequently, such samples underwent a complete chemical characterization on the basis of the methodology and data processing described by [259].

Indoor and outdoor school-time PNC, Dp, and LDSA concentrations were measured by the two DiscMinis in the 39 schools of Barcelona.

Simultaneous measurements of particle number concentrations at urban background were performed through the water-based condensation particle counter CPC 3785 TSI (minimum detectable particle equal to 5 nm).

6.1.2.2 Experimental analysis in Cassino

The following instruments were used in the experimental campaign performed in Cassino (Table 16):

- a butanol-based Condensation Particle Counters (CPC 3775, TSI Inc.) to monitor total particle number concentration down to 4 nm with 1-s sampling time;
- a Scanning Mobility Particle Sizer (SMPS 3936, TSI Inc.), made of a further CPC 3775 and an Electrostatic Classifier (EC 3080 TSI), to measure particle number distributions in the range of 15-700 nm with a 64-channel per decade size resolution and used with a 180-s time resolution in the present experimental analysis;

- a water-based condensation particle counter CPC 3785 TSI able to measure the total particle number concentration down to 5 nm in particle diameter with 1-s sampling time;
- a sampler Zambelli 6000 Plus to collect PM_{10} through the gravimetric method [260] at a fixed flow rate of 2.3 m^3 h^{-1} .

Three schools were monitored in Cassino during the school-time (08.30 am to 01.30 pm for two schools and 08.30 am to 04.30 pm for another one); each school was monitored for two weeks.

Outdoor school-time PM_{10} samples were collected daily through the gravimetric method (gravimetric sampler Zambelli 6000 plus). Such samples underwent a chemical characterization through the nuclear not-destructive technique Instrumental Neutron Activation Analysis (INAA) for the inorganic composition analysis (more details are reported in [121, 261, 262]), whereas the organic composition was performed through the gas chromatography–mass spectrometry methodology already applied and described in [263] and [264]. No PM samples in indoors were collected.

School-time particle number concentrations and distributions in outdoor were measured through the SMPS 3936, whereas school-time indoor particle number concentrations were measured through the CPC 3775. On the basis of the outdoor particle number distribution data, surface area distributions were estimated considering spherical particles. Thus, alveolar- and tracheobronchial-deposited surface area concentrations in outdoor were evaluated on the basis of the dosimetry model developed by the [136] considering the fractional deposition for children (normal nose breathers) performing sitting activities. In indoor the same procedure to estimate the lung-deposited surface area concentrations was adopted: in particular, since no sub-micron particle indoor sources were present in the investigated classroom [91, 114, 115, 147, 265-267], the same particle number distribution measured in outdoor was applied and normalized to the indoor particle number concentration measured through the CPC placed in the classrooms. The authors highlight that this approach could be considered a limitation of the study since the particle penetration is size-dependent and, thus, the indoor particle size distributions could be slightly modified. Measurements of particle number concentrations at the background site were

performed through a condensation particle counter CPC 3775 TSI. The CPCs and the SMPS were also calibrated in the European Accredited Laboratory at the University of Cassino and Southern Lazio by comparison with a TSI 3068B Aerosol Electrometer, using NaCl particles generated through a Submicrometer Aerosol Generator (TSI 3940): details on the experimental analysis and calibration procedures are reported in [104, 121].

Table 16 *Scheme of the instrumentation used at the different sampling sites during the experimental campaigns performed in Barcelona and Cassino.*

City	Particle metrics	Sampling sites		
		School Indoor	School Outdoor	Urban background
Barcelona	Number concentration	DiscMini (Matter Aerosol)	DiscMini (Matter Aerosol)	CPC 3785 TSI
	Lung-deposited surface area concentration	DiscMini (Matter Aerosol)	DiscMini (Matter Aerosol)	-
	Online PM_1, $PM_{2.5}$, PM_{10}	DustTrak™ DRX 8533	DustTrak™ DRX 8533	Grimm model 180
	Gravimetric $PM_{2.5}$	high-volume sampler MCV CAV-A/mb (30 m^3 h^{-1})	high-volume sampler MCV CAV-A/mb (30 m^3 h^{-1})	high-volume sampler MCV CAV-A/mb (30 m^3 h^{-1})
Cassino	Number concentration	CPC 3775 TSI	SMPS 3936 TSI	CPC 3775 TSI
	Gravimetric PM_{10}	-	Sampler Zambelli 6000 (2.3 m^3 h^{-1})	-

6.1.3 Data post-processing

In order to obtain particle number, PM_{10} and chemical compound concentrations representative of the whole school year (then not limited to the sampling periods) the annual weighted average for each pollutant was evaluated. To this end a seasonal adjustment of the daily values measured at school was conducted on the basis of the approach applied by [83] and [268]. In particular, a back-extrapolation in time was performed considering the annual trend of such pollutants continuously measured at fixed sampling sites. As an example, long-term pollutant levels at school in Barcelona, both in indoor and outdoor, were obtained by "deseasonalization" of the one-week data measured at school on the basis of annual trend of the pollutant concentrations measured at the urban monitoring stations (placed in Eixampl, Gracia-SantGervasi and

Placa Universitat). In particular, data measured at schools were multiplied by the ratio between the average concentration measured on that day at the three fixed air quality urban background monitoring stations and the annual average background value of such pollutant at urban background. The same procedure was applied for Cassino, here the deseasonalization was performed on the basis of the abovementioned particle concentrations measured at the background site, whereas PM_{10} and chemical compound background values were obtained from the regional Agency for Environmental Protection (ARPA Lazio, available at arpalazio.net).

6.1.4 Evaluation of the daily dose and excess lifetime cancer risk received by students

Particle surface area doses received in the tracheobronchial and alveolar regions of the lungs by pupils attending lessons indoors in a typical school day (here considered of 8 h [269]) were calculated on the basis of the median exposure data of lung deposited surface area concentrations and time activity patterns. In particular, the median surface area dose (δ_{Alv+TB}) is expressed as the sum of alveolar and tracheobronchial contributions and was obtained using the lung-deposited surface area time-series measured through the DiSCmini in Barcelona and the estimated through the particle distribution measured in Cassino [137]:

$$\boldsymbol{\delta_{Alv+TB} = IR_{activity} \cdot S_{Alv+TB} \cdot T} \quad (8)$$

where $IR_{activity}$ ($m^3\ h^{-1}$) is the inhalation rate (which depends on children age and activity, in this study an IR of 0.42 $m^3\ h^{-1}$ was considered as characteristics of pupils aged 6-10 years performing a sedentary activity, i.e. studying), T is the time spent on the activity (the school-time, in this case 8 h), S_{Alv+TB} is the sum of alveolar- and tracheobronchial-deposited particle surface area concentrations (S_{Alv} and S_{TB}, respectively). The authors point out that the calculation of the dose and risk received by the children was performed considering the break periods as they were spent in the classrooms.

To evaluate the pupil's median excess lifetime cancer risk (ELCR) for the 5-year primary school period (please note that primary school period for Spanish children is 6 years but here the first 5 years were considered to perform a proper comparison with Italian schools), the risk assessment model carried out by [57] was used. This model considers the lung cancer effect due to both sub-micron particles, expressed in terms

of median particle surface area dose (δ_{Alv+TB}, $nm^2\ day^{-1}$), and super-micron particles, expressed as median PM_{10} dose (δ_{PM10}, $mg\ day^{-1}$). In fact, a coefficient (named c_f) to correlate the particle surface area-based cancer potency of the chemical to the mass-based cancer potency of the chemical was evaluated by Sze-To, et al. [57] as equal to 6.60×10^{-13} $mg\ nm^2$. The median particle surface area dose (δ_{Alv+TB}) is calculated as reported in eq. (8), whereas the median PM_{10} dose (δ_{PM10}) was evaluated by multiplying the median PM_{10} concentration during school-time by the typical particle deposition fraction for super-micron particles (here a deposition fraction equal to 0.2 was considered), by the IR (0.42 $m^3\ h^{-1}$), and by the exposure time T. The overall excess lifetime cancer risk due to the *i* pollutant and for 5 years of exposure was expressed as [270]:

$$\boldsymbol{ELCR_{5\ years}} = \sum_i \left[\sum_{y=1}^{5} \frac{\boldsymbol{SF_i}}{\boldsymbol{BW_y}} \cdot \left(\frac{\boldsymbol{m_{i\_out}}}{\boldsymbol{PM_{out}}} \cdot \boldsymbol{c_f} \cdot \boldsymbol{\delta_{Alv+TB}} + \frac{\boldsymbol{m_{i\_in}}}{\boldsymbol{PM_{in}}} \boldsymbol{\delta_{PM_{10}}} \right) \right] \cdot \frac{\boldsymbol{ST}}{\boldsymbol{70}} \quad (9)$$

where:

- SF_i ($kg\ d\ mg^{-1}$) is the inhalation cancer slope factor used to describe the cancer potency of the *i*-th pollutant and obtained from the Office of Environmental Health Hazard Assessment [271] equal to 1.51×10^{1}, 6.30×10^{0}, 9.10×10^{-1} and 3.90×10^{0} $kg\ d\ mg^{-1}$ for As, Cd, Ni and BaP, respectively;
- BW_y is the body weight of the *y*-th year for 6-10 aged pupils obtained from Zoppi, et al. [272] as function of the students' gender and in the range 22-33 kg and 21-34 kg for male and female, respectively (please note that different weights were used since median ELCR values for males and females were calculated separately);
- m_i/PM is the median mass concentration of each pollutant condensed on $PM_{2.5}$ (in Barcelona) or PM_{10} (in Cassino);
- *ST* is the ratio between the school days and total days of the year (in this case roughly 200/365).

The term $SF_i\times m_i/PM$ is known as slope factor of the mixture of the *n* carcinogenic pollutants on PM and will be hereinafter reported as SF_m. Since no major indoor sources of sub-micron particles were present in the classrooms, the resulting concentrations of number and surface area metrics measured in indoors for naturally

ventilated buildings were mostly due to the abovementioned penetration from outdoors [113]. Therefore, the chemical composition of sub-micron particles in indoor is the same of the outdoor ones. Thus, to evaluate the toxicity of sub-micron particles inhaled in schools the same chemical composition of the outdoor ones was adopted: to this end the particle surface area dose received in indoor was multiplied by the outdoor mass fraction of chemical compounds (m_{i_out}/PM_{out}). On the contrary, super-micron particles in indoors (mostly contributing to PM metrics) are generated by indoor sources too (e.g. chalk emission, resuspension of dust carried inside from outdoors), thus the chemical composition (and then the toxicity) of indoor PM is different from the outdoor one [83, 91, 100, 114, 115, 147, 265, 273]. For this reason, the PM_{10} dose received in indoor was multiplied by the indoor mass fraction of chemical compounds (m_{i_in}/PM_{in}).

The authors point out that, since most of the indoor PM sources are related to mechanical processes (e.g. resuspension) their contribution is more related to coarse particle range ($PM_{2.5-10}$) than the $PM_{2.5}$ fraction [273]. Nonetheless, the chemical analyses for schools in Barcelona were performed on $PM_{2.5}$ samples, then not including the $PM_{2.5-10}$ fraction: this could lead to a possible underestimation of the indoor-generated PM toxicity. However, the possible underestimation of the ELCR value is expected to be negligible since such indoor mass fractions are multiplied by the PM_{10} dose contribution which is generally unimportant with respect to the surface area dose contribution [169, 270]. Similarly, as regard the Cassino case-study, the contribution of the PM_{10} dose was neglected since no indoor PM data were available and the contribution of the surface area dose solely was considered in ELCR evaluation for students in Cassino. Nonetheless, as hereinafter reported, the underestimation of the ELCR when the PM_{10} dose contribution is not included was considered negligible.

6.2 Results and discussion

6.2.1 Exposure in schools

In **Figure 16** statistics of the particle concentrations measured inside and outside the 39 schools investigated in Barcelona are reported. In particular, data of the different airborne particle metrics are shown: particle number, lung-deposited surface area (expressed as the sum of alveolar and tracheobronchial contributions, S_{Alv+TB}), and PM fraction (PM_1, $PM_{2.5}$, and PM_{10}) concentrations [274].

Median particle number concentrations measured outdoor ranged roughly between 1×10^4 to 4×10^4 #· cm^{-3} (median value of 1.96×10^4 #·cm^{-3}): such variability was mainly due to the location of the schools; indeed, higher values were detected in schools flanking densely-trafficked main streets of the city. Particle number concentrations at outdoor school sites were higher than the simultaneous median concentration at the urban background station (1.32×10^4 #·cm^{-3}). Major details concerning the effect of the school localization on measured outdoor concentrations are reported in [83]. As expected, indoor concentrations resulted lower than outdoor ones (median value of 1.35×10^4 #·cm^{-3}) with a median outdoor-to-indoor penetration ratio (N_{in}/N_{out}) equal to 0.7 which is within the typical values reported for naturally ventilated buildings [91, 94, 115, 265, 275, 276]. Such lower indoor concentrations are due to the lack of sub-micron particle sources in classrooms, therefore indoor concentrations are mostly due to the outdoor-to-indoor penetration of particles produced in urban area.

A similar behavior was recognized in terms of lung-deposited surface area concentrations (**Figure 16**b), with median values equal to 41.2 and 33.7 μm^2 cm^{-3} measured outdoors and indoors, respectively. Both number and lung-deposited surface area metrics are governed by sub-micron particle dynamics, and this is the reason why analogous statistics were measured for the two metrics.

As regard the schools investigated in Cassino, median outdoor and indoor concentrations in terms of PNC /LDSA resulted equal to 1.96×10^4 #·cm^{-3}/111 μm^2 cm^{-3} and 1.60×10^4 #·cm^{-3}/90 μm^2 cm^{-3}, respectively, with a resulting median N_{in}/N_{out} ratio similar to that measured in Barcelona (0.8). The higher concentrations measured in Cassino agree with the data reported in previous papers [60, 133].

From the statistics of indoor and outdoor PM_1, $PM_{2.5}$, and PM_{10} concentrations of the 39 schools in Barcelona (**Figure 16**c) the different behavior of super-micron particles, with respect to the sub-micron, was highlighted. Median values of indoor and outdoor PM_{10} concentrations were equal to 60.7 $\mu g/m^3$ and 50.1 $\mu g/m^3$, respectively. Indoor concentrations were higher than outdoor ones due to the presence of indoor sources of super-micron particles (e.g. chalk and particle resuspension due to students' movements [83, 273, 277]. This is not a novel aspect, since, differently from sub-micron particles, PM_{10} data in schools from several studies reported indoor-to-outdoor PM_{10} ratios (here equal to 1.2) larger than one [115, 278-280]. As an example [115] showed that, differently from gases produced in indoors (e.g. CO_2), the sudden mass-based particle emissions in classrooms cannot be easily diluted even when longer airing periods are adopted. Nonetheless, the data reported in **Figure 16**c revealed that for PM_1 and $PM_{2.5}$ indoor and outdoor concentrations were quite similar (PM_{1_in}/PM_{1_out}=0.9; $PM_{2.5\_in}/PM_{2.5\_out}$=1.0), demonstrating that the higher indoor PM_{10} concentration is due to mechanical processes mainly affecting the coarse particle fraction (i.e. $PM_{2.5-10}$). In any case, it is interesting to note that [83] and [273] demonstrated that the continuous mechanical grinding of playground sand yielded to unusually high concentrations of mineral dust in the $PM_{2.5}$ fraction. This accounted for extremely high levels of $PM_{2.5}$ in both indoor and playgrounds, near doubling the typical $PM_{2.5}$ urban background concentrations of Barcelona. As regards the PM_{10} data measured in outdoor in Cassino, values larger than those measured in Barcelona were recognized: this is in agreement with the typical high PM_{10} outdoor concentrations measured in that area [141].

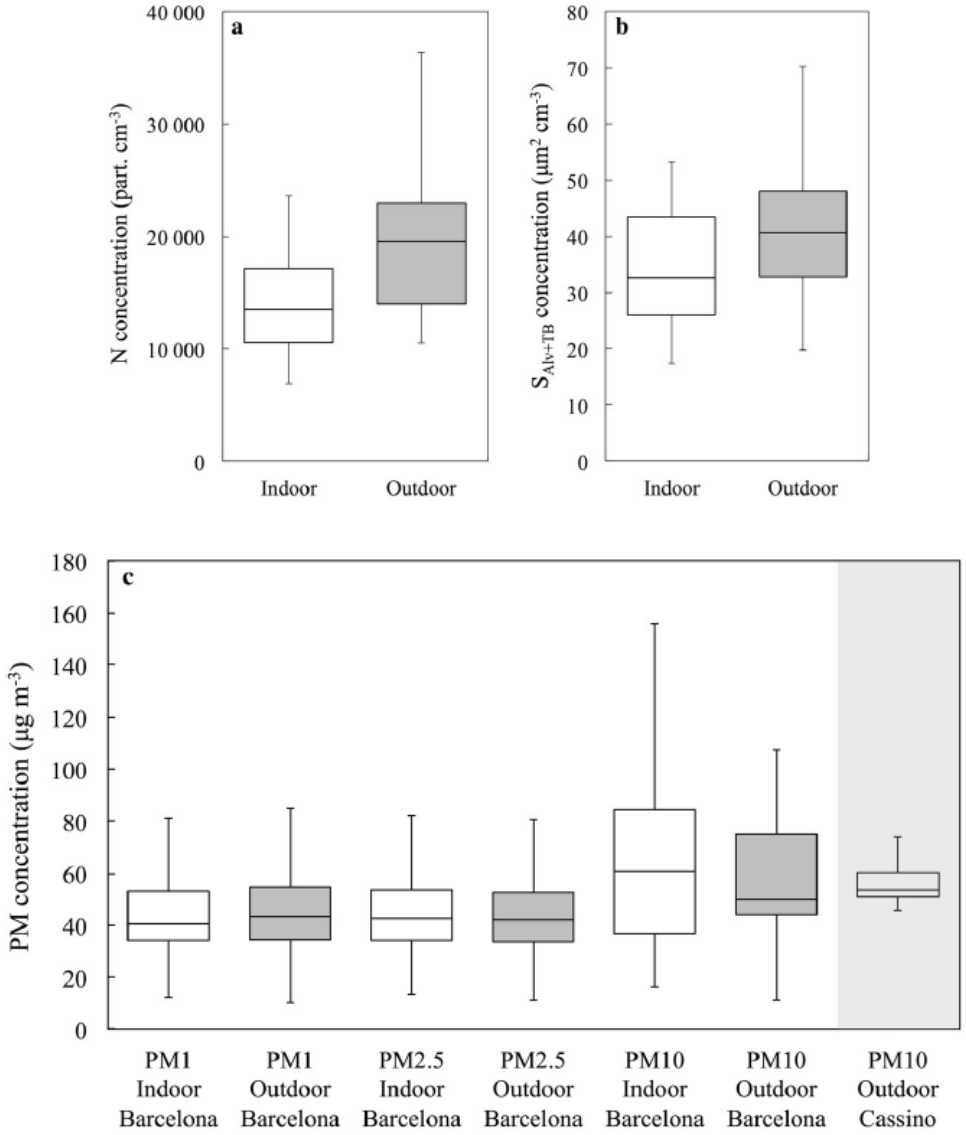

Figure 16 *Statistics of indoor and outdoor airborne particle concentrations measured in the schools of Barcelona and Cassino in terms of a) number (Barcelona), b) lung-deposited surface area (Barcelona), and c) PM fraction concentrations (Barcelona and Cassino). Box-plots report 5th and 95th percentiles, 1st (Q_1) and 3rd (Q_3) quartiles, mean and median value.*

6.2.2 Chemical characterization

Concentrations of toxic compounds in PM sampled in outdoor and indoor school environments in both the cities are reported in **Table 17**. Data clearly show the higher outdoor concentrations of PAH (expressed as equivalent BaP) measured in Cassino (0.71 ng·m^{-3}) with respect to Barcelona (0.09 ng·m^{-3}): such higher concentrations in Cassino are likely due to the combustion of biomass for residential heating purpose

typically used during wintertime in the region [141]. Larger outdoor concentrations of Cd were also measured in Cassino with respect to Barcelona as it is also a tracer of biomass combustion processes [281]. On the contrary, higher As and Ni outdoor concentrations were measured in Barcelona due to the larger anthropogenic emissions (mainly industrial; [179, 273]). Indoor concentrations of As, Cd and Ni in Barcelona resulted lower than the outdoor ones, confirming the different chemical composition of particles present indoors. Once again, the authors highlight that such difference in As, Cd and Ni concentrations between indoor and outdoor sites could be underestimated since the chemical analysis in Barcelona was performed on $PM_{2.5}$ samples then not including the coarse particle fraction, although Amato et al. (2009) reported that in Barcelona most of these elements occur in the $PM_{2.5}$ fraction.

In **Table 18** median values of mass fractions of carcinogenic compounds on PM measured at the outdoor and indoor sampling sites of the schools investigated are reported. As regard the schools placed in Barcelona higher mass fractions were measured in outdoors then resulting in a higher slope factor of the mixture with respect to the indoor one (SF_m, **Table 18**). The larger contribution to the SF_m both at indoor and outdoor sites in Barcelona is due to As (>60%) and Ni (>20%) which represent typical markers of the anthropogenic emissions. At outdoor sampling sites in Cassino the median mass fractions resulted in a larger SF_m than Barcelona one. In Cassino the larger contribution to the SF_m was linked to Cd (>50%), and a not negligible influence of BaP (>10%) was also recognized as an effect of the biomass combustion during the heating period. The SF_m values for both Barcelona and Cassino resulted higher than those measured by Sze-To, et al. [57] for cooking-generated particulate matter but lower than the incinerator plant [282] and cigarette ones [139].

Table 17 *Median As, Cd, Ni and BaP annual concentration measured at the outdoor and indoor sampling sites of the schools investigated.*

City and sampling location	As ($ng \cdot m^{-3}$)	Cd ($ng \cdot m^{-3}$)	Ni ($ng \cdot m^{-3}$)	BaP ($ng \cdot m^{-3}$)
Barcelona outdoor	0.54	0.19	3.56	0.09
Barcelona indoor	0.48	0.16	2.74	0.10
Cassino outdoor	0.17	1.69	1.75	0.71

Table 18 *Median mass fractions of carcinogenic compounds on PM (expressed as ppm) measured at the outdoor and indoor sampling sites of the schools investigated and corresponding SF of the mixture (SF_m). Mass fractions were referred to $PM_{2.5}$ and PM_{10} for samples collected in Barcelona and Cassino, respectively.*

City and sampling site	m_{As}/PM (ppm)	m_{Cd}/PM (ppm)	m_{Ni}/PM (ppm)	m_{BaP}/PM (ppm)	SF_m	Contribution to the SF_m
Barcelona outdoor	10.7	3.76	71.1	1.72	2.57×10^{-4}	As=63%, Cd=9%, Ni=25%, BaP= 3%
Barcelona indoor	7.92	2.65	45.2	1.60	1.84×10^{-4}	As=65%, Cd=9%, Ni=22%, BaP= 3%
Cassino outdoor	3.22	31.5	32.5	13.2	3.08×10^{-4}	As=18%, Cd=54%, Ni=15%, BaP=12%

6.2.3 Dose and risk received by students

In ***Figure 17*** statistics of the dose received by students in classrooms in Barcelona during the school-time (8 h) are reported in terms of particle surface area. As mentioned above, the dose values represent the sum of alveolar and tracheobronchial contributions (δ_{Alv+Tb}). Dose received varied in a wide range due to the wide exposure data variability (as an effect of school location and road traffic). In particular, the dose received by students in Barcelona ranged between 58.4 mm^2 and 179 mm^2, with a median value of 110 mm^2, whereas in Cassino the median dose received in 8 h was 303 mm^2, i.e. almost three-fold with respect to that received in Barcelona. Such dose experienced in Cassino is quite high considering that no indoor sub-micron particle sources are in operation in such classrooms: indeed, as a comparison, this value is not much lower than the overall daily dose received by the population living in Barcelona and Cassino (roughly 600 mm^2 and 1000 mm^2 respectively, [283]), and still larger than those received in offices by people exposed to of about one hour of laser and 3D printing activities [145, 146].

In **Table 19** the ELCR data for primary school students (6-10 years old) in Barcelona and Cassino are reported. The median overall risk due to the five-year exposure ($ELCR_{5\ years}$) for male and female students in Barcelona resulted equal to 2.88×10^{-5} and 2.94×10^{-5}, respectively. The slight difference in risk received by males and females is merely due to the different body weight values [272] since the same inhalation rates and deposition fractions were considered as obtained from the

International Commission on Radiological Protection [136]. Such ELCR values corresponding to the 5-year primary school exposure is comparable to the maximum tolerable ELCR, 1×10^{-5} according to the U.S. Environmental Protection Agency [284] risk assessment. Five-year median ELCR values received by primary-school students in Cassino resulted about one order of magnitude higher than Barcelona ones (1.35×10^{-4} and 1.38×10^{-4} for males and females, respectively). This is due to both (a) higher particle toxicity (SF_m higher than that measured in Barcelona, **Table 18**) and (b) larger dose (median surface area dose in Cassino almost more than three-fold compared to that experienced in Barcelona). The higher toxicity of the particles inhaled in Cassino is mainly due to the significant influence of the biomass burning phenomena in cold season, whereas the larger dose can be ascribed to the high concentrations measured, in particular, during the thermal inversion periods [60, 133]. The authors point out that the ELCR received during the five-year primary school period is two orders of magnitude lower than the lifetime risk of typical Italian population (roughly 2×10^{-2} [169, 270]). ELCR data reported in **Table 19** clearly confirmed the negligible contribution to the risk of the super-micron particles (i.e. $PM_{2.5\text{-}10}$) for students in Barcelona (about three orders of magnitude lower than the surface area contribution). These data confirm that it is reasonable to consider negligible the abovementioned unaccounted different mass fraction due to the indoor-generated coarse particles in Barcelona as well as the possible underestimation of the ELCR for students in Cassino addressable to the lack of PM_{10} dose data. Concerning the contribution of the different chemical compounds to the risk (**Table 18**), the higher contribution is due to As in Barcelona (causing an ELCR of about 2×10^{-5} on 5-year basis) and Cd in Cassino (providing an ELCR of about 1.3×10^{-4} on 5-year basis).

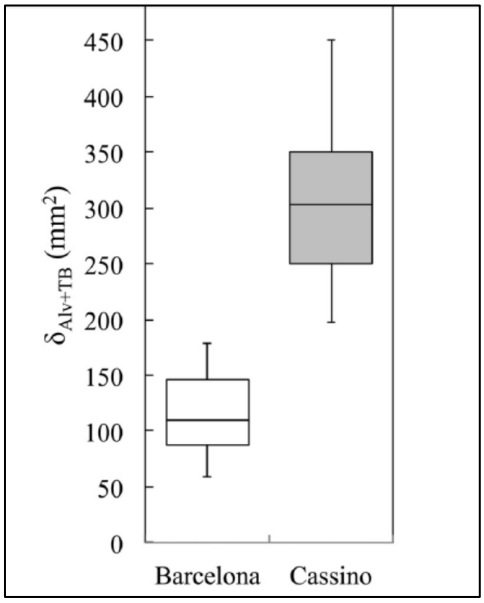

Figure 17 *Statistics of the total particle surface area doses received by students in classroom in Barcelona and Cassino during school time. Box-plots report 5th and 95th percentiles, 1st (Q_1) and 3rd (Q_3) quartiles, mean and median value of the δAlv+Tb.*

Table 19 *Median ELCR values of the primary school students in Barcelona and Cassino for the five-year primary school period (ELCR5 years) and contribution of the different metrics (surface area, S_{Alv+TB}, and PM_{10}).*

City	Gender	$ELCR_{5\ years}$	$ELCR_{5\ years}$ (S_{Alv+Tb})	$ELCR_{5\ years}$ (PM_{10})
Barcelona	male	2.88×10^{-5}	2.88×10^{-5}	2.69×10^{-8}
	female	2.94×10^{-5}	2.94×10^{-5}	2.74×10^{-8}
Cassino	male	1.35×10^{-4}	1.35×10^{-4}	-
	female	1.38×10^{-4}	1.38×10^{-4}	-

7 REAL-WORLD EFFECTIVENESS OF COMMERCIAL FACE MASKS TO REDUCE PERSONAL PM EXPOSURE

As already said commuters may be exposed to higher airborne particle concentrations due to their proximity to vehicle emission. Cyclists and pedestrians are among the categories of travellers most at risk of encountering adverse health effect related to high exposure to traffic pollution, due not only to the proximity of the springs but also to the high rate of breath. In fact, some study found a mean (standard deviation) value of real-word breathing rate for cyclist equal to 59.1(13.7) $L \cdot min^{-1}$ and 46.2 (10.6) $L \cdot min^{-1}$ for man and woman respectively [132]. To try to protect them self from the exposure to airborne particles people started to use personal protectors as face masks. Cloth face masks come with an elastic strap, which needs to be worn behind the head or over the ears to maintain an adequate fitting to the face, and they have a filter designed to reduce particle penetration into the breathing area. However, the effectiveness of such filters in reducing PM exposure will depend not only on the filter used but also on the tightness of the seal between the mask and the face of each individual. Therefore, two factors have to be introduced in order to describe the overall efficiency of respirators:

- Total Inward Leakage (TIL), which refers to the penetration directly through the respective filter [285]. In this context, it has been established that nanoparticles in the range 4-20nm are efficiently captured by respirator filters [286].
- Fit Factor (FF), which describes the penetration as leak around the filter and towards the breathing zone, has been introduced to express how good the fit of a respirator is on the face of a given individual during a certain use. The

protection offered by a face respirator has been found to be depended on the FF [287], while the FF itself could be influenced by a number of factors such as the type of user´s activity [288] and facial characteristics [289].

Some studies assessed the effectiveness of these face masks, as an example, Grinshpun, et al. [290] investigated the penetration of NaCl particles through the filter material of an N95 and surgical face mask, or Bowen [291] using saline particles have tested different type of RP as a pre-shaped dust mask, bandana, surgical mask or N95 mask. Other study by Rengasamy, et al. [292] through NIOSH method have compared the penetration from different household fabrics, commonly used during pandemic respiratory infections with N95 respirator material. Jung, et al. [293] compared masks and handkerchiefs generally used by people to protect them self against particulate air pollution from yellow sand, or Mueller, et al. [294] investigated the efficiency of several RP against volcano ash. None of these studies takes into account the efficiency of commercial face masks under a real exposure to urban outdoor aerosol neither looking at the effectiveness of face mask response to different metric as PM, LDSA, BC or PNC at the same time. In addition, they do not take into account the possible different response of face masks effectiveness under different breathing rates.

The present study aims to evaluate the real-world effectiveness of nine different low-cost face masks to reduce the level of exposure to the airborne particle in terms of particle mass concentration ($PM_{2.5}$), Particle Number Concentration (PNC), Lung Deposited Surface Area (LDSA) and Black Carbon concentrations (BC). Face mask performances were assessed in a typically traffic-affected urban background environment in the city of Barcelona under three different breathing patterns in order to investigate the influence of flowrate in face mask effectiveness.

7.1 Materials and Methods

In order to evaluate the effectiveness of each face mask in reducing exposure to airborne particles an experimental campaign was carried out in November 2017 at the urban background monitoring station of Palau Reial in Barcelona (Spain). The study analysed nine different face masks, all commercially available in a price range of ≈1€ to 44€ (low cost respirators) and commonly used by cyclists and pedestrians. Two

dummy heads were located outdoors (at the height of 1.60 m in order to replicate the cyclist and pedestrian exposure) during working hours, only one of them being fitted with a face mask. The mouth of each dummy head was fitted with an anti-electrostatic inlet tube and a splitter separating air flow into 4 channels, driving isokinetically airborne particles to:

- A DustTrak^{TM} DRX aerosol monitor (Model 8533, TSI incorporated) to measure PM2.5, based on the light scattering with an operating stream of 3 $L \cdot min^{-1}$;
- A diffusion charger counter (DiscMini, Matter Aerosol AG) able to measure PNC (# cm^{-3}), average particle size and Lung Deposited Surface Area concentration in the particle size range of 10-700 nm with an operating stream of 1 $L \cdot min^{-1}$;
- A micro-aethalometer model AE51 (Magee Scientific) for BC, which register the rate of change in absorption of transmitted light due to continuous collection of aerosol deposit on a filter, with an operating stream of 0.1 $L \cdot min^{-1}$. The filters were changed every 9 hours of sampling;
- A dry vacuum (BECKER VT 4.8 I) pump for adjusting the remaining flow. at different cyclist breathing rates (32, 42 and 52 $L \cdot min^{-1}$[131, 295]), to obtain a simulation of different breathing scenarios. Air flows were checked after each test.

In addition, we used another reference BC concentration as measured by a Multi Angle Absorption Photometer (MAAP, Thermo scientific) at the Palau Reial station, in the cases when the micro-aethalometer suffered technical issues.

All instruments were set to one-minute time resolution, except for the DiscMini (10 seconds). Prior to the sampling campaign, the devices were inter-compared and corrected by a linear regression fit in order to minimize any measuring differences between paired instruments. The correction factors were: PM2.5: cf=0.7557 R^2=0.47, PNC: cf=0.6963 R^2=0.79, LDSA: cf=0.6531 R^2=0.88, BC cf=0.9042 R^2=0.85. The entire set-up is shown in Figure 18.

Both dummy heads were made by paper-mache, and they represented an adult human's head. The dummy head cranial circumference is 61 cm with a size of 20x15x20 cm

(high x width x depth). Detailed information regarding the nine face masks studied are listed in **Table 20**. These respirators comprise a filter, that can be located in the whole face mask or just at a certain point (i.e. in dedicated valves). Eight of the nine face masks have an exhalation valve that allows air exit and obstructs air entry, the exception being MASK 3.

Table 20 *Face mask models, characteristics and filtration typology (based on info found on producers' websites march 2018), different filter layers information was obtained in laboratory.*

MASK	*PRICE €*	*CHARACTERISTICS*	*FILTRATION TYPOLOGY*	*DIFFERENT FILTER LAYERS*
1	44	Organic cotton, 2 exhalation valves	N99 filter layer, carbon filter	2
2	36	Neoprene, filter separated from the mask, 2 exhalation valves	Combination filter for chemical and particle filtration	2
3	28	Soft-Tech Material, 2 exhalation valves	Electrostatic filter	1
4	8	Exhalation valve	Filter FFP3	3
5	3	Exhalation valve	Filter FFP1	3
6	1	Not available	Not available	2
7	20	Soft material, filter separated from the mask, 2 exhalation valves	Active carbon filter	3
8	27	Washable technical mesh, filter separated from the mask, Exhalation valve	Electrostatic and active carbon filter, 1 valve	3
9	9	Fibber cloth, 2 exhalation valves	Non-woven fabric filter	2

Each test lasted 60 min and followed the same procedure: during the first 30 min both dummy heads were not wearing any mask. After 30 min from the start of the measurements, one of the dummy heads was fitted with a face mask, attempting the best possible fit for each respirator in order to avoid infiltration of air from the mask edges. A total of 27 tests (3 breathing rates for 9 different masks) were performed. In 5 cases the AE51, on the dummy head without face mask, had a poor correlation with the one located in the other dummy head, and for these cases the values of MAAP (sampling in the same location) were used in the data treatment instead. Details on the experimental campaign are reported in **Table 21**.

Table 21 *Details on experimental campaign*

Location	*Average Temperature (°C)*	*Average Humidity (%)*	*Period*	*Number of masks*	*Breathing Rate ($L \cdot min^{-1}$)*	*Number of tests*	*Duration of each test (min)*
IDAEA-CSIC Barcelona	17.5	55	November 2017	9	32, 42, 52	27	60

The effectiveness of each face mask was calculated as:

$$\boldsymbol{effectiveness} = (\mathbf{1} - \frac{\boldsymbol{H_M}}{\boldsymbol{H_{WM}}}) \times \mathbf{100} \quad (10)$$

where H_{WM} is the value measured without face mask, while H_M is the value measured with the face mask. In order to evaluate the real-world effectiveness of commercial face masks to reduce personal exposure, a campaign was carried out in an environment with an outdoor concentration levels in a range of (maximum - minimum) 25-5 μg m^{-3} for $PM_{2.5}$, 3.3×10^4 - 3×10^3 #· cm^{-3} for PNC, 73-5 μm^2 cm^{-3} for LDSA and 4.3-0.2 μg m^{-3} for BC.

The presented method used to evaluate the different respirators had two limitations:

The test considers breathing only as inhalation without the exhalation part. Since during exhalation a positive pressure is generated, the fit of the respirator might be compromised and unfiltered aerosol could enter in the breathing zone, this is especially true for respirators without exhalation valves. Due to the above an overestimation of the measured efficiency might have occurred.

The increased of the simulated breathing rate might have led to a tighter fit of the respirator, as the applied flow rate was increased. However, in reality intense exercise like cycling increase the frequency of inhalation and exhalations per time unit, as well as the intensity of those. Thus, in real conditions the fit of the mask might be compromised with intensive breathing, while high simulated breathing rates might lead to improved fitting and better filtration in some cases.

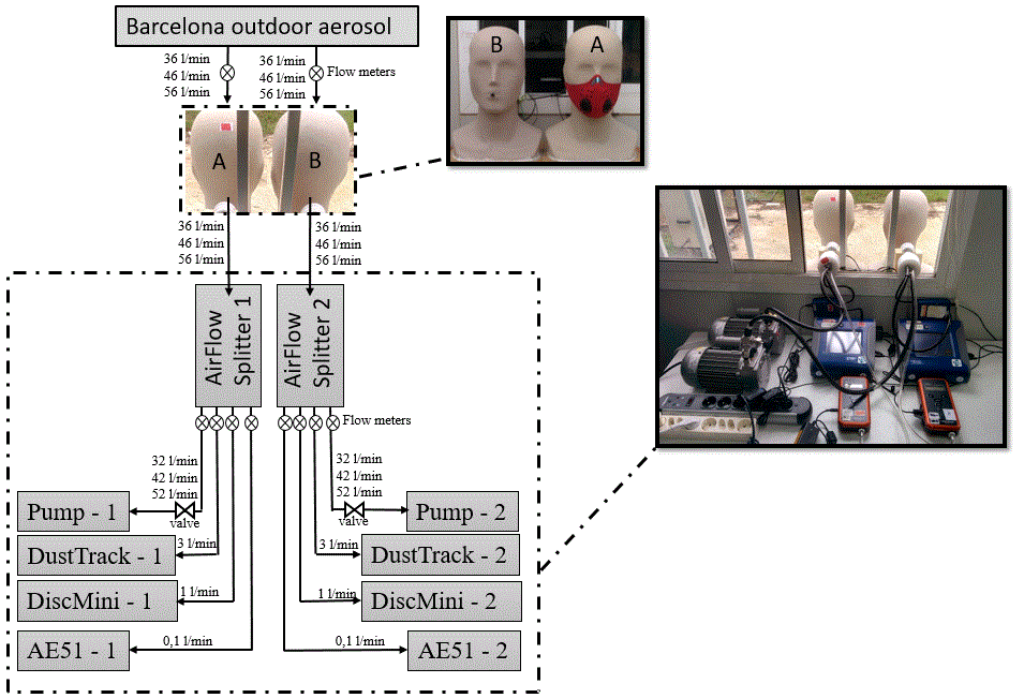

Figure 18 Scheme of measurement set-up.

7.2 Results

The data demonstrate that the effect of face mask application on pollutant exposure is immediate (**Figure 19**). The examples shown in **Figure 19** demonstrate measurements made with MASK 7 (at different breathing rates), which was the best performing mask for every metric ($PM_{2.5}$, PNC, LDSA, BC). At the beginning of each measurement, with both dummy heads (A and B) without masks, a similar concentration trend is measured by the two instruments. Once the face mask is applied to one of the dummy heads (A), concentrations continue to follow a similar trend but their levels are lower with respect to other dummy head (B). The same trend is recognisable for all metrics immediately after the application of the face mask.

In **Figure 20** the individual exposure reduction to airborne particles, in terms of $PM_{2.5}$, PNC, LDSA and BC for all the face masks under investigation is shown, merging the data for the three ventilation rates investigated. The highest individual exposure reduction to airborne particles concerns $PM_{2.5}$, with a median value of 43% although presenting a large variation between the different face masks from 14% to 96%. No cost-effectiveness relationship was found in this study, indicating that the price is not

an indicator of the mask efficiency, furthermore the cost seems to be more related to the esthetics of the mask than to the effectiveness. As an example, MASK 6 was not the mask with the lowest effectiveness but it was the cheapest and with a poor esthetic design. The effectiveness in terms of PNC and LDSA is equal to 19% and 22% (median value) respectively, and their variation is in a range of 4 to 70%. For BC the effectiveness of the mask is lower than LDSA, showing a 19 % median value with a range variation between 6% and 61%. For all metrics under investigation except for $PM_{2.5}$, the median value is always less than 30% and also the variation between minimum and maximum is very large, highlighting the importance in choosing the most efficient mask. Despite such large variation however, the results highlight that there is generally a good reduction in the range of super-micron particles whereas the ability of the masks used in this study to reduce individual exposure is lower for sub-micron and ultrafine particles.

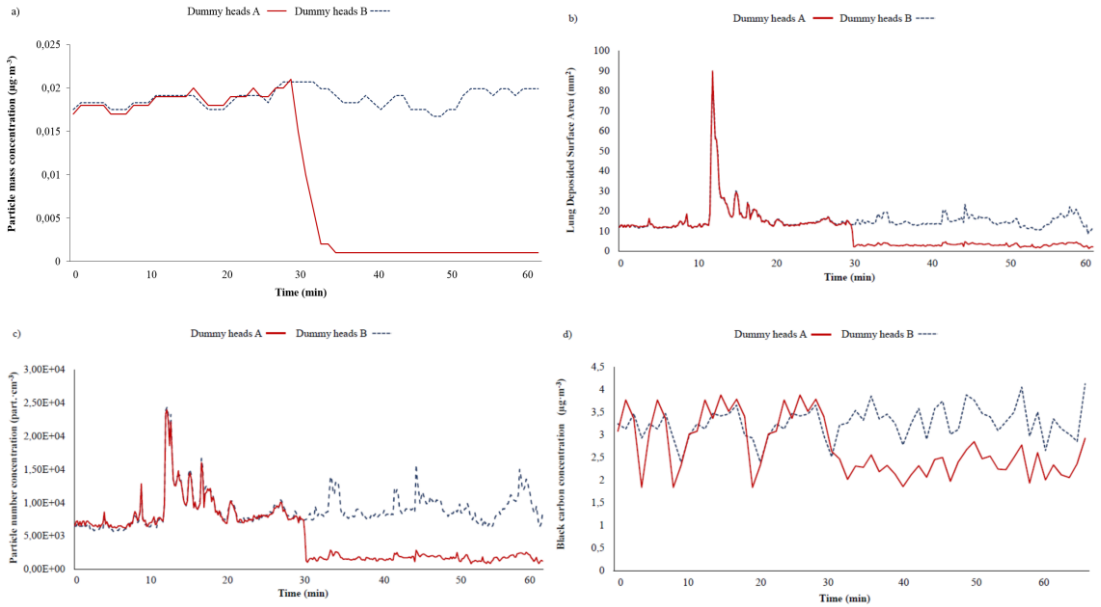

Figure 19 *Examples of sampling in terms of: a) particle mass concentration related to mask 7 at 52 L·min^{-1}; b) Lung Deposited Surface Area related to mask 7 at 32 L·min^{-1}, c) particle number concentration related to mask 7 at 32 L·min^{-1}; d) black carbon concentration related to mask 7 at 32 L·min^{-1}. In each example are shown both cases, with and without face mask (dummy head A and dummy head B).*

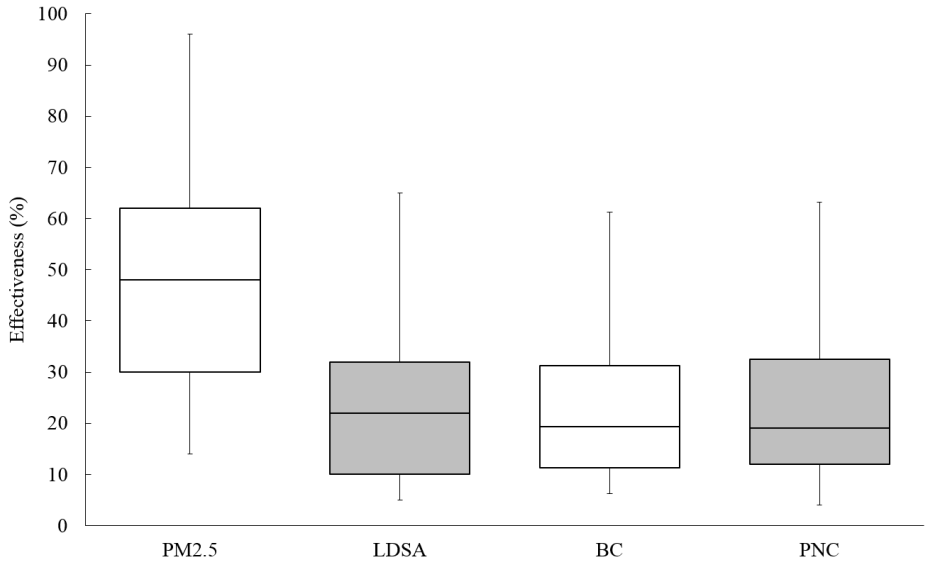

Figure 20 *Airborne particle reduction for the entire campaign for all face masks under investigation collected for different metrics express as a boxplot showing maximum, minimum and 75th, 50th and 25th percentiles.*

In **Table 22** the concentrations observed in both dummy heads for each face mask and breathing rates are shown. There is not a clear relationship between the change of breathing rate and the face mask effectiveness (**Table 22**). In **Figure 21** are shown the effectiveness of face masks for the three breathing rates take into account related to $PM_{2.5}$ that was the metric in which we found the best performance.

Four reduction trends are detectable overall depending which face mask is being evaluated: (i) effectiveness increases with breathing rates (mask 2 and 7 per $PM_{2.5,}$ mask 9 per PNC); (ii) effectiveness decreases with the increase of the breathing rate (masks 3,4,8 and 9 per $PM_{2.5}$, masks 1,3,4 per LDSA, mask 4 per BC and PNC); (iii) the lowest effectiveness was found with a breathing rate of 42 $L \cdot min^{-1}$ (masks 1,5 and 6 per $PM_{2.5}$, masks 5,6 and 9 per LDSA, mask 9 per BC and masks 3,5 and 6 per PNC); (iv) the highest effectiveness was found with a breathing rate of 42 $L \cdot min^{-1}$ (masks 2,7 and 8 per LDSA, mask 1 per BC and masks 1,2,7 and 8 per PNC). Such differences are due to the different type of construction material and the different types of filter used. In terms of $PM_{2.5}$, the ambient concentration average range variation in which face masks were tested was from 5 to 25 $\mu g \cdot m^{-3}$, and the mask with the highest effectiveness in terms of $PM_{2.5}$ was the MASK 7 with a value of 89%, while the lowest

value was found for MASK 3 equal to 35% (merging the data for the three types of breathing). In terms of PNC, the highest effectiveness was found for the MASK 7 as well as for the other metrics were always more than 80% (as average of the three breathing rates), while the lowest value in terms of PNC as well as for LDSA and BC concentration were related to the MASK 3 (for PNC =9%, LDSA =11% and BC =11%, values are shown as an average between the reduction values for the three breathings). These two masks (7 and 3) show differences in terms of material and filter: in MASK 7 the entire surface of the face mask has a filter except in the 2 exhalation valves where air cannot enter but just exit; the mask adheres well to the human face due to the washable technical mesh material. On the other hand, MASK 3 is made of a plastic soft material that does not adhere so well to the dummy head, and the filter is located only in the 2 valves that lead the entering and the exit of the air. Moreover, MASK 3 is the only mask under investigation without exhalation valve (details in **Table 20**). Interesting results are shown in **Table 22** concerning MASK 7, which was the mask with the highest effectiveness for all the pollutant take into account and also for three breathing rates. High effectiveness of MASK 7 may be due to the combination of different characteristics of this mask including (i) filter quality, as shown in **Figure 22** MASK 7 has three different filter layers which have three different textures; (ii) presence of the filter in the entire area of the masks (except in the exhalation valves); (iii) good adhering to the human face thanks to the mask coating material technical mash. The highest effectiveness for each breathing rate is related to $PM_{2.5}$ concentrations for all the masks.

Table 22 *Measured values (average ± standard deviation) of $PM_{2.5}$ ($\mu g \cdot m^{-3}$), PNC ($\#\cdot cm^{-3}$), LDSA ($\mu m^2 \cdot c\ m^{-3}$) and BC ($\mu g \cdot m^{-3}$) collected for the 9 different masks for each breathing rate BR ($L \cdot min^{-1}$) for both situations without and with face masks and face masks effectiveness E (%). C_A and C_B are concentration range measured in dummy heads A and B respectively for the related metrics.*

		$PM_{2.5}$			PNC			LDSA			BC		
Mask	***BR***	C_A	C_B	***E***	C_A	C_B	***E***	C_A	C_B	***E***	C_A	C_B	***E***
1	32	4.5±1.1 - 3.3±0.6	7.3±0.6 - 8.5±0.6	61	$6.3\times10^3\pm3.9\times10^3$- $2.81\times10^3\pm6.3\times10^2$	$6.9\times10^3\pm4.2\times10^3$- $2.96\times10^3\pm8.2\times10^2$	5	8±5 - 3.72±0.9	9.6±8.2 - 8.5±0.6	19	0. 4 ± 0.2 - 0.20 ± 0.09	0.4±0.3 - 0.24±0.11	19
	42	12±1 - 10±0.7	14±1 - 14±1.4	28	$9.4\times10^3\pm6.7\times10^3$- $7\times10^3\pm1\times10^3$	$9.4\times10^3\pm6.8\times10^3$- $8.4\times10^3\pm1.2\times10^3$	16	17±8 - 14±1.8	17±8 - 16±1.8	15	0.6 ± 0.2 - 0.4 ± 0.14	0.6 ± 0.3- 0.5±0.16	31
	52	5±0.6 - 3.7±0.4	7.3±1.5 - 12.8±1	71	$7.7\times10^3\pm2.8\times10^3$- $8.3\times10^3\pm3.5\times10^3$	$7.9\times10^3\pm3.3\times10^3$- $8.9\times10^3\pm4\times10^3$	7	12±3.7 - 12±5	12±4 - 13±5	5	NA 0.24±0.18	NA - 0.3±0.2	20
2	32*	13±2- 13±2	14±1- 16±3	21	$2.7\times10^4\pm4\times10^3$- $3.1\times10^4\pm6.6\times10^3$	$3.3\times10^4\pm5\times10^3$- $3.2\times10^4\pm9.6\times10^3$	4	58±8 - 66±11	73±9 - 70±17	7	3.4 ± 1.2 - 3.9 ± 1	4 ± 1.4 - 4.3±1.8	14
	42	11±0.5 - 9±0.3	13±0.4 - 14±0.5	37	$9\times10^3\pm4\times10^3$- $7.5\times10^3\pm1.6\times10^3$	$1\times10^4\pm4.4\times10^3$- $1\times10^4\pm2.2\times10^3$	26	20±5 - 15±2	22±6 - 20±3	25	NA	NA	NA
	52	3.2±0.4 - 2±1.3	2.9±0.4 - 6±2.2	61	$7.0\times10^3\pm1\times10^4$- $5\times10^3\pm1\times10^3$	$7.6\times10^3\pm1\times10^4$- $7\times10^3\pm1\times10^3$	25	9±13 - 7±2.6	9±13 - 9±3	24	1±0.3 - 0.9±0.1	3±1 - 1.2±0.9	31
3	32	3±0.5 - 3±0.7	6±0.4 - 6±0.9	52	$3.2\times10^3\pm3.6\times10^2$- $5\times10^3\pm5\times10^3$	$4.9\times10^3\pm4.3\times10^2$- $5.7\times10^3\pm6.7\times10^3$	14	5±0.8 - 6±5.3	5±0.8 - 8±7.6	22	NA	NA	NA
	42	9±0.5 - 9±0.7	11±0.5 - 12±0.6	27	$5.9\times10^3\pm6\times10^2$- $7.9\times10^3\pm2.4\times10^3$	$5.3\times10^3\pm6\times10^2$- $8\times10^3\pm3\times10^3$	4	11±1.3 - 14±3.3	11±1.3 - 15±3.9	6	0.3 ± 0.2 – 0.5±0.1	0.4±0.2- 0.6±0.3	18
	52	6±1 - 5±0.6	10±0.7 - 7±0.3	25	$9.6\times10^3\pm2.5\times10^3$- $8\times10^3\pm3.4\times10^3$	$9\times10^3\pm2.7\times10^3$- $8.7\times10^3\pm4\times10^3$	8	14±3 - 12.8±4.1	13.2±3 - 13.4±4.4	5	0.23±0.17 - 0.31±0.11	0.24±0.20 0.33±0.24	9
4	32	3±0.5 - 2.3±0.35	6±0.4 - 6±0.6	60	$1.1\times10^4\pm2\times10^3$- $6\times10^3\pm3\times10^3$	$1.2\times10^4\pm3\times10^3$- $7.5\times10^3\pm3\times10^3$	19	11±4 - 7±3	13±6 - 9±3	24	0.3 ± 0.1 – 0.3 ± 0.1	0.3 ± 0.1- 0.4±0.3	43
	42	7.5±0.8 - 11±6	11±0.4 - 15±5.4	28	$1.5\times10^4\pm4\times10^3$- $1.6\times10^4\pm3\times10^3$	$1.6\times10^4\pm4\times10^3$- $1.9\times10^4\pm3.6\times10^3$	17	23±5 - 25±8	24±5 - 29±10	15	0.4 ± 0.3 - 0.9 ± 0.1	1.± 0.3 1 ± 0.3	11
	52	6±1 - 5±0.6	11±0.7 - 7±0.3	25	$9.6\times10^3\pm2.5\times10^3$- $7.9\times10^3\pm3.4\times10^3$	$8.9\times10^3\pm2.7\times10^3$- $8.6\times10^3\pm4\times10^3$	8	14±3 - 12.8±4	13±3 - 13.4±4	5	0.2±0.1 - 0.31±0.1	0.2±0.2 - 0.33±0.1	9
5	32*	2±0.3 - 2±0	5±0.2 - 5±0.3	63	$8\times10^3\pm2.2\times10^3$- $6.2\times10^3\pm1.7\times10^3$	$9\times10^3\pm2.5\times10^3$- $9.3\times10^3\pm2.6\times10^3$	33	8.9±1.7 - 6±1.1	8.4±1.6 - 9±1.8	35	0.16 ± 0.13– 0.18 ± 0.09	0.15±0.2- 0.2±0.1	13
	42	15±3 - 5.6±0.4	17.7±2.4 - 11±0.4	48	$1.7\times10^4\pm2.9\times10^3$- $9.8\times10^3\pm1\times10^3$	$1.7\times10^4\pm3.2\times10^3$- $1.1\times10^4\pm2\times10^3$	11	34±7 - 15±1	35±7.2 - 17±3	11	NA	NA	NA
	52*	9.5±1.2 - 5.9±0.3	14±1.6 - 12±0.6	51	$6.9\times10^3\pm2.5\times10^3$- $5\times10^3\pm1.5\times10^3$	$7.5\times10^3\pm1.1\times10^3$- $7.8\times10^3\pm2.5\times10^3$	37	15.8±2.5 - 10±2	16.4±2.7 - 15±3	33	0.5±0.2 - 0.6±0.17	0.9±0.7 - 0.64±0.16	46
6	32*	2.65±0.5- 2±0.4	5.7±0.5 - 5.4±0.4	64	$1.1\times10^4\pm5.4\times10^3$- $5.1\times10^3\pm1.3\times10^3$	$1.3\times10^4\pm6.7\times10^3$- $8\times10^3\pm2\times10^3$	36	10±4.4 - 5±1	12±7.3 - 8±1.6	42	0.2 ± 0.12 - 0.15± 0.08	0.2±0.3 - 0.18±0.14	21
	42	12±5 - 16±0.8	15±4 - 19±1.5	14	$1.1\times10^4\pm5\times10^3$- $1.1\times10^4\pm1.5\times10^3$	$1.1\times10^4\pm5\times10^3$- $1.3\times10^4\pm1.7\times10^3$	13	20±7 - 25±3	22±8 - 27±3.3	9	NA	NA	NA
	52*	4.7±0.7 - 4±0	9.2±0.3 - 9.7±0.5	32	$7.7\times10^3\pm2\times10^3$- $7\times10^3\pm2\times10^3$	$7.4\times10^3\pm2\times10^3$- $9.7\times10^3\pm2.9\times10^3$	28	12.5±2 - 10±2	12±2 - 13±2.9	26	0.3±0.2 - 0.2±0.08	0.3±0.2 - 0.3±0.1	6
7	32	4.7±1.2 - 1.13±0.25	9.3±0.8 - 7.7±0.7	86	$6.3\times10^3\pm2.3\times10^3$- $1.3\times10^3\pm7.8\times10^2$	$7.1\times10^3\pm2.8\times10^3$- $7.2\times10^3\pm1.3\times10^3$	82	11±7 - 2±1.3	14±8 - 12±2	81	0.7± 0.2 - 0.7± 0.2	0.6 ± 0.3- 0.8±0.3	NA
	42	11.5±7 - 2±0.2	7.8±1.3 - 13±0.6	85	$7.3\times10^3\pm4.1\times10^3$- $7.9\times10^2\pm1.1\times10^3$	$7.8\times10^3\pm1.2\times10^3$- $7.5\times10^3\pm1.3\times10^3$	89	15±8 - 2±2	16±2 - 15±2	89	NA	NA	NA
	52	19±1 - 1±0.2	18±1 - 25±1.3	96	$8.9\times10^3\pm1\times10^3$- $1.7\times10^3\pm1\times10^3$	$8.9\times10^3\pm1\times10^3$- $1.1\times10^4\pm1.4\times10^3$	84	23±1.7 - 4±2.3	23±1.7 - 25±2.3	83	1.8±0.4 - 0.2±0.1	1.6±0.6 - 2±0.5	89
8	32	6.2±1 - 4.5±2	6.7±1 - 12.3±2	64	$9.4\times10^3\pm4.8\times10^3$- $6\times10^3\pm2\times10^3$	$8.9\times10^3\pm4.5\times10^3$- $7\times10^3\pm2\times10^3$	14	17±7 - 11±3	15±6 - 12±3	9	0.3 ± 0.3 - 0.57 ± 0.2	0.4 ± 0.3- 0.62±0.2	11
	42	12.6±0.7 - 8.8±0.5	15±0.7 - 14±1	38	$1\times10^4\pm3.7\times10^3$- $8.4\times10^3\pm3.4\times10^3$	$1\times10^4\pm3.7\times10^3$- $1.1\times10^4\pm4\times10^3$	22	21±6 - 18±6	21±6 - 22±6.4	20	NA	NA	NA
	52	13±0.5 - 8.7±3.9	15±1.1 - 14±9.4	36	$8.2\times10^3\pm2.3\times10^3$- $4.8\times10^3\pm3.2\times10^3$	$7.6\times10^3\pm1.4\times10^3$- $5.9\times10^3\pm3.9\times10^3$	19	19±4 - 12±7	18±3 - 14±9	19	0.8±0.3- 0.8±0.5	0.8±0.6 - 0.9±07	11
9	32	9.4±1.4 - 7.8±1.8	12±1.3 - 14±2.6	43	$2.35\times10^4\pm3.2\times10^3$- $1.94\times10^4\pm2.51\times10^3$	$2.64\times10^4\pm4.04\times10^3$- $2.61\times10^4\pm4.52\times10^3$	26	40±3 - 25±6.0	48±4.0 - 52±9.0	51	2.4 ± 1.2 – 2.1 ± 0.2	2.4±1.3 - 3±0.3	39
	42	9.5±0.6 - 8±0.4	13±0.5- 14±0.6	42	$8.73\times10^3\pm1.96\times10^3$- $6.40\times10^3\pm2.37\times10^3$	$9.35\times10^3\pm2.47\times10^3$- $9.37\times10^3\pm2.52\times10^3$	32	17±3.0 - 14±4	19±4.0 - 19±3	28	0.83 ± 0.5 - 0.59 ± 0.16	0.75±0.2- 0.74±0.1	25
	52	8.1±0.6 - 8±0.6	8±0.5 - 13±0.9	41	$7.45\times10^3\pm1.68\times10^3$- $6.30\times10^3\pm6.1\times10^2$	$4.92\times10^3\pm1.21\times10^3$- $1.02\times10^4\pm9.6\times10^2$	36	19±3 - 18±2	12±2 - 27±1.7	31	0.9±0.2 - 1±0.2	0.9±0.2- 1.3±0.4	28

Another aspect that should be taken into account, as Gao, et al. [296] demonstrated, is that the variation of relative humidity (RH) can alter the efficiency of a face respirator. The effect of RH on the filter efficiency varies depending on the aerosols type, particles size, and the filter material [297]. Haghighat, et al. [298] found that the penetration of the filters increased with the increasing RH. Conversely, Yang and Lee [299] reported that RH had no effect on the filter performance. Hence, different RH variations may have a different effect on different face respirators. In the current study all the respirators were tested under similar ambient RH conditions.

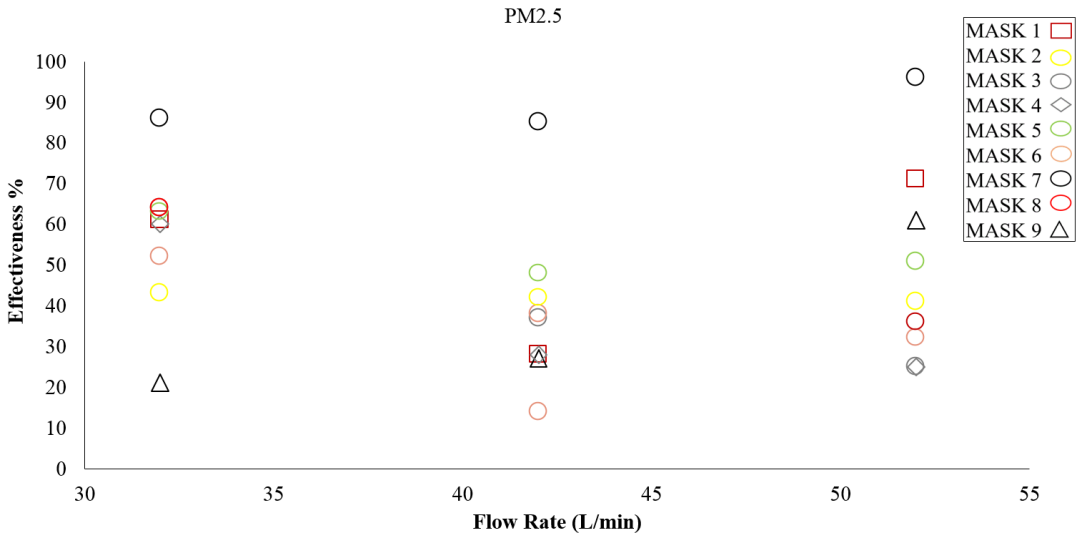

Figure 21 *Effectiveness of face masks for the three different breathing rates for PM2.5.*

Figure 22 *Different filter layers of MASK.*

8 EFFECT OF VENTILATION STRATEGIES AND AIR PURIFIERS ON THE CHILDREN' EXPOSURE TO AIRBORNE PARTICLES AND GASEOUS POLLUTANTS IN SCHOOL GYMS

Amongst the school environments, besides the classrooms, children spend time in school gyms to perform physical activities. School gyms are recognized as environments with high PM_{10} concentrations mainly due to the resuspension phenomena occurring during the physical activity itself [300-303]. Furthermore, no effective reduction strategies are typically adopted in gyms since the ventilation of such environments (as for classrooms) mostly relies upon natural ventilation (air exchange with closed windows) and manual airing via window opening. Few papers have recently been published on characterizing the efficiency of the air purifiers and their effectiveness in reducing the exposure in indoor environments [126-129]. The present study investigates the effect of the air purifiers as well as of the ventilation strategies on the children's exposure in school gyms to different pollutants. This paper uses the measured data for sub-micron particles (expressed as particle number, PNC, and black carbon, BC, concentrations), super-micron particles (expressed as particle mass concentrations), NO_2 and CO_2 through experimental campaigns in two different school gyms in Barcelona, Spain.

8.1 Materials and Methods

8.1.1 Site description

Two public primary school gyms located in the urban area of Barcelona (Spain) were selected to perform the experimental campaigns. The school gym A is placed on the Northeast side of the Montjuic hill (40 m above sea level) and it is not directly exposed to streets with high traffic density. The school gym B is located in the area of Vila Olimpica, it is quite close to the sea as well as to one of the most highly trafficked roads in Barcelona (about 215 m from Ronda Litoral, characterized by a daily traffic >100000 vehicles day^{-1}). Both school gyms present a rectangular floor shape with volumes of 430 and 2400 m^3 for gym A and B, respectively. Hot-water plants are installed in the gyms (fancoils and radiators for gym A and B, respectively) for heating purposes, and no *ad-hoc* mechanical ventilation systems were present in the gyms. Air ventilation only relied upon leakages of the envelope (natural ventilation) or window opening (manual airing). The school-time of both gyms is 08.30-17.30, during which they are used by different school classes for different physical activities.

8.1.2 Methodology and experimental apparatus

The experimental analysis was carried out in the period February-April 2015 for four weeks in each school gym. Measurements were performed in two monitoring sites in both schools: a) in the school gym, and b) at an outdoor site within the school area. The monitoring location inside the school gym was near one of the walls not directly exposed to the air purifiers (when used); whereas the outdoor site was outside the gym within few meters from the windows in order to properly measure indoor-to-outdoor (I/O) concentration ratios. At both indoor and outdoor monitoring sites, the instruments were placed on a desk.

Within the four-week campaigns, four different types of tests were carried out by considering four different ventilation strategies (one week of measurements for each strategy and for each school):

- Natural ventilation (NV), i.e. windows kept closed during the school-time (ventilation just due to the leakages of the envelope);
- Manual airing (MA), i.e. windows open during the school time;

- Natural ventilation and air purifiers (NV+AP), i.e. windows kept closed during the school-time as for the NV scenario, air purifiers running during the school time (turned on about half an hour before the school start time and turned off at school end time);
- Manual airing and air purifiers (MA+AP), i.e. windows open during the school time as for the MA scenario, air purifiers running during the school time (turned on about half an hour before the school start time and turned off at school end time).

The following pollutants/parameters were measured:

- Particle mass concentration of super-micron particles; in particular, the particle mass fraction in the 1-10 µm diameter range (PM_{1-10}) was evaluated on the basis of particle number distribution measurements performed through (i) an optical counter (OPC 1.108, Grimm; measurement range 0.3-20 µm, measurement frequency 6 s) and (ii) an Aerodynamic Particles Sizer (APS 3321, TSI Inc.; measurement range 0.5-20 µm; measurement frequency 1 s). The PM_{1-10} was estimated from the measured particle number distributions considering the particles as unit density spheres;
- Particle number concentration (PNC) of sub-micron particles measured by means of two diffusion charger particle counters (Testo DiSCmini; measurement range 10-700 nm; measurement frequency 1 s);
- Particle number size distributions through a portable scanning mobility particle sizer (Nanoscan SMPS 3091, TSI Inc.; measurement range 10-420 nm, measurement frequency 60 s);
- Black carbon (BC) measured by means of portable aethalometers (AE51 Magee Scientific; measurement frequency 1 s);
- Carbon dioxide (CO_2) measured by means of Non-Dispersive Infrared sensor (Q-TRAK indoor air quality monitor 7575, TSI Inc.; measurement range 0-5000 ppm, measurement frequency 20 s);

- Nitrogen dioxide (NO_2) measured through chemiluminescence analyzer (Thermo Scientific™; measurement range 0-20 ppm, measurement frequency 120 s);

In particular, the following instruments were installed at the indoor monitoring site in both the schools: the APS 3321, a Testo DiSCmini, the Q-TRAK 7575, the chemiluminescence analyzer, a portable aethalometer AE51, and the Nanoscan SMPS 3091 (in the school gym A only); whereas the following instruments were installed at the outdoor monitoring site in both the schools: the OPC 1.108, a Testo DiSCmini, and a portable aethalometer AE51. All the data were post-processed as 10-min average values.

Prior to the experimental campaigns, the devices were inter-compared by means of an *ad-hoc* experimental analysis performed in the urban area of Barcelona (at the official air quality station of Palau Reial, Barcelona, Spain) in order to minimize any measuring difference between paired instruments. Correction factors were evaluated through a linear regression fit: in particular, correction factors equal to 0.74 (R^2=0.93), 1.30 (R^2=0.97), and 1.05 (R^2=0.98) were obtained for PM_{1-10} (OPC-APS), particle number concentrations (two DiscMinis), and BC (two aethalometers). Moreover, before each measurement week, a further comparison between the two DiscMinis, the OPC and APS, and the two aethalometers was performed in order to take into account for the possible on-field effects on the instruments (e.g. the specific aerosol under investigation) and for unexpected instrument drift.

8.1.2.1 Air purifier characteristics and operation

The campaigns using air purifiers (NV+AP and MA+AP tests) were performed using six identical devices: four air purifiers were installed in the four corners of the gyms and two air purifiers along the longest walls of the gym (in the middle of the walls). Characteristics of the air purifier used in this study at the maximum power (which is that used during the campaign) are: maximum flow rate of 660 $m^3 h^{-1}$, dimensions of 60×73×55 cm, power of 178 W, electrical intensity of 1.1 A. Regarding filtration characteristics, the purifiers adopted present: i) pre-filtration with a glass microfiber filter class F7 for particles with a diameter <0.2 µm; ii) a filter for gaseous pollutants

containing a mixture of active carbon and absorbent media able to filter H_2S, SO_2, NO, NO_2, HCHO, as well as hydrocarbons, chlorine and volatile organic compounds; iii) a glass microfiber HEPA filter H14 for sub-micron and UFP.

The six purifiers used at the maximum power provided a total flow rate of 3960 $m^3 h^{-1}$. The manufacturer suggested to adopt a ratio between the total flow rate provided by the purifiers and the gym volume (hereinafter reported as "Air Changes per Hour, ACH") roughly equal to 1.5 h^{-1}. This is the reason why six purifiers were adopted; indeed, the total flow rate of the six purifiers in the larger gym (school gym B) allowed to obtain an ACH=1.7 h^{-1}. As mentioned above, the manufacturers' suggestion represents mainly a rule of thumb, in fact, values >10 h^{-1} are elsewhere suggested. To this end, in order to check the behavior of the purifiers with a higher ACH value, the same air purifier configuration was adopted in the smaller gym (school gym A) then obtaining an ACH=9.2 h^{-1}.

In order to evaluate the effect of the air purifiers in terms of airborne particle concentration reduction, the total removal rate of different particle metrics for NV and NV+AP strategies was also evaluated. The total removal rate is due to the contributions of particle exfiltration (related to the air exchange rate of the gym, *AER*) and the particle deposition (evaluated by means of the particle deposition rate, *k*) [304, 305]. Such removal rate (*AER*+*k*) was evaluated measuring the exponential decay of the particle concentration from an initial concentration N_0 to a lower concentration measured after a time period *t*:

$$(\boldsymbol{AER} + \boldsymbol{k}) = -\ln\frac{\boldsymbol{N_{(t)}}}{\boldsymbol{N_0}} \cdot \boldsymbol{t} \quad (11)$$

With this aim, tests were performed measuring as soon as the children left the room (N_0 concentration) for about one hour. The *AER*+*k* values for NV and NV+AP strategies were obtained performing measurements with windows kept closed without, $(AER+k)_{NV}$, and with air purifiers in operation, $(AER+k)_{NV+AP}$, respectively. The total removal rate for the following metrics were evaluated: (i) total particle number concentration (PNC) measured through the diffusion charger, (ii) $PM_{1\text{-}10}$, $PM_{1\text{-}2.5}$, and $PM_{2.5\text{-}10}$ fractions estimated from the APS measurements, and (iii) particle number concentration of particles smaller than 40 nm ($PNC_{<40}$), between 40 nm and 130 nm

(PNC_{40-130}), and larger than 130 nm ($PNC_{>130}$) measured through the Nanoscan SMPS 3091 (as mentioned above, the Nanoscan was used in the school gym A only).

8.2 Results

In this section data collected during the two experimental campaigns are summarized and discussed. Median concentrations (and 25^{th} - 75^{th} ranges) of PNC, BC and PM_{1-10} measured during the four-week campaigns at the outdoor sites of the schools were equal to 1.10×10^4 part. cm^{-3} ($0.90\text{-}1.41\times10^4$ part. cm^{-3}) and 1.21×10^4 part. cm^{-3} ($0.93\text{-}1.51\times10^4$ part. cm^{-3}), 2.3 µg m^{-3} (1.7 - 3.2 µg m^{-3}) and 1.2 µg m^{-3} (0.8 - 1.9 µg m^{-3}), 15.8 µg m^{-3} (10.9 – 21.0 µg m^{-3}) and 6.8 µg m^{-3} (4.1 – 11.6 µg m^{-3}) for school A and B, respectively. The PNC values at the two outdoor sites, tested through the non-parametric Kruskal-Wallis test ($p<0.01$), resulted statistically similar, whereas statistically higher BC and PM_{1-10} levels were measured at the outdoor site of the school B; this is likely due to the influence of the position of the school within the city: indeed, the school B is closer to a highly trafficked road with respect to the school A. Nonetheless, the study is not focused on the evaluation of the outdoor air quality in the city (which mostly represents a local aspect), therefore, rather than the absolute outdoor concentrations, the behaviour of the indoor values with respect to the outdoor ones will be hereinafter discussed.

In Figure 23, by way of example, 24-h trends of PNC, BC, and PM_{1-10} measured on one day of the entire measurement week of each scenario (NV, NV+AP, MA, and MA+AP), both indoor (gym) and outdoor, are presented for the school gym B.

The PNC and BC trends clearly highlight, as expected, that sub-micron particle sources are mostly placed outdoors: indeed, for all the scenarios investigated, the outdoor PNC and BC during the school gym time resulted higher than the indoor ones. Therefore, the indoor concentrations of such metrics characteristics of the sub-micron particles are just affected by the outdoor ones. Nonetheless, the different ventilation and air purifier scenarios affect differently the indoor levels: in particular, when the windows are kept closed during the school gym time (NV scenario) the indoor concentrations (PNC and BC) follow the outdoor ones but the concentrations are significantly lower than those measured at the outdoor site due to the shielding effect of the gym envelope

(i.e. the building airtightness and, thus, its air exchange rate). On the contrary, when the windows are open to obtain a manual airing of the gym (MA scenario), the indoor levels of sub-micron particles reach the outdoor ones due to higher air exchange rate [122, 306, 307]. When the air purifiers are adopted, a positive effect was recognized on both PNC and BC metrics. In particular, the air purifiers were extremely effective with windows closed (NV+AP scenario), in this case the dependence of the indoor PNC and BC levels upon the outdoor ones resulted almost negligible then demonstrating the effectiveness of the air purifiers in filtrating the sub-micron particles. Such effect is even more clear for the school gym A characterized by a higher ACH as hereinafter discussed (Table 23). Nonetheless, when the air purifiers are adopted with windows open (MA+AP scenario) their effect is much less important, in that case the high air exchange rate of the gym due to the manual airing likely favor the infiltration of sub-micron particles indoors: this is recognizable from the indoor PNC and BC trends that clearly approach to the outdoor ones but with lower indoor-to-outdoor ratios with respect to the MA scenario as hereinafter discussed (Table 23). Super-micron particles were investigated through the PM_{1-10} metrics. The observed indoor PM_{1-10} concentrations were higher than the outdoors during all the investigated scenarios. This is due to the presence of indoor sources (children's physical activities leading to particle resuspension) which affect the indoor PM_{1-10} concentrations to a greater extent than the outdoor ones [122, 303, 308]. The presence of the indoor source implies that the worst exposure scenario in terms of PM_{1-10} for the children is the NV one: the reduced air exchange rate due to the windows closed doesn't allow a proper exfiltration of indoor-generated particles. Such dynamics was a little bit improved when the manual airing is adopted (MA scenario) then obtaining a corresponding indoor/outdoor (I/O) ratio smaller than the NV scenario one (Table 23). The adoption of the air purifiers is able to reduce such indoor over-exposure with respect to the outdoor PM_{1-10} concentrations. In particular, the most efficient strategy for such aerosol metrics is the adoption of the combined effect of manual airing and air purifier (MA+AP scenario). This is likely due to the concomitant positive effects of the increased air exchange rate and the recirculation/filtration guaranteed by the purifiers as confirmed by the data hereinafter reported (Table 23). Besides the airborne particle

metrics, the ventilation strategies and the adoption of air purifiers affect the gaseous pollutants/markers too. In Figure 24, by way of example, 24-h trends of NO_2 and CO_2 measured for one day of the entire measurement week of each scenario (NV, NV+AP, MA, and MA+AP) at indoor monitoring site (gym), are reported for the school gym B. Unfortunately, no outdoor values are available for those gases. Nonetheless, the indoor concentrations allow to draw some qualitative conclusions. In particular, the CO_2 levels, as expected [122], are not influenced by the presence of the purifiers, indeed lower indoor concentrations were measured for scenarios characterized by higher air exchange rates (i.e. MA and MA+AP) as typical of indoor-generated gases. On the contrary, the outdoor-generated gaseous pollutants, such as NO_2, present lower indoor values for ventilation scenarios with windows closed (NV and NV+AP). For air purifiers able to trap NO_2 too (as those considered in the present study), the scenarios with purifiers in operation (NV+AP and MA+AP) are able to reduce the indoor exposure with respect to the corresponding scenarios without purifiers (NV and MA, respectively).

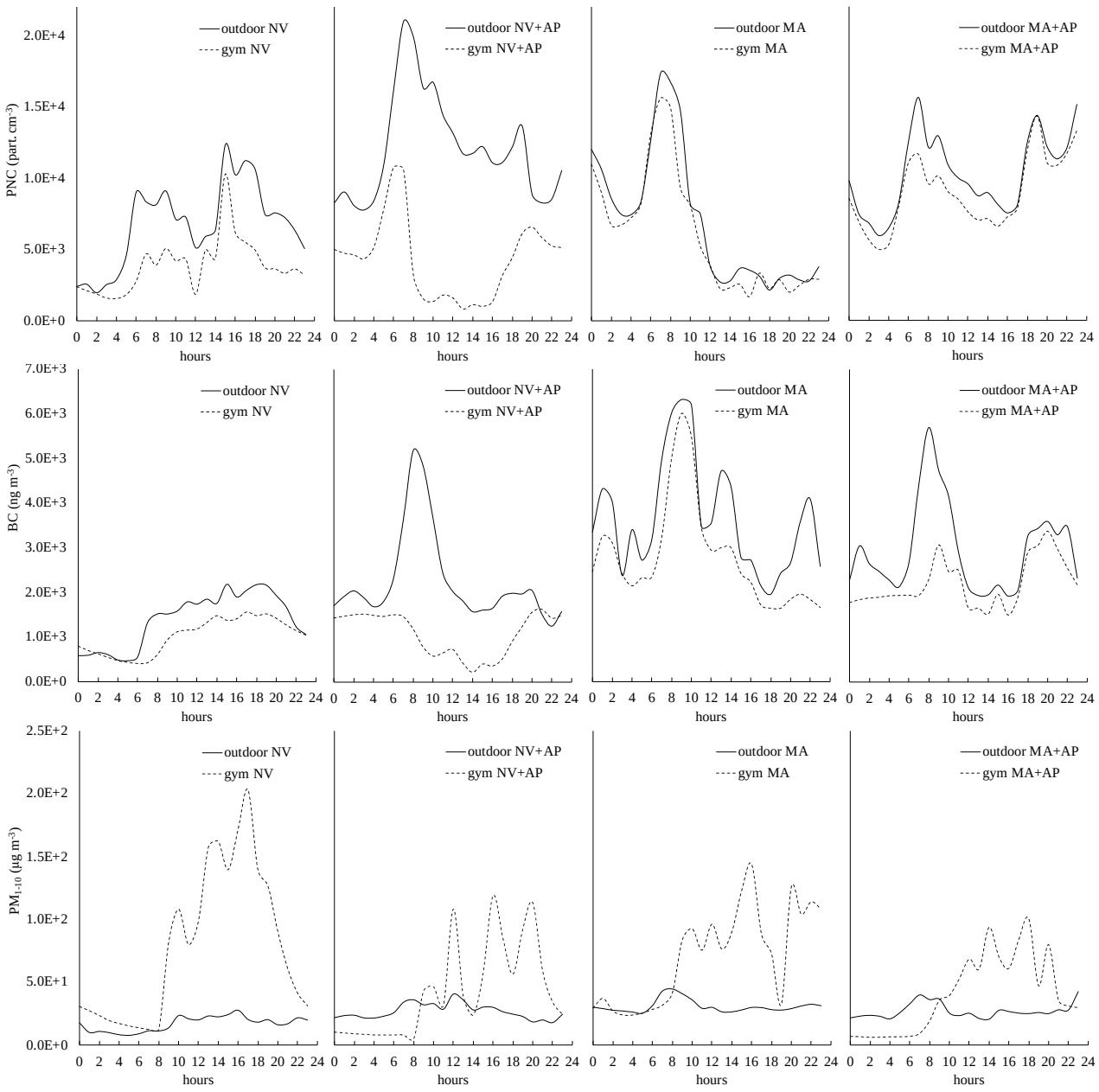

Figure 23 *Example of indoor (gym) and outdoor 24-h trends of total particle number concentrations (PNC), BC, and $PM_{1\text{-}10}$ measured for one day during the one week of monitoring campaign for the different scenarios (NV, NV+AP, MA, and MA+AP) in the school gym B. The shaded area represents the school gym time.*

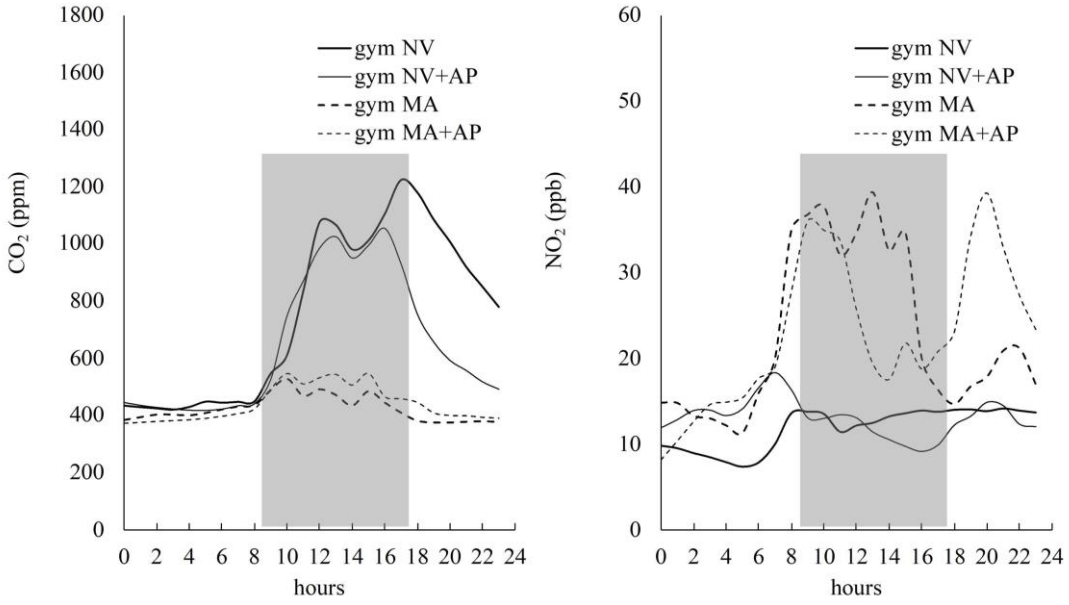

Figure 24 *Example of indoor (gym) 24-h trends of NO_2 and CO_2 measured for one day during the one week of monitoring campaign for the different scenarios (NV, NV+AP, MA, and MA+AP) in the school gym B. The shaded area represents the school gym time.*

The illustrative trends reported in Figure 23 and Figure 24 are referred to one day of measurements adopted to characterize each scenario in the school gym B. In order to quantify the effectiveness of the different scenarios, in Figure 25 and Figure 26 the box-plots of indoor (gym) and outdoor (if any) trends of the airborne particle and gaseous pollutants investigated are reported for both the school gyms. Such box-plots represent the statistics of school gym time period and include the entire measurement period for each scenario (one week). Therefore, the data reported in the box-plots allow to carry out more robust results with respect to the one-day descriptive trends due to the longer averaging period which provides a larger amount of data and reduces possible miscalculations caused by variations of the physical activity/number of children/operating hours on different days. In particular, the box-plot highlights even better the effectiveness of the air purifiers in reducing the sub-micron particle concentrations with respect to the outdoor ones; indeed, in both the school gyms, the PNC resulted roughly lower than 0.15×10^4 part. cm^{-3}, whereas the simultaneous outdoor concentrations were higher than 1×10^4 part. cm^{-3}. Thus, the sub-micron particle concentrations were reduced approximately by a factor of 10 (I/O in NV+AP) as hereinafter summarized in Table 23. A similar reduction was obtained in terms of

BC. An effect of the air purifiers was also recognized in terms of deviation of indoor sub-micron concentrations; indeed, during NV+AP and MA+AP scenarios, the indoor PNC and BC data resulted in clearly narrower box-plots with respect to the scenarios with no air purifiers in operation (NV and MA). As regard the super-micron particle concentrations (PM_{1-10}), the box-plot confirm a reduction of indoor levels when air purifiers are used; nonetheless such a positive effect is lower than that reachable on sub-micron particles (as hereinafter detailed in Table 23) likely due to the presence of the indoor sources. The authors point out that they are not discussing the absolute concentration values which mostly represent local data, but the effect of the different strategies under investigation are examined in terms of indoor-to-outdoor (I/O) concentration ratios. Indeed, on the basis of the median values of Figure 25, the I/O concentration ratios were calculated and reported in Table 23. In particular, I/O concentration ratios are shown, for all scenarios (NV, NV+AP, MA, MA+AP) and the particle metrics under investigation (PNC, BC, and PM_{1-10}.).

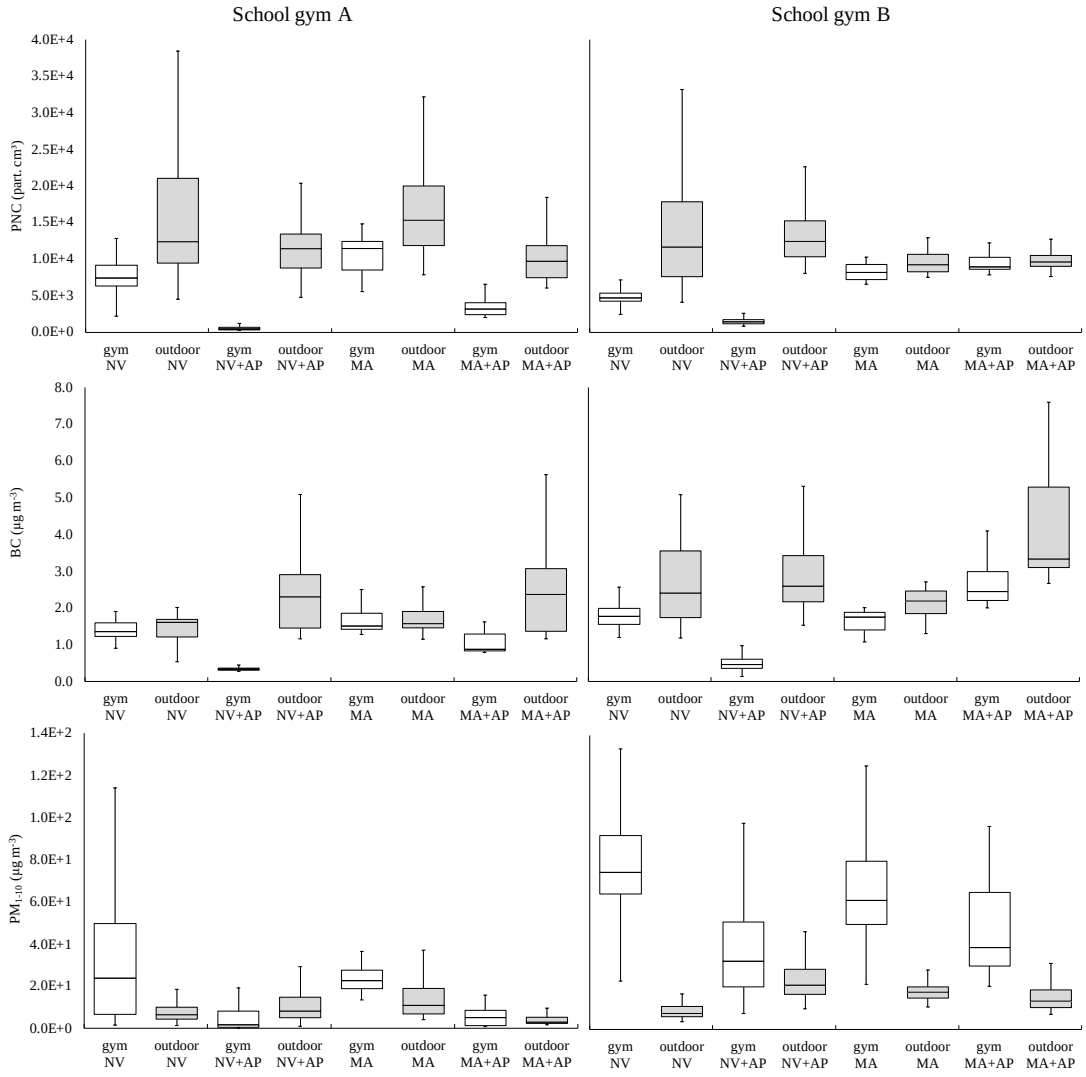

Figure 25 *Box-plots of airborne particle concentration levels (PNC, BC, PM_{1-10}) measured during the school gym time for the whole experimental campaign performed in the two school gyms at indoor (gym) and outdoor monitoring sites for the different scenarios (NV, NV+AP, MA, and MA+AP).*

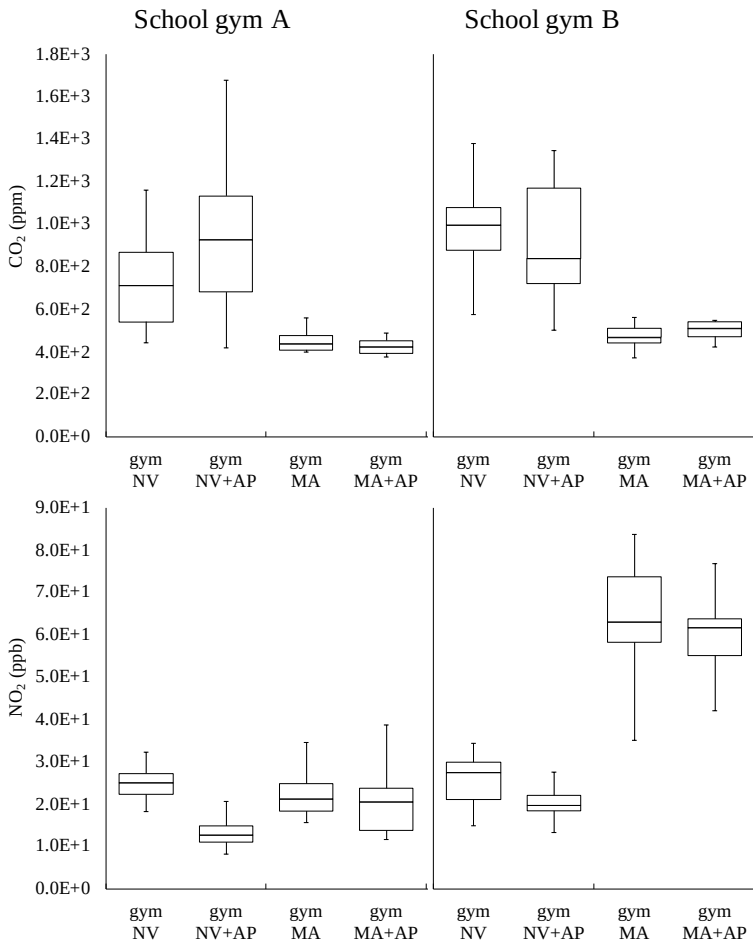

Figure 26 *Box-plots of CO_2 and NO_2 measured during the school gym time for the whole experimental campaign performed in the two school gyms at indoor (gym) monitoring site for the different scenarios (NV, NV+AP, MA, and MA+AP).*

Figure 26 reports the indoor NO_2 concentrations in school gym A and B. Despite simultaneous outdoor NO_2 levels are not available, the box-plots seem to confirm an effect of the air purifier: this is obviously more evident in the scenarios with windows closed (NV+AP vs. NV); nonetheless, a similar trend was also recognized for manual airing approaches (MA+AP vs. MA). These behaviors can be recognized in both the school gyms; nonetheless the graph clearly show that indoor NO_2 concentrations for MA and MA+AP scenarios are higher in the school gym B likely due to the different location of the school within the city: indeed, the school gym B is close to one of the major urban road of Barcelona.

As regard the particle number concentration, the I/O ratios are reduced from 0.60 and 0.40 in the NV scenario to 0.04 and 0.12 for NV+AP scenario in the school gyms A

and B, respectively. As expected, a larger reduction was obtained for the school gym A (93% vs. 70%) characterized by a greater ACH. The MA scenario implies an increase of I/O PNC ratios with respect to the NV ones (0.74 and 0.88 in school gyms A and B, respectively) because of the larger infiltration of outdoor-generated sub-micron particles during the windows airing. When the air purifiers are used during the manual airing strategy (MA+AP) a reduction of the I/O PNC ratio with respect to the manual airing alone is recognized: the reduction is still large in the school gym B (from 0.74 to 0.32, 57%) due to the high ACH, whereas is almost negligible (6%) in the school B since the ACH is comparable to the typical AER of window opened [122]. Similar data were measured for BC since it is an airborne particle metric characteristics of the traffic-related emission too [309].

PM_{1-10} I/O ratios for NV scenario resulted equal to 3.69 and 9.79 in the school gyms A and B, respectively. The extremely high indoor values with respect to outdoor ones are due to the high intensity of the physical activities performed in the gym with respect to the school classrooms [115]. Nonetheless, the use of air purifiers allowed an important reduction since the I/O ratios dropped to 0.19 and 1.53 then obtaining a reduction of 95% and 84% for school gyms A and B, respectively. The manual airing scenario also reduce the PM_{1-10} I/O ratios with respect to the NV one (I/O ratios of 2.09 and 3.45 for school gyms A and B, respectively), nonetheless, such reduction is limited with respect NV+AP scenario. The simultaneous use of air purifier and manual airing (MA+AP), that could be roughly considered a first attempt to reduce indoor-generated pollutants and filtrate the outdoor-generated ones, shows a further reduction of PM_{1-10} I/O ratios with respect to the MA ones, but the ratios are still larger than 1 whatever the ACH value amongst those investigated.

Table 23 *Indoor/outdoor (I/O) median concentration ratios measured for all scenarios under investigation (NV, NV+AP, MA, MA+AP) in terms of particle number concentration (PNC), BC, and $PM_{1\text{-}10}$ and for both school gyms under investigation.*

airborne particle metrics	School gym A				School gym B			
	NV	NV+AP	MA	MA+AP	NV	NV+AP	MA	MA+AP
PNC	0.60	0.04	0.74	0.32	0.40	0.12	0.88	0.83
BC	0.84	0.15	0.95	0.37	0.74	0.18	0.79	0.74
$PM_{1\text{-}10}$	3.69	0.19	2.09	1.74	9.79	1.53	3.45	2.87

The different percent reduction of the I/O ratios in the two school gyms are strictly related to the different ACH values adopted (9.2 h^{-1} and 1.7 h^{-1} for school gyms A and B, respectively), indeed, higher ACH values imply a faster gym air recirculation and consequent filtration. To confirm this aspect, the total removal rate for different airborne particle metrics were evaluated through decay tests in both the gyms as described in the section "Air purifier characteristics and operation". In Table 24 the difference of total removal rate between NV+AP and NV scenarios ($(AER+k)_{NV+AP} - (AER+k)_{NV}$, expressed as h^{-1}) is reported for particle number concentrations (PNC, $PNC_{<40}$, $PNC_{40\text{-}130}$, and $PNC_{>130}$) and PM fractions ($PM_{1\text{-}10}$, $PM_{1\text{-}2.5}$, and $PM_{2.5\text{-}10}$). The data clearly show that for all the particle metrics the total removal rates are larger for the school gym A than for the B one. The removal rates measured for super-micron particles are quite similar within the entire 1-10 μm diameter range with a slightly higher decay for the coarse fraction ($PM_{2.5\text{-}10}$) which is the one mostly influenced by resuspension phenomena. As regard the sub-micron particles, the removal rate of particles smaller than 130 nm is quite similar to the total PNC removal rate (roughly 1 h^{-1}), whereas a slightly slower decay was observed for particles larger than 130 nm likely due to the typical reduced filter efficiency in that size range [310].

Table 24 *Difference of total removal rate amongst NV+AP and NV scenarios ($(AER+k)_{NV+AP} - (AER+k)_{NV}$, h^{-1}) in terms of particle number (PNC, $PNC_{<40}$, PNC_{40-130}, $PNC_{>130}$) and mass concentration (PM_{1-10}, $PM_{1-2.5}$, and $PM_{2.5-10}$) for both the investigated school gyms. Values reported represents the differences amongst the median $((AER+k)_{NV+AP}$ and $((AER+k)_{NV}$ values.*

airborne particle metrics	School gym A	School gym B
PNC	0.99 h^{-1}	0.23 h^{-1}
$PNC_{<40}$	1.02 h^{-1}	-
PNC_{40-130}	1.05 h^{-1}	-
$PNC_{>130}$	0.87 h^{-1}	-
PM_{1-10}	3.62 h^{-1}	1.19 h^{-1}
$PM_{1-2.5}$	3.60 h^{-1}	0.93 h^{-1}
$PM_{2.5-10}$	3.63 h^{-1}	1.20 h^{-1}

9 CONCLUSION

In the present thesis an assessment of the influence of the lifestyle on the exposure to airborne particles (including ultrafine particles) throughout a "direct exposure assessment approach" was performed. It was also estimated the typical daily doses received by different populations, taking into account different characteristics of the populations under investigation (like gender, age and origin). Moreover, a risk assessment of ELCR was performed taking into account two crucial environments. Besides, was also evaluated the efficiency of some possible solution in reducing the levels of the ELCR by means a reduction of the received dose of airborne particles.

In detail: an investigation of the daily dose in terms of particle surface area received by different Western populations was performed in order to show the effect of the age, gender, microenvironment, and nationality (lifestyle, culture, and built-up environment) on the overall daily dose. Airborne particle concentration data (obtained through measurements at a personal scale, i.e. direct exposure assessment method), time activity patterns (obtained from national statistics institutes) and inhalation rates, were combined through a Monte Carlo simulation to obtain the most probable dose received by populations living in Barcelona (Spain), Cassino (Italy), Guilford (UK), Lund (Sweden) and Brisbane (Australia). The contribution of the main microenvironments was also investigated.

Data on particle concentration levels demonstrate a high exposure during cooking and eating activities for all the populations investigated. Nonetheless, the typical concentration to which people are exposed in Lund are much lower than that in other cities: this can be related to the widespread use of the mechanical ventilation systems indoor (including homes). Higher concentrations are typically measured during eating and cooking times in Cassino and Guilford (median value $>5\times10^4$ part. cm^{-3}) whereas

the median concentration values in transport and outdoor environments are generally considerably lower.

Particle surface area doses received were significantly larger than 1000 mm^2 for people living in Cassino and Guilford, about 600-800 mm^2 for those residing in Barcelona and Brisbane, and around 100 mm^2 for Lund inhabitants. The main parameter influencing the dose received by people is the lifestyle: the time spent in highly-polluted microenvironments (e.g. during cooking and eating activities), which strongly affect the total daily dose. On the contrary, the outdoor air quality in studied cities has low impact on the dose received by people, due to both short exposure time and not significantly high concentration levels (when compared to indoor sources/exposures). Nonetheless, the findings of our study demonstrate that the dose received indoors (even when cooking and eating activities were conducted) can be remarkably reduced through the improvement in the overall indoor air quality by means of both local extractors and general mechanical ventilation systems (with up to date filtration units), utilization of which leads to the increase in the air exchange rates.

One of the crucial environments that could lead to high exposure to airborne particles due to the high levels of concentration is transport, to this reason a study was performed to investigate on Vehicle Interior Air Quality (VIAQ). Data of this campaign reveals real air quality conditions experienced by taxi drivers and their passengers travelling day-to-day through a traffic-congesting city such as Barcelona, and reinforces the critical importance of air exchange rates to VIAQ. Both ultra-fine particle numbers (PNC) in the size range of 10-700 nm, and lung deposited surface area (LDSA) measurements offer sensitive indicators of VIAQ and the likelihood of negative health effects. Despite the high city centre traffic volumes, and even with a dominance of diesel vehicles on the road, taxis driven under closed ventilation conditions can suppress median levels of UFP to around PNC=10000 $\#\cdot cm^{-3}$ or less. Such levels are considerably lower than PNC values reported for UFP breathed when travelling by public transport (bus, metro, tram) in the same city [69]. In contrast, if taxi windows are left open then median PNC values will rise above 20000 and can approach 100000 $\#\cdot cm^{-3}$, with transient peak exposures capable of exceeding PNC=1000000 $\#\cdot cm^{-3}$. Similarly, median LDSA levels can rise from <20 $\mu g^2\cdot cm^{-3}$

under closed conditions to >200 $\mu g^2 \cdot cm^{-3}$ with windows open and with transient peak levels exceeding 1000 $\mu g^2/cm^{-3}$. Median UFP sizes of 36 nm (non-diesel) and 46 nm (diesel) reflect the presence of accumulation mode particles undergoing processes such as coagulation within the confined and relatively undiluted microenvironment of the vehicle interior. Evidence for the presence of exhaust contaminants generated by the vehicle being driven ("self-pollution") is implicated by higher BC and CO levels, and larger UFP sizes, measured inside the diesel taxi as compared to their non-diesel pair. Higher concentrations of CO (>2 ppm) are most commonly associated with older diesel taxis with >500000 km on the odometer. PM_{10} concentrations measured inside the taxis were variable but averaged 67 $\mu g \cdot m^{-3}$, which is more than treble the urban background for the same period and mostly attributable to increased levels of organic and elemental carbon. Source apportionment calculations indicate the main source of PM_{10} measured inside the taxis was vehicle exhaust followed by non-exhaust particles emitted by vehicle wear. The trace metal signature of PM_{10} collected within the taxis shows significant enhancements in Cr, Cu, Sn, Sb and a "High Field Strength Element" group characterised by Zr accompanied by Hf, Nb, Y and U. This signature is attributed mainly to the presence of brake PM and, in the case of the HFSE group, to the abrasive mineral zircon. Volatile organic compounds measured inside the taxi are dominated by 2-methylbutane and n-pentane, both of which are presumably sourced from the combustion of light hydrocarbon fuels. Other common VOCs include toluene, m-xylene, o-xylene, 1,2,4-trimethylbenzene, ethylbenzene, p-xylene, benzene, and 1,3,5-trimethylbenzene, all interpreted as exhaust emissions sourced from a mix of fuels. The youngest taxi (fuelled by natural gas) registered the highest content of alkanes and aromatics (possibly due at least in part due to off-gassing), and the VOC composition inside a closed electric taxi was strongly influenced by the presence of an air freshener. Carbon dioxide concentrations stayed at around ambient levels (400 ppm) with taxi windows open, but quickly climbed to undesirable levels under closed ventilation conditions. In one example it took just 33 minutes to reach a CO_2 concentration of 2500 ppm and stayed above that level for 4.5 hours of the 6-hour monitoring period.

Taxi drivers (and their passengers) would benefit from greater awareness of the known hazards associated with breathing traffic pollutants. Such knowledge would encourage them to make intelligent use of interior ventilation to reduce both the infiltration of outside contaminants and the build-up of indoor-generated pollutants.

A particular urban configuration easy to find in the city in which people could receive high levels of deposited dose that lead to high levels of ELCR is the street canyons. A novel modelling approach was proposed in order to evaluate the ELCR for people exposed to fine and ultrafine particles emitted by light duty and heavy-duty vehicles (both gasoline and diesel fuelled) in urban street canyons. To this end, the literature data of PAHs, heavy metals PCDD/Fs and PM_{10} deposited on particle surface, detected in emission from the vehicles, were used for the evaluation of the ELCR at the tailpipe. This value was then imposed in a numerical CFD model as input data, in order to evaluate the lung cancer risk of people living in the street canyon, at street level (at a height of 1.5 m), as a function of the wind speed and canyon geometry (aspect ratio, H/W), and considering two exposure scenarios. The ELCR calculated at the tailpipe was found to be equal to 2.1×10^{-2}, meaning that for every 100000 people hypothetically breathing directly at the tailpipe of the vehicles 24 hours per day for 70 years, 2 100 will develop lung cancer. On the basis of this value, imposed as input data in the numerical CFD model, the ELCR for people living inside the canyon was obtained. In particular, for an extreme scenario of people living 24 hours per day for 70 years in the street canyon, the maximum ELCR value found equal to 5.2×10^{-2} (5 200 new lung cancer cases over a population of 100000) on the leeward side of the H/W=3 street canyon configuration, with a wind speed of 1 m/s, according to the proposed model, showing the presence of an accumulation zone inside the canyon that significantly worsen the air quality. In the same extreme scenario, the lower ELCR value of 4.1×10^{-4} is relative to the windward side of the H/W=1 configuration, with wind speed of 5 m/s, meaning that 41 people will develop cancer over a population of 100000. For a more realistic scenario of people spending 15 minutes per day in the street canyon for 20 years, the worst condition was observed on the leeward side of the H/W=3 configuration, with wind speed of 1 m/s (ELCR equal to 1.5×10^{-4} – 15 new lung cancer cases over 100000 peoples), while the lower ELCR is relative to the

windward side of the H/W=1 street canyon, with 5 m/s of wind speed (1.2×10^{-6} – 0.12 new lung cancer cases over 100000 peoples). From the parametric analysis, it was found that the ELCR value at 1.5 m from the ground is higher on the leeward side for aspect ratios equal to 1 and 3, while for aspect ratio equal to 2 the ELCR is higher on the windward side, for all the three wind speeds analysed. In addition, the simulations showed that with the increasing of wind speed the ELCR becomes lower everywhere in the street canyon, due to the strengthened interaction between the free-stream flow and the flow inside the canyon. Finally, the risk calculated in this work (considering the scenario of people exposed 15 minutes per day for 20 years) results lower if compared to the ELCR target limit of 1×10^{-5} reported by WHO and can be considered "safe" if compared to the EPA target risk range of 10^{-6} – 10^{-4}, under the assumption described in the proposed methodology.

With the proposed approach, that allows to consider the dispersion of particles and relative toxicity, it will be possible to evaluate the effect of different sources that contribute to the total ELCR in urban area. Anyway a not negligible amount of uncertainty can be associated to the proposed methodology, and that a proper uncertainty budget of the ELCR model is quite complex as it depends on measurement uncertainties, on model uncertainty itself, and on the uncertainty of the assumptions made (choice of fleet and fuel spread, fractional deposition, spherical shape of the particles etc.). Therefore, an ad-hoc study focused on a more accurate risk and correlated uncertainty evaluation, together with the evaluation of different particle sources in urban area that contribute to the total ELCR, could likely represent a future development of this work.

Moving the attention in indoor environments the school represent one of the most crucial environments. To better understand the levels of the indoor air quality where children are exposed an experimental campaign was carried out in two different European cities involving more than 30 schools. Exposure data to airborne particle metrics and carcinogenic compounds were used to evaluate the school-time dose received by students and the related lung cancer risk. To this end an ad-hoc model able to take into account the contribution of both particle surface area and mass metrics was adopted.

Number and lung-deposited surface area concentrations (characteristics of sub-micron particles) in classrooms resulted lower than the outdoor values due to the sub-micron penetration factors lower than 1 (0.7-0.8 in terms of particle number concentrations for the experimental campaigns here shown). Values in Cassino resulted larger than the Barcelona ones due to the contribution of biomass-burning emitted particles. Indeed, median lung-deposited surface area concentrations in classrooms resulted equal to 34 and 90 $\mu m^2\ cm^{-3}$ in Barcelona and Cassino, respectively. On the contrary, PM_{10} concentrations in classrooms (characteristics of super-micron particles) resulted larger than the outdoor ones due to the typical coarse-particle generation and re-suspension in schools.

The cancer potency of the mixture of the different carcinogenic pollutants on PM (i.e. slope factor) was evaluated on the basis of the compounds mass fractions: the slope factor of particles collected in Cassino resulted larger than the Barcelona one likely due to the presence of compounds typical emitted by biomass burning heating systems. The median surface area dose received during school-time by students in Barcelona and Cassino resulted equal to 110 mm^2 and 303 mm^2, respectively, with larger dose received by students in Cassino due to the higher concentrations values.

The lung cancer risk due to the five-year primary school period exposure to airborne particles in Barcelona ($>2\times10^{-5}$) resulted quite similar to the maximum tolerable values commonly accepted (1×10^{-5}). On the contrary, the risk for students in Cassino (roughly 1.4×10^{-4}) is significantly higher than the limit value suggested by the EPA: this is likely due to the larger dose received by students and cancer potency of particles.

In light of results found in these experimental campaigns, we can say that the concentrations of pollutants, as well as the time we spend in the environment or doing the activity, have a strong influence on personal exposure to air pollutions. A possible solution to reduce the exposure and consequent increase of ELCR are represented by (i) personal protectors as face masks, (ii) strategies ventilation, (iii) air purifiers. To better understand the effectiveness of these methods two experimental campaigns were carried out under real conditions.

The first study involved Nine different face masks (varying in a price range of 1 - 44€) and aims to evaluate their effectiveness to reduce exposure to $PM_{2.5}$, PNC, LDSA and BC. Three different breathing rates were considered (32 $L\cdot min^{-1}$, 42 $L\cdot min^{-}$

^{1}, and 52 L·min^{-1}) in order to cover the range of cyclist breath rates. Results show that effectiveness is immediate and its median value among the face masks under study was 48% for $PM_{2.5}$ but less than 30 % for other metrics (PNC=19%, LDSA=22% and BC=19%). We found a rather large variability among different face masks, one of them clearly shown higher performances than other masks in each metrics taken into account. The common feature is higher effectiveness for $PM_{2.5}$ than for BC, PNC and LDSA, possibly related to particle size distribution. The differences observed among different face masks are likely due to the different fit, filter material, filtration and technology of each mask, but no cost-effectiveness relationship was found. A limitation of this study is due to the different initial range of concentration in which were exposed the masks since the sampling was carried out under real conditions of outdoor exposure of airborne particles. No clear relationship between the change in breathing rate and effectiveness was observed. With all breathing rates, the highest effectiveness for each mask is related to $PM_{2.5}$ concentrations, and the highest performance was found for all pollutants with the same mask (MASK 7).

Given the wide range of variability of performance obtained in this study, it is clear that more attention must be given to the choice of commercial face masks with respect to their ability to reduce individual air pollutant exposure. Since the price is not a good indicator of the best performance, it is better to focus more in characteristics of the quality of the filter as a filtration typology, number of different filter layers and how the mask fits to the human face.

The second study was designed and performed in two school gyms to investigate about the effect of different strategies, including the adoption of different ventilation methods and the use of air purifiers, to reduce the exposure of children in school gyms to airborne particles and gaseous pollutants. Different scenarios were taken into account: (i) natural ventilation (windows closed), (ii) natural ventilation and use of air purifiers, (iii) manual airing (windows open), and (iv) manual airing along with air purifiers in operation. The air purifiers, when used, provided an air change per hour (ACH) equal to 9.2 h^{-1} and 1.7 h^{-1} in the school A and B, respectively.

One-week indoor (in the gym) and outdoor measurements of particle number, black carbon, and PM_{1-10} concentrations were performed for each scenario along with indoor measurements of CO_2 and NO_2.

The results of the campaign highlighted that the different airborne particle metrics are differently affected by the ventilation method and the use of purifiers. In particular, for natural ventilation scenario, which is the typical condition adopted in colder periods (at least in non-extremely cold countries), the concentrations of airborne particle metrics mostly affected by sub-micron particles (i.e. particle number and black carbon) are lower than the outdoor ones as they are mostly emitted by outdoor sources. On the contrary, super-micron particles (here evaluated in terms of PM_{1-10}) can reach indoor-to-outdoor ratios (I/O) extremely high due to the particle resuspension related to the physical activity of the children themselves (up to 9 in the smaller school). The adoption of air purifiers with windows closed leads to promising results, indeed, a significant of I/O reduction for both sub- and super-micron particles was recognized whatever the ACH value. In particular, the particle number and PM_{1-10} I/O ratios were reduced by 93% and 95% in the school characterized by an ACH=9.2 h^{-1} and by 70% and 84% in the school characterized by an ACH=1.7 h^{-1}. The different reduction is due to the different ACH values: the higher the ACH value (9.2 vs. 1.7 h^{-1}), the faster the total removal rate (e.g. 0.99 vs 0.23 h^{-1} in terms of particle number concentration) measured through *ad-hoc* particle decay tests performed as soon as the children left the gyms. The natural ventilation method and the simultaneous use of air purifiers can also significative reduce the indoor concentrations of NO_2 penetrating from outdoors when such purifiers are equipped with *ad-hoc* NO_2 filters. On the contrary, no effect on the indoor-generated CO_2 can be guaranteed: the reduction of indoor-generated pollutants that cannot be filtrated by the purifiers (e.g. CO_2, radon) can be just obtained by increasing the air exchange rate (e.g. using the manual airing in naturally ventilated buildings). Nonetheless, the manual airing scenario itself can reduce the concentration of indoor generated pollutants/gases (e.g. CO_2 and PM_{1-10}) but implies a simultaneous penetration of outdoor-generated sub-micron particles and gases. In that case, the simultaneous use of air purifiers provides a significant reduction of particle number

and black carbon concentrations just for high ACH values, otherwise it is almost negligible (about 6% for ACH=1.7 h^{-1}).

Summarizing, the use of air purifiers in school gyms close to busy traffic roads can be a suitable and easy-to-use solution in buildings where no mechanical ventilation systems are adopted. Indeed, even if reducing the exposure to outdoor-generated pollutants could be achieved by locating the gyms far from the outdoor sources (e.g. roads) or reducing traffic intensity around school, the super-micron particles are emitted by the children activity through resuspension phenomena independently from the location of the gym within the city; thus, using air purifiers can guarantee lower exposure to such size fraction.

In conclusion, from the data reported in the present thesis it is evidenced that there is a strong relationship between lifestyle and exposure to airborne particles, and that the indoor environment represents the most influencing contribution to the received dose with respect outdoor environments. In light of this, since of the strong dependence of the ELCR from the received dose of airborne particles, lifestyle represents a strong influencing parameter. Such a result opens the question on the possibility to reduce the ELCR and gives us as one of the possible solutions the reduction of the received dose of airborne particles. This reduction could be performed by changing some habits and/or adopting some precautionary/preventive measures as a (i) wear facemasks in outdoor environments (for example whereas are riding a bike close to some street with high vehicular density), and (ii) using an adequate strategy of ventilation or air purifiers in indoor environments (for example whereas are cooking or are at work).

REFERENCES

[1] EPA, "Exposure Factors Handbook 2011 Edition " 2011.

[2] B. Nemery, P. H. M. Hoet, and A. Nemmar, "The Meuse Valley fog of 1930: An air pollution disaster," *Lancet,* vol. 357, pp. 704-708, 2001.

[3] M. L. Bell and D. L. Davis, "Reassessment of the lethal London fog of 1952: Novel indicators of acute and chronic consequences of acute exposure to air pollution," *Environmental Health Perspectives,* vol. 109, pp. 389-394, 2001.

[4] EPA, "Clean Air Act."

[5] WHO, "Air Quality Guidelines for Europe," vol. second edition, 2000.

[6] E. E. Agency, "Europe's environment: the second assessment," 1998.

[7] E. E. Agency, "Air quality in Europe — 2018 report," 2018.

[8] WHO, "Overview of the environment and health in Europe in the 1990s: Third Ministerial Conference on Environment and Health, London,16–18 June 1999.," 1999.

[9] W. H. Organization, "Recommendations for concentration–response functions for cost–benefit analysis of particulate matter, ozone and nitrogen dioxide," *Health risks of air pollution in Europe – HRAPIE project,* 2013.

[10] O. Schmid, W. Möller, M. Semmler-Behnke, G. A. Ferron, E. Karg, J. Lipka, *et al.,* "Dosimetry and toxicology of inhaled ultrafine particles," *Biomarkers,* vol. 14, pp. 67-73, 2009.

[11] G. Buonanno, G. Marks, and L. Morawska, "Health effects of daily airborne particle dose in children: direct association between personal dose and respiratory health effects," *Environmental Pollution,* vol. 180, pp. 246-250, 2013.

[12] S. Buteau and M. S. Goldberg, "A structured review of panel studies used to investigate associations between ambient air pollution and heart rate variability," *Environ Res,* vol. 148, pp. 207-47, Jul 2016.

[13] R. D. Brook, M. Jerrett, J. R. Brook, R. L. Bard, and M. M. Finkelstein, "The relationship between diabetes mellitus and traffic-related air pollution," *J Occup Environ Med,* vol. 50, pp. 32-8, Jan 2008.

[14] A. H. Auchincloss, A. V. Diez Roux, J. T. Dvonch, P. L. Brown, R. G. Barr, M. L. Daviglus, *et al.,* "Associations between Recent Exposure to Ambient Fine Particulate Matter and Blood Pressure in the Multi-Ethnic Study of Atherosclerosis (MESA)," *Environmental Health Perspectives,* vol. 116, pp. 486-491, 01/24

09/19/received

01/10/accepted 2008.

[15] M. C. Power, M. G. Weisskopf, S. E. Alexeeff, B. A. Coull, A. Spiro, 3rd, and J. Schwartz, "Traffic-related air pollution and cognitive function in a cohort of older men," *Environ Health Perspect,* vol. 119, pp. 682-7, May 2011.

[16] R. Beelen, M. Stafoggia, O. Raaschou-Nielsen, Z. J. Andersen, W. W. Xun, K. Katsouyanni, *et al.*, "Long-term exposure to air pollution and cardiovascular mortality: An analysis of 22 European cohorts," *Epidemiology*, 2014.

[17] International Agency for Research on Cancer, "IARC: Outdoor air pollution a leading environmental cause of cancer deaths," Lyon/Geneva, 17 October 201317 October 2013 2013.

[18] C. A. Pope III and D. W. Dockery, "Health effects of fine particulate air pollution: Lines that connect," *Journal of the Air and Waste Management Association*, vol. 56, pp. 709-742, 2006.

[19] J. H. Seinfeld and S. N. Pandis, *Atmospheric Chemistry And Physics: From Air Pollution to Climate Change (2nd edition)*, 1998.

[20] I. Nikolova, S. Janssen, K. Vrancken, P. Vos, V. Mishra, and P. Berghmans, "Size resolved ultrafine particles emission model - A continues size distribution approach," *Science of the Total Environment*, vol. 409, pp. 3492-3499, 2011.

[21] Y. Zhu, D. C. Fung, N. Kennedy, W. C. Hinds, and A. Eiguren-Fernandez, "Measurements of ultrafine particles and other vehicular pollutants inside a mobile exposure system on Los Angeles freeways," *Journal of the Air and Waste Management Association*, vol. 58, pp. 424-434, 2008.

[22] S. Bhuyan and A. Biswas, "Investigations on self-starting and performance characteristics of simple H and hybrid H-Savonius vertical axis wind rotors," *Energy Conversion and Management*, vol. 87, pp. 859-867, 2014.

[23] M. Scungio, G. Buonanno, F. Arpino, and G. Ficco, "Influential parameters on ultrafine particle concentration downwind at waste-to-energy plants," *Waste Management*, vol. 38, pp. 157-163, 2015.

[24] I. Neft, M. Scungio, N. Culver, and S. Singh, "Simulations of aerosol filtration by vegetation: Validation of existing models with available lab data and application to near-roadway scenario," *Aerosol Science and Technology*, vol. 50, pp. 937-946, 2016.

[25] P. J. Landrigan, R. Fuller, N. J. R. Acosta, O. Adeyi, R. Arnold, N. Basu, *et al.*, "The Lancet Commission on pollution and health," *The Lancet*, vol. 391, pp. 462-512, 2018/02/03/ 2018.

[26] K. Unfried, C. Albrecht, L.-O. Klotz, A. Von Mikecz, S. Grether-Beck, and R. P. F. Schins, "Cellular responses to nanoparticles: Target structures and mechanisms," *Nanotoxicology*, vol. 1, pp. 52-71, 2007/01/01 2007.

[27] E. G. Cauda, B. K. Ku, A. L. Miller, and T. L. Barone, "Toward developing a new occupational exposure metric approach for characterization of diesel aerosols," *Aerosol Science and Technology*, vol. 46, pp. 1370-1381, 2012.

[28] R. Hauser, J. J. Godleski, V. Hatch, and D. C. Christiani, "Ultrafine Particles in Human Lung Macrophages," *Archives of Environmental Health: An International Journal*, vol. 56, pp. 150-156, 2001/03/01 2001.

[29] B. Giechaskiel, B. Alföldy, and Y. Drossinos, "A metric for health effects studies of diesel exhaust particles," *Journal of Aerosol Science*, vol. 40, pp. 639-651, 2009.

[30] T. Stoeger, C. Reinhard, S. Takenaka, A. Schroeppel, E. Karg, B. Ritter, *et al.*, "Instillation of six different ultrafine carbon particles indicates a surface area threshold dose for acute lung inflammation in mice," *Environmental Health Perspectives*, vol. 114, pp. 328-333, 2006.

[31] O. Schmid and T. Stoeger, "Surface area is the biologically most effective dose metric for acute nanoparticle toxicity in the lung," *Journal of Aerosol Science*, vol. 99, pp. 133-143, 9// 2016.

[32] EPA, "Report to congress on black carbon," 2010.
[33] United Nations, "Effects of Air Pollution on Health - Report from the fifteenth meeting of the Joint Task Force on the Health Aspects of Air Pollution," Economic and Social Council - Economic Commission for Europe, Geneve2012.
[34] N. Janssen, M. Simic-Lawson, G. Hoek, P. Fischer, B. Brunekreef, R. Atkinson, *et al.*, "Black Smoke as an Additional Indicator to Evaluate the Health Benefits of Traffic-related Policy Measures: A Systematic Review of the Health Effects of Black Smoke Compared to PM Mass," *Epidemiology*, vol. 22, pp. S199-S200 10.1097/01.ede.0000392294.88487.14, 2011.
[35] P. Vanderstraeten, Forton, M., Brasseur, O., Offer, Z.Y.,, "Black Carbon Instead of Particle Mass Concentration as an Indicator for the Traffic Related Particles in the Brussels Capital Region," *Journal of Environmental Protection*, vol. 2, pp. 525-532, 2011.
[36] E. H. Wilker, A. Baccarelli, H. Suh, P. Vokonas, R. O. Wright, and J. Schwartz, "Black carbon exposures, blood pressure, and interactions with single nucleotide polymorphisms in microRNA processing genes," *Environmental Health Perspectives*, vol. 118, pp. 943-948, 2010.
[37] D. Q. Rich, J. Schwartz, M. A. Mittleman, M. Link, H. Luttmann-Gibson, P. J. Catalano, *et al.*, "Association of short-term ambient air pollution concentrations and ventricular arrhythmias," *American Journal of Epidemiology*, vol. 161, pp. 1123-1132, 2005.
[38] R. J. Delfino, T. Tjoa, D. L. Gillen, N. Staimer, A. Polidori, M. Arhami, *et al.*, "Traffic-related air pollution and blood pressure in elderly subjects with coronary artery disease," *Epidemiology*, vol. 21, pp. 396-404, 2010.
[39] A. Zanobetti, A. Baccarelli, and J. Schwartz, "Gene-Air Pollution Interaction and Cardiovascular Disease: A Review," *Progress in Cardiovascular Diseases*, vol. 53, pp. 344-352, 2011.
[40] S. F. Suglia, A. Gryparis, J. Schwartz, and R. J. Wright, "Association between traffic-related black carbon exposure and lung function among urban women," *Environmental Health Perspectives*, vol. 116, pp. 1333-1337, 2008.
[41] J. Schneider, U. Kirchner, S. Borrmann, R. Vogt, and V. Scheer, "In situ measurements of particle number concentration, chemically resolved size distributions and black carbon content of traffic-related emissions on German motorways, rural roads and in city traffic," *Atmospheric Environment*, vol. 42, pp. 4257-4268, 2008.
[42] K. H. Kim, K. Sekiguchi, S. Kudo, and K. Sakamoto, "Characteristics of atmospheric elemental carbon (char and soot) in ultrafine and fine particles in a roadside environment, Japan," *Aerosol and Air Quality Research*, vol. 11, pp. 1-12, 2011.
[43] X. Zhou, J. Gao, T. Wang, W. Wu, and W. Wang, "Measurement of black carbon aerosols near two Chinese megacities and the implications for improving emission inventories," *Atmospheric Environment*, vol. 43, pp. 3918-3924, 2009.
[44] M. Brines, M. Dall'Osto, D. C. S. Beddows, R. M. Harrison, F. Gómez-Moreno, L. Núñez, *et al.*, "Traffic and nucleation events as main sources of ultrafine particles in high-insolation developed world cities," *Atmospheric Chemistry and Physics*, vol. 15, pp. 5929-5945, 2015.
[45] S. Weichenthal, "Selected physiological effects of ultrafine particles in acute cardiovascular morbidity," *Environmental Research*, vol. 115, pp. 26-36, 2012.
[46] M. Semmler, J. Seitz, F. Erbe, P. Mayer, J. Heyder, G. Oberdörster, *et al.*, "Long-term clearance kinetics of inhaled ultrafine insoluble iridium particles from the

rat lung, including transient translocation into secondary organs," *Inhalation Toxicology,* vol. 16, pp. 453-459, 2004.

[47] D. Loomis, "Sizing up air pollution research," *Epidemiology,* vol. 11, pp. 2-4, 2000.

[48] C. A. Pope, "What do epidemiologic findings tell us about health effects of environmental aerosols?," *Journal of Aerosol Medicine: Deposition, Clearance, and Effects in the Lung,* vol. 13, pp. 335-354, 2000.

[49] U. Franck, S. Odeh, A. Wiedensohler, B. Wehner, and O. Herbarth, "The effect of particle size on cardiovascular disorders - The smaller the worse," *Science of the Total Environment,* vol. 409, pp. 4217-4221, 2011.

[50] P. Kumar, L. Morawska, W. Birmili, P. Paasonen, M. Hu, M. Kulmala, *et al.*, "Ultrafine particles in cities," *Environment International,* vol. 66, pp. 1-10, 2014.

[51] T. M. Sager and V. Castranova, "Surface area of particle administered versus mass in determining the pulmonary toxicity of ultrafine and fine carbon black: comparison to ultrafine titanium dioxide," *Particle and Fibre Toxicology,* vol. 6, pp. 15-15, 05/04

09/30/received

05/04/accepted 2009.

[52] D. M. Brown, M. R. Wilson, W. MacNee, V. Stone, and K. Donaldson, "Size-dependent proinflammatory effects of ultrafine polystyrene particles: A role for surface area and oxidative stress in the enhanced activity of ultrafines," *Toxicology and Applied Pharmacology,* vol. 175, pp. 191-199, 2001.

[53] U. C. Nygaar, M. Samuelsen, A. Aase, and M. Løvik, "The capacity of particles to increase allergic sensitization is predicted by particle number and surface area, not by particle mass," *Toxicological Sciences,* vol. 82, pp. 515-524, 2004.

[54] C. M. Sayes, K. L. Reed, and D. B. Warheit, "Assessing toxicology of fine and nanoparticles: Comparing in vitro measurements to in vivo pulmonary toxicity profiles," *Toxicological Sciences,* vol. 97, pp. 163-180, 2007.

[55] G. Oberdorster, E. Oberdorster, and J. Oberdorster, "Nanotoxicology: an emerging discipline evolving from studies of ultrafine particles," *Environ Health Perspect,* vol. 113, pp. 823-39, Jul 2005.

[56] C. L. Tran, D. Buchanan, R. T. Cullen, A. Searl, A. D. Jones, and K. Donaldson, "Inhalation of poorly soluble particles. II. Influence Of particle surface area on inflammation and clearance," *Inhal Toxicol,* vol. 12, pp. 1113-26, Dec 2000.

[57] G. N. Sze-To, C. L. Wu, C. Y. H. Chao, M. P. Wan, and T. C. Chan, "Exposure and cancer risk toward cooking-generated ultrafine and coarse particles in Hong Kong homes," *HVAC and R Research,* vol. 18, pp. 204-216, 2012.

[58] *EU Directive 2008/50/EC of the European Parliament and of the Council of 21 May 2008 on ambient air quality and cleaner air for Europe, 2008,* L 152/1, 2008.

[59] G. Buonanno, M. Dell'Isola, L. Stabile, and A. Viola, "Critical Aspects of the Uncertainty Budget in the Gravimetric PM Measurements," *Measurement,* vol. 44, pp. 139-147, 2010.

[60] V. Rizza, L. Stabile, G. Buonanno, and L. Morawska, "Variability of airborne particle metrics in an urban area," *Environmental Pollution,* vol. 220, pp. 625-635, 2017.

[61] S. Kaur, M. J. Nieuwenhuijsen, and R. N. Colvile, "Pedestrian exposure to air pollution along a major road in Central London, UK," *Atmospheric Environment,* vol. 39, pp. 7307-7320, 2005/12/01/ 2005.

[62] P. Kumar, M. Ketzel, S. Vardoulakis, L. Pirjola, and R. Britter, "Dynamics and dispersion modelling of nanoparticles from road traffic in the urban atmospheric environment—A review," *Journal of Aerosol Science,* vol. 42, pp. 580-603, 2011/09/01/ 2011.

[63] M. Cepeda, J. Schoufour, R. Freak-Poli, C. M. Koolhaas, K. Dhana, W. M. Bramer, *et al.*, "Levels of ambient air pollution according to mode of transport: a systematic review," *The Lancet Public Health,* vol. 2, pp. e23-e34, 2017/01/01/ 2017.

[64] G. Hoek, R. M. Krishnan, R. Beelen, A. Peters, B. Ostro, B. Brunekreef, *et al.*, "Long-term air pollution exposure and cardio- respiratory mortality: a review," *Environmental Health,* vol. 12, p. 43, 2013/05/28 2013.

[65] F. Amato, M. Pandolfi, T. Moreno, M. Furger, J. Pey, A. Alastuey, *et al.*, "Sources and variability of inhalable road dust particles in three European cities," *Atmospheric Environment,* vol. 45, pp. 6777-6787, 2011/12/01/ 2011.

[66] Y. Zhu, W. C. Hinds, S. Kim, S. Shen, and C. Sioutas, "Study of ultrafine particles near a major highway with heavy-duty diesel traffic," *Atmospheric Environment,* vol. 36, pp. 4323-4335, 2002.

[67] E. S. Lee, M. K. Stenstrom, and Y. Zhu, "Ultrafine particle infiltration into passenger vehicles. Part I: Experimental evidence," *Transportation Research Part D: Transport and Environment,* vol. 38, pp. 156-165, 2015/07/01/ 2015.

[68] A. Leavey, N. Reed, S. Patel, K. Bradley, P. Kulkarni, and P. Biswas, "Comparing on-road real-time simultaneous in-cabin and outdoor particulate and gaseous concentrations for a range of ventilation scenarios," *Atmospheric Environment,* vol. 166, pp. 130-141, 2017/10/01/ 2017.

[69] T. Moreno, C. Reche, I. Rivas, M. Cruz Minguillón, V. Martins, C. Vargas, *et al.*, "Urban air quality comparison for bus, tram, subway and pedestrian commutes in Barcelona," *Environmental Research,* vol. 142, pp. 495-510, 10// 2015.

[70] G. Buonanno, G. Giovinco, L. Morawska, and L. Stabile, "Tracheobronchial and alveolar dose of submicrometer particles for different population age groups in Italy," *Atmospheric Environment,* vol. 45, pp. 6216-6224, 2011.

[71] C. A. Pope III and D. W. Dockery, "Health effects of fine particulate air pollution: lines that connect," *Journal of Air and Waste Management Association,* vol. 56, pp. 707-742, 2006.

[72] D. Brugge, J. L. Durant, and C. Rioux, "Near-highway pollutants in motor vehicle exhaust :a review of epidemiologic evidence of cardiac and pulmonary health risks," *Environmental Health,* vol. 6, 2007.

[73] Z. J. Andersen, M. Ketzel, S. Loft, and O. Raaschou-Nielsen, "Association between short-term exposure to ultrafine particles and hospital admissions for stroke in Copenhagen, Denmark," *European Heart Journal,* vol. 16, pp. 2034-2040, 2010.

[74] H. Kikumoto and R. Ooka, "A study on air pollutant dispersion with bimolecular reactions in urban street canyons using large-eddy simulations," *Journal of Wind Engineering and Industrial Aerodynamics,* vol. 104-106, pp. 516-522, 2012.

[75] D. Hertwig, G. C. Efthimiou, J. G. Bartzis, and B. Leitl, "CFD-RANS model validation of turbulent flow in a semi-idealized urban canopy," *Journal of Wind Engineering and Industrial Aerodynamics,* vol. 111, pp. 61-72, 2012.

[76] M. Scungio, F. Arpino, L. Stabile, and G. Buonanno, "Numerical simulation of ultrafine particle dispersion in urban street canyons with the spalart-allmaras

turbulence model," *Aerosol and Air Quality Research,* vol. 13, pp. 1423-1437, 2013.

[77] M. Scungio, F. Arpino, G. Cortellessa, and G. Buonanno, "Detached eddy simulation of turbulent flow in isolated street canyons of different aspect ratios," *Atmospheric Pollution Research,* vol. 6, pp. 351-364, 2015.

[78] X. Querol, A. Alastuey, C. R. Ruiz, B. Artiñano, H. C. Hansson, R. M. Harrison, *et al.*, "Speciation and origin of PM10 and PM2.5 in selected European cities," *Atmospheric Environment,* vol. 38, pp. 6547-6555, 2004.

[79] M. Eeftens, M.-Y. Tsai, C. Ampe, B. Anwander, R. Beelen, T. Bellander, *et al.*, "Spatial variation of PM2.5, PM10, PM2.5 absorbance and PMcoarse concentrations between and within 20 European study areas and the relationship with NO2 – Results of the ESCAPE project," *Atmospheric Environment,* vol. 62, pp. 303-317, 12// 2012.

[80] L. R. Crilley, G. A. Ayoko, E. Stelcer, D. D. Cohen, M. Mazaheri, and L. Morawska, "Elemental Composition of Ambient Fine Particles in Urban Schools: Sources of Children’s Exposure," *Aerosol and Air Quality Research,* vol. 14, pp. 1906-1916, 2014.

[81] C. Reche, I. Rivas, M. Pandolfi, M. Viana, L. Bouso, M. Àlvarez-Pedrerol, *et al.*, "Real-time indoor and outdoor measurements of black carbon at primary schools," *Atmospheric Environment,* vol. 120, pp. 417-426, 2015.

[82] M. C. Minguillón, I. Rivas, T. Moreno, A. Alastuey, O. Font, P. Córdoba, *et al.*, "Road traffic and sandy playground influence on ambient pollutants in schools," *Atmospheric Environment,* vol. 111, pp. 94-102, 2015/06/01/ 2015.

[83] I. Rivas, M. Viana, T. Moreno, M. Pandolfi, F. Amato, C. Reche, *et al.*, "Child exposure to indoor and outdoor air pollutants in schools in Barcelona, Spain," *Environment International,* vol. 69, pp. 200-212, 2014/08/01/ 2014.

[84] R. L. Brent and M. Weitzman, "The Vulnerability, Sensitivity, and Resiliency of the Developing Embryo, Infant, Child, and Adolescent to the Effects of Environmental Chemicals, Drugs, and Physical Agents as Compared to the Adult: Preface," *Pediatrics,* vol. 113, pp. 933-934, 2004.

[85] A. Makri and N. I. Stilianakis, "Vulnerability to air pollution health effects," *International Journal of Hygiene and Environmental Health,* vol. 211, pp. 326-336, 2008.

[86] G. L. Ginsberg, B. P. Foos, and M. P. Firestone, "Review and analysis of inhalation dosimetry methods for application to children's risk assessment," *Journal of Toxicology and Environmental Health - Part A,* vol. 68, pp. 573-615, 2005.

[87] J. Heinrich and R. Slama, "Fine particles, a major threat to children," *International Journal of Hygiene and Environmental Health,* vol. 210, pp. 617-622, 2007.

[88] T. F. Bateson and J. Schwartz, "Children's response to air pollutants," *Journal of Toxicology and Environmental Health - Part A: Current Issues,* vol. 71, pp. 238-243, 2008.

[89] M. K. Selgrade, C. G. Plopper, M. I. Gilmour, R. B. Conolly, and B. S. Foos, "Assessing the health effects and risks associated with children's inhalation exposures--asthma and allergy," *J Toxicol Environ Health A,* vol. 71, pp. 196-207, 2008.

[90] OECD, *How long do students spend in the classroom?*: OECD Publishing, 2012.

[91] L. Stabile, M. Dell'Isola, A. Frattolillo, A. Massimo, and A. Russi, "Effect of natural ventilation and manual airing on indoor air quality in naturally ventilated Italian classrooms," *Building and Environment,* vol. 98, pp. 180-189, 3// 2016.

[92] B. Stephens and J. A. Siegel, "Penetration of ambient submicron particles into single-family residences and associations with building characteristics," *Indoor Air,* vol. 22, pp. 501-13, Dec 2012.

[93] C. Chen and B. Zhao, "Review of relationship between indoor and outdoor particles: I/O ratio, infiltration factor and penetration factor," *Atmospheric Environment,* vol. 45, pp. 275-288, 1// 2011.

[94] Y. Zhu, W. C. Hinds, M. Krudysz, T. Kuhn, J. Froines, and C. Sioutas, "Penetration of freeway ultrafine particles into indoor environments," *Journal of Aerosol Science,* vol. 36, pp. 303-322, 2005.

[95] M. Viana, S. Díez, and C. Reche, "Indoor and outdoor sources and infiltration processes of PM1 and black carbon in an urban environment," *Atmospheric Environment,* vol. 45, pp. 6359-6367, 2011.

[96] N. Tippayawong, P. Khuntong, C. Nitatwichit, Y. Khunatorn, and C. Tantakitti, "Indoor/outdoor relationships of size-resolved particle concentrations in naturally ventilated school environments," *Building and Environment,* vol. 44, pp. 188-197, 2009.

[97] R. W. Atkinson, G. W. Fuller, H. R. Anderson, R. M. Harrison, and B. Armstrong, "Urban ambient particle metrics and health: a time-series analysis," *Epidemiology,* vol. 21, pp. 501-11, Jul 2010.

[98] S. Lanzinger, A. Schneider, S. Breitner, M. Stafoggia, I. Erzen, M. Dostal, *et al.*, "Associations between ultrafine and fine particles and mortality in five central European cities - Results from the UFIREG study," *Environ Int,* vol. 88, pp. 44-52, Mar 2016.

[99] B. Ostro, A. Tobias, A. Karanasiou, E. Samoli, X. Querol, S. Rodopoulou, *et al.*, "The risks of acute exposure to black carbon in Southern Europe: results from the MED-PARTICLES project," *Occup Environ Med,* vol. 72, pp. 123-9, Feb 2015.

[100] I. Rivas, M. Viana, T. Moreno, L. Bouso, M. Pandolfi, M. Alvarez-Pedrerol, *et al.*, "Outdoor infiltration and indoor contribution of UFP and BC, OC, secondary inorganic ions and metals in PM2.5 in schools," *Atmospheric Environment,* vol. 106, pp. 129-138, 2015/04/01/ 2015.

[101] M. Stafoggia, A. Schneider, J. Cyrys, E. Samoli, Z. J. Andersen, G. B. Bedada, *et al.*, "Association Between Short-term Exposure to Ultrafine Particles and Mortality in Eight European Urban Areas," *Epidemiology,* vol. 28, pp. 172-180, Mar 2017.

[102] J. Sunyer, M. Esnaola, M. Alvarez-Pedrerol, J. Forns, I. Rivas, M. Lopez-Vicente, *et al.*, "Association between traffic-related air pollution in schools and cognitive development in primary school children: a prospective cohort study," *PLoS Med,* vol. 12, p. e1001792, Mar 2015.

[103] Health Effects Institute, "Understanding the Health Effects of Ambient Ultrafine Particles. HEI Perspectives 3.," Boston, MA2013.

[104] G. Buonanno, F. C. Fuoco, L. Morawska, and L. Stabile, "Airborne particle concentrations at schools measured at different spatial scales," *Atmospheric Environment,* vol. 67, pp. 38-45, 2013.

[105] A. Pacitto, L. Stabile, M. Viana, M. Scungio, C. Reche, X. Querol, *et al.*, "Particle-related exposure, dose and lung cancer risk of primary school children

in two European countries," *Science of the Total Environment,* vol. 616-617, pp. 720-729, 2018.

[106] M. J. Mendell and G. A. Heath, "Do indoor pollutants and thermal conditions in schools influence student performance? A critical review of the literature," *Indoor Air,* vol. 15, pp. 27-52, 2005/01/01 2005.

[107] J. Jiang, D. Wang, Y. Liu, Y. Xu, and J. Liu, *A study on pupils' learning performance and thermal comfort of primary schools in China* vol. 134, 2018.

[108] M. Schweiker, G. M. Huebner, B. R. M. Kingma, R. Kramer, and H. Pallubinsky, "Drivers of diversity in human thermal perception – A review for holistic comfort models," *Temperature,* vol. 5, pp. 308-342, 2018/10/02 2018.

[109] J. G. Allen, P. MacNaughton, U. Satish, S. Santanam, J. Vallarino, and J. D. Spengler, "Associations of Cognitive Function Scores with Carbon Dioxide, Ventilation, and Volatile Organic Compound Exposures in Office Workers: A Controlled Exposure Study of Green and Conventional Office Environments," *Environmental health perspectives,* vol. 124, pp. 805-812, 2016.

[110] European Committee for Standardisation, "UNI EN 15251 - Indoor environmental input parameters for design and assessment of energy performance of buildings addressing indoor air quality, thermal environment, lighting and acoustics," ed. Brussels, Belgium: European Committee for Standardisation, 2008.

[111] L. Chatzidiakou, D. Mumovic, and A. Summerfield, "Is CO2 a good proxy for indoor air quality in classrooms? Part 1: The interrelationships between thermal conditions, CO2 levels, ventilation rates and selected indoor pollutants," *Building Services Engineering Research and Technology,* vol. 36, pp. 129-161, 2015.

[112] U. Satish, M. J. Mendell, K. Shekhar, T. Hotchi, D. Sullivan, S. Streufert, *et al.*, "Is CO2 an indoor pollutant? Direct effects of low-to-moderate CO2 concentrations on human decision-making performance," *Environmental health perspectives,* vol. 120, pp. 1671-1677, 2012.

[113] L. Morawska, G. A. Ayoko, G. N. Bae, G. Buonanno, C. Y. H. Chao, S. Clifford, *et al.*, "Airborne particles in indoor environment of homes, schools, offices and aged care facilities: The main routes of exposure," *Environ Int,* vol. 108, pp. 75-83, Nov 2017.

[114] T. Salthammer, E. Uhde, T. Schripp, A. Schieweck, L. Morawska, M. Mazaheri, *et al.*, "Children's well-being at schools: Impact of climatic conditions and air pollution," *Environment International,* vol. 94, pp. 196-210, 9// 2016.

[115] L. Stabile, M. Dell'Isola, A. Russi, A. Massimo, and G. Buonanno, "The effect of natural ventilation strategy on indoor air quality in schools," *Science of the Total Environment,* vol. 595, pp. 894-902, 2017.

[116] M. Cipolla, M. Bruzzone, E. Stagnaro, M. Ceppi, A. Izzotti, C. Culotta, *et al.*, "Health Issues of Primary School Students Residing in Proximity of an Oil Terminal with Environmental Exposure to Volatile Organic Compounds," *BioMed research international,* vol. 2016, pp. 4574138-4574138, 2016.

[117] S. Clifford, M. Mazaheri, F. Salimi, W. N. Ezz, B. Yeganeh, S. Low-Choy, *et al.*, "Effects of exposure to ambient ultrafine particles on respiratory health and systemic inflammation in children," *Environment International,* vol. 114, pp. 167-180, 2018/05/01/ 2018.

[118] K. Gordon, P. D. Terry, X. Liu, T. Harris, D. Vowell, B. Yard, *et al.*, "Radon in Schools: A Brief Review of State Laws and Regulations in the United States,"

International journal of environmental research and public health, vol. 15, p. 2149, 2018.

[119] V. Rizza, L. Stabile, D. Vistocco, A. Russi, S. Pardi, and G. Buonanno, "Effects of the exposure to ultrafine particles on heart rate in a healthy population," *Sci Total Environ*, vol. 650, pp. 2403-2410, Feb 10 2019.

[120] J. A. Swenberg, B. C. Moeller, K. Lu, J. E. Rager, R. C. Fry, and T. B. Starr, "Formaldehyde carcinogenicity research: 30 years and counting for mode of action, epidemiology, and cancer risk assessment," *Toxicologic pathology*, vol. 41, pp. 181-189, 2013.

[121] L. Stabile, G. Buonanno, P. Avino, and F. C. Fuoco, "Dimensional and chemical characterization of airborne particles in schools: Respiratory effects in children," *Aerosol and Air Quality Research*, vol. 13, pp. 887-900, 2013.

[122] L. Stabile, G. Buonanno, A. Frattolillo, and M. Dell'Isola, "The effect of the ventilation retrofit in a school on CO 2 , airborne particles, and energy consumptions," *Building and Environment*, vol. 156, pp. 1-11, 2019.

[123] Intelligent Energy for Europe Programme, "Energy Efficiency Trends and Policies in the Household and Tertiary Sectors. An Analysis Based on the ODYSSEE and MURE Databases," http://www.odyssee-mure.eu/publications/br/energy-efficiency-in-buildings.html2015.

[124] W. Chan, S.-C. Lee, A. Hon, L. Liu, D. Li, and N. Zhu, "Management learning from air purifier tests in hotels: Experiment and action research," *International Journal of Hospitality Management*, vol. 44, pp. 70-76, 2015/01/01/ 2015.

[125] M. Kim, G.-T. Lim, Y.-J. Kim, B. Han, C. G. Woo, and H.-J. Kim, "A novel electrostatic precipitator-type small air purifier with a carbon fiber ionizer and an activated carbon fiber filter," *Journal of Aerosol Science*, vol. 117, pp. 63-73, 2018/03/01/ 2018.

[126] H. Ma, H. Shen, T. Shui, Q. Li, and L. Zhou, "Experimental Study on Ultrafine Particle Removal Performance of Portable Air Cleaners with Different Filters in an Office Room," *International journal of environmental research and public health*, vol. 13, p. 102, 2016.

[127] K.-C. Noh and S.-J. Yook, "Evaluation of clean air delivery rates and operating cost effectiveness for room air cleaner and ventilation system in a small lecture room," *Energy and Buildings*, vol. 119, pp. 111-118, 2016/05/01/ 2016.

[128] H.-J. Oh, I.-S. Nam, H. Yun, J. Kim, J. Yang, and J.-R. Sohn, "Characterization of indoor air quality and efficiency of air purifier in childcare centers, Korea," *Building and Environment*, vol. 82, pp. 203-214, 2014/12/01/ 2014.

[129] R. L. Peck, S. A. Grinshpun, M. Yermakov, M. B. Rao, J. Kim, and T. Reponen, "Efficiency of portable HEPA air purifiers against traffic related combustion particles," *Building and Environment*, vol. 98, pp. 21-29, 2016/03/01/ 2016.

[130] S. Schumacher, D. Spiegelhoff, U. Schneiderwind, H. Finger, and C. Asbach, "Performance of New and Artificially Aged Electret Filters in Indoor Air Cleaners," *Chemical Engineering & Technology*, vol. 41, pp. 27-34, 2018/01/01 2018.

[131] M. Zuurbier, G. Hoek, P. V. D. Hazel, and B. Brunekreef, "Minute ventilation of cyclists, car and bus passengers: An experimental study," *Environmental Health: A Global Access Science Source*, vol. 8, 2009.

[132] L. Int Panis, B. De Geus, G. Vandenbulcke, H. Willems, B. Degraeuwe, N. Bleux, *et al.*, *Exposure to Particulate Matter in Traffic: A Comparison of Cyclists and Car Passengers* vol. 44, 2010.

[133] G. Buonanno, L. Stabile, and L. Morawska, "Personal exposure to ultrafine particles: the influence of time-activity patterns," *Science of the Total Environment,* vol. 468–469, pp. 903–907, 2014.

[134] C. Schweizer, R. D. Edwards, L. Bayer-Oglesby, W. J. Gauderman, V. Ilacqua, M. Juhani Jantunen, *et al.*, "Indoor time-microenvironment-activity patterns in seven regions of Europe," *J Expos Sci Environ Epidemiol,* vol. 17, pp. 170-181, 05/17/online 2006.

[135] G. Bekö, B. U. Kjeldsen, Y. Olsen, J. Schipperijn, A. Wierzbicka, D. G. Karottki, *et al.*, "Contribution of various microenvironments to the daily personal exposure to ultrafine particles: Personal monitoring coupled with GPS tracking," *Atmospheric Environment,* vol. 110, pp. 122-129, 6// 2015.

[136] International Commission on Radiological Protection, "Human respiratory tract model for radiological protection. A report of a Task Group of the International Commission on Radiological Protection.," *Annals of the ICRP*, vol. 24, pp. 1-482, 1994.

[137] G. Buonanno, L. Morawska, L. Stabile, L. Wang, and G. Giovinco, "A comparison of submicrometer particle dose between Australian and Italian people," *Environmental Pollution,* vol. 169, pp. 183-189, 2012/10/01/ 2012.

[138] N. E. Klepeis, "Modeling human exposure to air pollution," in *Exposure Analysis*, L. A. Wallace, Steinemann, A.C., Ott, W.R., Ed., ed: CRC Press, 2006, pp. 445–470.

[139] L. Stabile, G. Buonanno, G. Ficco, and M. Scungio, "Smokers' lung cancer risk related to the cigarette-generated mainstream particles," *Journal of Aerosol Science,* vol. 107, pp. 41-54, May 2017.

[140] L. Wallace and W. Ott, "Personal exposure to ultrafine particles," *Journal of Exposure Science and Environmental Epidemiology,* vol. 21, pp. 20-30, 2011.

[141] European Environmental Agency, "Air quality in Europe - 2016 report," Luxembourg2016.

[142] C. Isaxon, A. Gudmundsson, E. Z. Nordin, L. Lönnblad, A. Dahl, G. Wieslander, *et al.*, "Contribution of indoor-generated particles to residential exposure," *Atmospheric Environment,* vol. 106, pp. 458-466, 4// 2015.

[143] P. Kumar and A. Goel, "Concentration dynamics of coarse and fine particulate matter at and around signalised traffic intersections," *Environ Sci Process Impacts,* vol. 18, pp. 1220-35, Sep 14 2016.

[144] M. Mazaheri, S. Clifford, R. Jayaratne, M. A. Megat Mokhtar, F. Fuoco, G. Buonanno, *et al.*, "School Children's Personal Exposure to Ultrafine Particles in the Urban Environment," *Environmental Science & Technology,* vol. 48, pp. 113-120, 2014/01/07 2014.

[145] L. Stabile, M. Scungio, G. Buonanno, F. Arpino, and G. Ficco, "Airborne particle emission of a commercial 3D printer: the effect of filament material and printing temperature," *Indoor Air,* vol. 27, pp. 398-408, 2017.

[146] M. Scungio, T. Vitanza, L. Stabile, G. Buonanno, and L. Morawska, "Characterization of particle emission from laser printers," *Science of the Total Environment,* vol. 586, pp. 623-630, 2017.

[147] L. Morawska, A. Afshari, G. N. Bae, G. Buonanno, C. Y. Chao, O. Hanninen, *et al.*, "Indoor aerosols: from personal exposure to risk assessment," *Indoor Air,* vol. 23, pp. 462-87, Dec 2013.

[148] Z. Bakó-Biró, D. J. Clements-Croome, N. Kochhar, H. B. Awbi, and M. J. Williams, "Ventilation rates in schools and pupils' performance," *Building and Environment,* vol. 48, pp. 215-223, 2// 2012.

[149] *Customised Report. Cat. No. 4430.0.*, Australian Bureau of Statistics EPA 600/P-99/002aF-bF, 2010.
[150] M. E. Soggiu, C. Vollono, and A. Bastone, "Human exposure assessment to environmental contaminants: exposure scenarios.," Istituto Superiore di Sanità (Italy)2010.
[151] D. Lader, S. Short, and J. Gershuny, *The Time Use Survey, 2005. How we spend our time*. London: Office for National Statistics, 2006.
[152] F. McGinnity, H. Russel, J. Williams, and S. Blackwell, *Time use in Ireland, 2005. Survey Report.* Dublin: The Economic and Social Research Institute, 2005.
[153] Statistics Sweden Economic Welfare Statistics Unit, *Swedish Time Use Survey 2010/11*. vol. Living Conditions Report 123. Orebro, 2012.
[154] Instituto Nacional de Estadística. Encuesta de Empleo del Tiempo 2009-2010. Resultados definitivos available at http://www.ine.es [Online].
[155] G. Buonanno, L. Morawska, and L. Stabile, "Particle emission factors during cooking activities," *Atmospheric Environment*, vol. 43, pp. 3235-3242, 2009.
[156] S. W. See and R. Balasubramanian, "Chemical characteristics of fine particles emitted from different gas cooking methods," *Atmospheric Environment*, vol. 42, pp. 8852-8862, 12// 2008.
[157] L. A. Wallace, W. R. Ott, and C. J. Weschler, "Ultrafine particles from electric appliances and cooking pans: experiments suggesting desorption/nucleation of sorbed organics as the primary source," *Indoor Air*, vol. 25, pp. 536-46, Oct 2015.
[158] I. Rivas, P. Kumar, and A. Hagen-Zanker, "Exposure to air pollutants during commuting in London: Are there inequalities among different socio-economic groups?," *Environ Int*, vol. 101, pp. 143-157, Apr 2017.
[159] G. Buonanno, F. C. Fuoco, and L. Stabile, "Influential parameters on particle exposure of pedestrians in urban microenvironments," *Atmospheric Environment*, vol. 45, pp. 1434-1443, 2011.
[160] A. M. Todea, S. Beckmann, H. Kaminski, D. Bard, S. Bau, S. Clavaguera, *et al.*, "Inter-comparison of personal monitors for nanoparticles exposure at workplaces and in the environment," *Sci Total Environ*, vol. 605-606, pp. 929-945, Dec 15 2017.
[161] W. H. Kruskal and W. A. Wallis, "Use of Ranks in One-Criterion Variance Analysis," *Journal of the American Statistical Association*, vol. 47, pp. 583-621, 1952/12/01 1952.
[162] M. Fierz, C. Houle, P. Steigmeier, and H. Burtscher, "Design, Calibration, and Field Performance of a Miniature Diffusion Size Classifier," *Aerosol Science and Technology*, vol. 45, pp. 1-10, 2011/01/01 2011.
[163] J. Marra, M. Voetz, and H. J. Kiesling, "Monitor for detecting and assessing exposure to airborne nanoparticles," *Journal of Nanoparticle Research*, vol. 12, pp. 21-37, 2010.
[164] G. Buonanno, E. R. Jayaratne, L. Morawska, and L. Stabile, "Metrological Performances of a Diffusion Charger Particle Counter for Personal Monitoring," *Aerosol and Air Quality Research*, vol. 14, pp. 156–167, 2014.
[165] A. Goel and P. Kumar, "A review of fundamental drivers governing the emissions, dispersion and exposure to vehicle-emitted nanoparticles at signalised traffic intersections," *Atmospheric Environment*, vol. 97, pp. 316-331, 11// 2014.
[166] P. Kumar, L. Pirjola, M. Ketzel, and R. M. Harrison, "Nanoparticle emissions from 11 non-vehicle exhaust sources – A review," *Atmospheric Environment*, vol. 67, pp. 252-277, 3// 2013.

[167] M.-A. Mokhtar, R. Jayaratne, L. Morawska, M. Mazaheri, N. Surawski, and G. Buonanno, "NSAM-derived total surface area versus SMPS-derived “mobility equivalent” surface area for different environmentally relevant aerosols," *Journal of Aerosol Science,* vol. 66, pp. 1-11, 12// 2013.

[168] L. Stabile, C. Vargas Trassierra, G. Dell'Agli, and G. Buonanno, "Ultrafine particle generation through atomization technique: the influence of the solution," *Aerosol and Air Quality Research,* vol. 13, pp. 1667–1677, 2013.

[169] G. Buonanno, L. Stabile, L. Morawska, G. Giovinco, and X. Querol, "Do air quality targets really represent safe limits for lung cancer risk?," *Science of the Total Environment,* vol. 580, pp. 74-82, 2017.

[170] L. Stabile, F. Arpino, G. Buonanno, A. Russi, and A. Frattolillo, "A simplified benchmark of ultrafine particle dispersion in idealized urban street canyons: A wind tunnel study," *Building and Environment,* vol. 93, Part 2, pp. 186-198, 11// 2015.

[171] A. Wierzbicka, M. Bohgard, J. H. Pagels, A. Dahl, J. Löndahl, T. Hussein, *et al.*, "Quantification of differences between occupancy and total monitoring periods for better assessment of exposure to particles in indoor environments," *Atmospheric Environment,* vol. 106, pp. 419-428, 4// 2015.

[172] S. An, X. Hu, and J. Wang, "Urban taxis and air pollution: a case study in Harbin, China," *Journal of Transport Geography,* vol. 19, pp. 960-967, 2011/07/01/ 2011.

[173] I. Alameddine, L. Abi Esber, E. Bou Zeid, M. Hatzopoulou, and M. El-Fadel, "Operational and environmental determinants of in-vehicle CO and PM2.5 exposure," *Science of The Total Environment,* vol. 551-552, pp. 42-50, 2016/05/01/ 2016.

[174] S. Fruin, D. Westerdahl, T. Sax, C. Sioutas, and P. M. Fine, "Measurements and predictors of on-road ultrafine particle concentrations and associated pollutants in Los Angeles," *Atmospheric Environment,* vol. 42, pp. 207-219, 2008/01/01/ 2008.

[175] N. Hudda and S. A. Fruin, "Carbon dioxide accumulation inside vehicles: The effect of ventilation and driving conditions," *Science of The Total Environment,* vol. 610-611, pp. 1448-1456, 2018/01/01/ 2018.

[176] L. Tartakovsky, V. Baibikov, J. Czerwinski, M. Gutman, M. Kasper, D. Popescu, *et al.*, "In-vehicle particle air pollution and its mitigation," *Atmospheric Environment,* vol. 64, pp. 320-328, 2013/01/01/ 2013.

[177] Y. Zhu, A. Eiguren-Fernandez, W. C. Hinds, and A. H. Miguel, "In-Cabin Commuter Exposure to Ultrafine Particles on Los Angeles Freeways," *Environmental Science & Technology,* vol. 41, pp. 2138-2145, 2007/04/01 2007.

[178] P. Paatero and U. Tapper, "Positive matrix factorization: A non-negative factor model with optimal utilization of error estimates of data values," *Environmetrics,* vol. 5, pp. 111-126, 1994.

[179] F. Amato, M. Pandolfi, A. Escrig, X. Querol, A. Alastuey, J. Pey, *et al.*, "Quantifying road dust resuspension in urban environment by Multilinear Engine: A comparison with PMF2," *Atmospheric Environment,* vol. 43, pp. 2770-2780, 2009/06/01/ 2009.

[180] P. Paatero and P. K. Hopke, "Discarding or downweighting high-noise variables in factor analytic models," *Analytica Chimica Acta,* vol. 490, pp. 277-289, 2003/08/25/ 2003.

[181] Paaetro, "End User's Guide to Multilinear Engine Applications.," 2007.

[182] P. Krecl, C. Johansson, A. C. Targino, J. Ström, and L. Burman, "Trends in black carbon and size-resolved particle number concentrations and vehicle emission factors under real-world conditions," *Atmospheric Environment,* vol. 165, pp. 155-168, 2017/09/01/ 2017.

[183] J.-Y. Chin and S. A. Batterman, "VOC composition of current motor vehicle fuels and vapors, and collinearity analyses for receptor modeling," *Chemosphere,* vol. 86, pp. 951-958, 2012/03/01/ 2012.

[184] J. Faber, K. Brodzik, A. Gołda-Kopek, and D. Łomankiewicz, "Benzene, toluene and xylenes levels in new and used vehicles of the same model," *Journal of Environmental Sciences,* vol. 25, pp. 2324-2330, 2013/11/01/ 2013.

[185] W. Y. Tsai, L. Y. Chan, D. R. Blake, and K. W. Chu, "Vehicular fuel composition and atmospheric emissions in South China: Hong Kong, Macau, Guangzhou, and Zhuhai," *Atmos. Chem. Phys.,* vol. 6, pp. 3281-3288, 2006.

[186] Z. Yao, X. Shen, Y. Ye, X. Cao, X. Jiang, Y. Zhang, *et al.*, "On-road emission characteristics of VOCs from diesel trucks in Beijing, China," *Atmospheric Environment,* vol. 103, pp. 87-93, 2015/02/01/ 2015.

[187] K. Brodzik, J. Faber, D. Łomankiewicz, and A. Gołda-Kopek, "In-vehicle VOCs composition of unconditioned, newly produced cars," *Journal of Environmental Sciences,* vol. 26, pp. 1052-1061, 2014/05/01/ 2014.

[188] J. Faber and K. Brodzik, *Air quality inside passenger cars*, 2016.

[189] L. Y. Chan, W. L. Lau, X. M. Wang, and J. H. Tang, "Preliminary measurements of aromatic VOCs in public transportation modes in Guangzhou, China," *Environment International,* vol. 29, pp. 429-435, 2003/07/01/ 2003.

[190] M. Riediker, R. Williams, R. Devlin, T. Griggs, and P. Bromberg, "Exposure to Particulate Matter, Volatile Organic Compounds, and Other Air Pollutants Inside Patrol Cars," *Environmental Science & Technology,* vol. 37, pp. 2084-2093, 2003/05/01 2003.

[191] H. Guo, S. C. Zou, W. Y. Tsai, L. Y. Chan, and D. R. Blake, "Emission characteristics of nonmethane hydrocarbons from private cars and taxis at different driving speeds in Hong Kong," *Atmospheric Environment,* vol. 45, pp. 2711-2721, 2011/05/01/ 2011.

[192] B. Xu, Y. Wu, Y. Gong, S. Wu, X. Wu, S. Zhu, *et al.*, "Investigation of volatile organic compounds exposure inside vehicle cabins in China," *Atmospheric Pollution Research,* vol. 7, pp. 215-220, 2016/03/01/ 2016.

[193] K.-w. You, Y.-s. Ge, B. Hu, Z.-w. Ning, S.-t. Zhao, Y.-n. Zhang, *et al.*, "Measurement of in-vehicle volatile organic compounds under static conditions," *Journal of Environmental Sciences,* vol. 19, pp. 1208-1213, 2007/01/01/ 2007.

[194] P. Joodatnia, P. Kumar, and A. Robins, "Fast response sequential measurements and modelling of nanoparticles inside and outside a car cabin," *Atmospheric Environment,* vol. 71, pp. 364-375, 2013/06/01/ 2013.

[195] L. D. Knibbs and R. J. de Dear, "Exposure to ultrafine particles and PM2.5 in four Sydney transport modes," *Atmospheric Environment,* vol. 44, pp. 3224-3227, 2010/08/01/ 2010.

[196] L. D. Knibbs, R. J. de Dear, L. Morawska, and K. L. Mengersen, "On-road ultrafine particle concentration in the M5 East road tunnel, Sydney, Australia," *Atmospheric Environment,* vol. 43, pp. 3510-3519, 2009/07/01/ 2009.

[197] L. Morawska, Z. Ristovski, E. R. Jayaratne, D. U. Keogh, and X. Ling, "Ambient nano and ultrafine particles from motor vehicle emissions: Characteristics,

ambient processing and implications on human exposure," *Atmospheric Environment,* vol. 42, pp. 8113-8138, 2008/11/01/ 2008.

[198] T. M. Sager and V. Castranova, "Surface area of particle administered versus mass in determining the pulmonary toxicity of ultrafine and fine carbon black: comparison to ultrafine titanium dioxide," *Particle and Fibre Toxicology,* vol. 6, p. 15, 2009/05/04 2009.

[199] G. Buonanno, S. Marini, L. Morawska, and F. C. Fuoco, "Individual dose and exposure of Italian children to ultrafine particles," *Science of the Total Environment,* vol. 438, pp. 271-277, 2012.

[200] O. Geiss, I. Bianchi, and J. Barrero-Moreno, "Lung-deposited surface area concentration measurements in selected occupational and non-occupational environments," *Journal of Aerosol Science,* vol. 96, pp. 24-37, 2016/06/01/ 2016.

[201] D. C. Quiros, E. S. Lee, R. Wang, and Y. Zhu, "Ultrafine particle exposures while walking, cycling, and driving along an urban residential roadway," *Atmospheric Environment,* vol. 73, pp. 185-194, 2013/07/01/ 2013.

[202] M. C. Fondelli, E. Chellini, T. Yli-Tuomi, I. Cenni, A. Gasparrini, S. Nava, *et al.*, "Fine particle concentrations in buses and taxis in Florence, Italy," *Atmospheric Environment,* vol. 42, pp. 8185-8193, 2008/11/01/ 2008.

[203] O. Nosko, J. Vanhanen, and U. Olofsson, "Emission of 1.3–10 nm airborne particles from brake materials," *Aerosol Science and Technology,* vol. 51, pp. 91-96, 2017/01/02 2017.

[204] F. Amato, F. R. Cassee, H. A. C. Denier van der Gon, R. Gehrig, M. Gustafsson, W. Hafner, *et al.*, "Urban air quality: The challenge of traffic non-exhaust emissions," *Journal of Hazardous Materials,* vol. 275, pp. 31-36, 2014/06/30/ 2014.

[205] T. Grigoratos and G. Martini, "Brake wear particle emissions: a review," *Environmental Science and Pollution Research,* vol. 22, pp. 2491-2504, February 01 2015.

[206] E. Adamiec, E. Jarosz-Krzemińska, and R. Wieszała, "Heavy metals from non-exhaust vehicle emissions in urban and motorway road dusts," *Environmental Monitoring and Assessment,* vol. 188, p. 369, May 26 2016.

[207] K. H. Cho, H. Jang, Y. S. Hong, S. J. Kim, R. H. Basch, and J. W. Fash, "The size effect of zircon particles on the friction characteristics of brake lining materials," *Wear,* vol. 264, pp. 291-297, 2008/02/04/ 2008.

[208] R. Montells, M. Aceves, and J. O. Grimalt, "Sampling and Analysis of Volatile Organic Compounds Emitted from Leaded and Unleaded Gasoline Powered Motor Vehicles," *Environmental Monitoring and Assessment,* vol. 62, pp. 1-14, May 01 2000.

[209] J. G. Watson, J. C. Chow, and E. M. Fujita, "Review of volatile organic compound source apportionment by chemical mass balance," *Atmospheric Environment,* vol. 35, pp. 1567-1584, 2001/03/01/ 2001.

[210] Y.-C. Chien, "Variations in amounts and potential sources of volatile organic chemicals in new cars," *Science of The Total Environment,* vol. 382, pp. 228-239, 2007/09/01/ 2007.

[211] M. J. Fedoruk and B. D. Kerger, "Measurement of volatile organic compounds inside automobiles†," *Journal of Exposure Science & Environmental Epidemiology,* vol. 13, pp. 31-41, 2003/01/01 2003.

[212] X. Zhang, P. Zhang, C. Li, Y. Li, C. Jin, and W. Zhang, "Characterization of two regulators of the TNF-α signaling pathway in Apostichopus japonicus: LPS-

induced TNF-α factor and baculoviral inhibitor of apoptosis repeat-containing 2," *Developmental & Comparative Immunology,* vol. 48, pp. 138-142, 2015/01/01/ 2015.

[213] L. Kajtár and L. Herczeg, "Influence of carbon-dioxide concentration on human well-being and intensity of mental work," *Idojaras,* vol. 116, pp. 145-169, 2012.

[214] F. Gany, S. Bari, L. Prasad, J. Leng, T. Lee, G. D. Thurston, *et al.*, "Perception and reality of particulate matter exposure in New York City taxi drivers," *Journal Of Exposure Science And Environmental Epidemiology,* vol. 27, p. 221, 05/11/online 2016.

[215] G. Buonanno, G. Giovinco, L. Morawska, and L. Stabile, "Lung cancer risk of airborne particles for Italian population," *Environmental Research,* vol. 142, pp. 443-451, 2015.

[216] M. Scungio, G. Buonanno, L. Stabile, and G. Ficco, "Lung cancer risk assessment at receptor site of a waste-to-energy plant," *Waste Management,* 2016.

[217] Office of Environmental Health Hazard Assessment, "Technical Support Document for Cancer Potency Factors: Methodologies for Derivation, Listing of Available Values, and Adjustments to Allow for Early Life Stage Exposures," C. E. P. Agency, Ed., ed. Sacramento, CA, 2009.

[218] European Environmental Agency, "EMEP/EEA air pollutant emission inventory guidebook 2016: Technical guidance to prepare national emission inventories," *EEA Technical Report (08/29/2013),* 2013.

[219] N. E. Klepeis, "Modelling human exposure to air pollution," *Human Exposure Analisys, ed., Ott et al., CRC Press,* pp. 445-470, 2006.

[220] International Commission on Radiological Protection, "Human respiratory tract model for radiological protection. A report of a Task Group of the International Commission on Radiological Protection," vol. 24, ed: Annals of the ICRP, 1994, pp. 1-482.

[221] F. C. Fuoco, L. Stabile, G. Buonanno, M. Scungio, M. Manigrasso, and A. Frattolillo, "Tracheobronchial and alveolar particle surface area doses in smokers," *Atmosphere,* vol. 8, 2017.

[222] R. P. F. Schins, J. H. Lightbody, P. J. A. Borm, T. Shi, K. Donaldson, and V. Stone, "Inflammatory effects of coarse and fine particulate matter in relation to chemical and biological constituents," *Toxicology and Applied Pharmacology,* vol. 195, pp. 1-11, 2004.

[223] C. Louis, Y. Liu, S. Martinet, B. D'Anna, A. M. Valiente, A. Boreave, *et al.*, "Dilution effects on ultrafine particle emissions from Euro 5 and Euro 6 diesel and gasoline vehicles," *Atmospheric Environment,* vol. 169, pp. 80-88, 2017.

[224] S. Jung, J. Lim, S. Kwon, S. Jeon, J. Kim, J. Lee, *et al.*, "Characterization of particulate matter from diesel passenger cars tested on chassis dynamometers," *Journal of Environmental Sciences (China),* vol. 54, pp. 21-32, 2017.

[225] D. M. Lou, P. Wan, P. Q. Tan, and Z. Y. Hu, "Effects of formulations of DOC+CDPF on characteristics of particle emission from a diesel bus," *Zhongguo Huanjing Kexue/China Environmental Science,* vol. 36, pp. 3280-3286, 2016.

[226] S. Marini, G. Buonanno, L. Stabile, and P. Avino, "A benchmark for numerical scheme validation of airborne particle exposure in street canyons," *Environmental Science and Pollution Research,* vol. 22, pp. 2051-2063, 2015.

[227] ACEA-European Automobile Manufacturers Association. (2017/18/07). *www.acea.be*.

[228] D. Moreira and M. Vilhena, *Air pollution and turbulence: modeling and applications*: CRC Press/Taylor & Francis, 2010.
[229] P. A. Baron and K. Willeke, *Aerosol Measurement - principles, techniques and applications*, Second ed.: Wiley Interscience, 2001.
[230] W. C. Hinds, *Aerosol Technology*, Second Edition ed.: John Wiley & Sons, INC., 1999.
[231] M. A. Parra, J. L. Santiago, F. Martín, A. Martilli, and J. M. Santamaría, "A methodology to urban air quality assessment during large time periods of winter using computational fluid dynamic models," *Atmospheric Environment*, vol. 44, pp. 2089-2097, 2010.
[232] J. L. Santiago, R. Borge, F. Martin, D. de la Paz, A. Martilli, J. Lumbreras, *et al.*, "Evaluation of a CFD-based approach to estimate pollutant distribution within a real urban canopy by means of passive samplers," *Science of the Total Environment*, vol. 576, pp. 46-58, 2017.
[233] C. He, L. Morawska, J. Hitchins, and D. Gilbert, "Contribution from indoor sources to particle number and mass concentrations in residential houses," *Atmospheric Environment*, vol. 38, pp. 3405-3415, 2004.
[234] Commission on Environmental Health, "Environment for Sustainable Heakth Development: An Action Plan for Sweden," vol. SOU 1996, Ministry of Health and Social Affairs, Ed., ed. Stockholm, 1996, pp. 1-136.
[235] EPA, "Risk Assessment Guidance for Superfund: Volume I - Human Health Evaluation Manual (Part B, Development of Risk-based Preliminary Remediation Goals)," vol. 540/R-92/003, O. o. R. a. Development, Ed., ed. Washinghton, DC: United States Environmental Protection Agency, 1991b.
[236] P. Blondeau, V. Iordache, O. Poupard, D. Genin, and F. Allard, "Relationship between outdoor and indoor air quality in eight French schools," *Indoor Air*, vol. 15, pp. 2-12, 2005.
[237] E. Diapouli, A. Chaloulakou, and N. Spyrellis, "Indoor and outdoor particulate matter concentrations at schools in the Athens area," *Indoor and Built Environment*, vol. 16, pp. 55-61, 2007.
[238] U. Heudorf, V. Neitzert, and J. Spark, "Particulate matter and carbon dioxide in classrooms - The impact of cleaning and ventilation," *International Journal of Hygiene and Environmental Health*, vol. 212, pp. 45-55, 2009.
[239] B. Brunekreef, N. A. H. Janssen, J. De Hartog, H. Harssema, M. Knape, and P. Van Vliet, "Air pollution from truck traffic and lung function in children living near motorways," *Epidemiology*, vol. 8, pp. 298-303, 1997.
[240] S. C. Lee and M. Chang, "Indoor and outdoor air quality investigation at schools in Hong Kong," *Chemosphere*, vol. 41, pp. 109-113, 2000.
[241] Y. H. Mi, D. Norbäck, J. Tao, Y. L. Mi, and M. Ferm, "Current asthma and respiratory symptoms among pupils in Shanghai, China: Influence of building ventilation, nitrogen dioxide, ozone, and formaldehyde in classrooms," *Indoor Air*, vol. 16, pp. 454-464, 2006.
[242] J. F. Mejía, S. L. Choy, K. Mengersen, and L. Morawska, "Methodology for assessing exposure and impacts of air pollutants in school children: Data collection, analysis and health effects - A literature review," *Atmospheric Environment*, vol. 45, pp. 813-823, 2011.
[243] World Health Organization, "WHO's global air-quality guidelines," *Lancet*, vol. 368, p. 1302, Oct 14 2006.

[244] L. Morawska, C. He, G. Johnson, H. Guo, E. Uhde, and G. Ayoko, "Ultrafine particles in indoor air of a school: Possible role of secondary organic aerosols," *Environmental Science and Technology,* vol. 43, pp. 9103-9109, 2009.

[245] Q. Zhang and Y. Zhu, "Characterizing ultrafine particles and other air pollutants at five schools in South Texas," *Indoor Air,* vol. 22, pp. 33-42, 2012.

[246] C. Y. H. Chao and T. C. Tung, "An empirical model for outdoor contaminant transmission into residential buildings and experimental verification," *Atmospheric Environment,* vol. 35, pp. 1585-1596, 2001.

[247] H. Guo, L. Morawska, C. He, and D. Gilbert, "Impact of ventilation scenario on air exchange rates and on indoor particle number concentrations in an air-conditioned classroom," *Atmospheric Environment,* vol. 42, pp. 757-768, 2008.

[248] P. H. Baker, S. Sharples, and I. C. Ward, "Air flow through cracks," *Building and Environment,* vol. 22, pp. 293-304, 1987.

[249] O. Poupard, P. Blondeau, V. Iordache, and F. Allard, "Statistical analysis of parameters influencing the relationship between outdoor and indoor air quality in schools," *Atmospheric Environment,* vol. 39, pp. 2071-2080, 2005.

[250] A. Gupta and K. W. David Cheong, "Physical characterization of particulate matter and ambient meteorological parameters at different indoor-outdoor locations in Singapore," *Building and Environment,* vol. 42, pp. 237-245, 2007.

[251] M. Mazaheri, C. Reche, I. Rivas, L. R. Crilley, M. Álvarez-Pedrerol, M. Viana, *et al.*, "Variability in exposure to ambient ultrafine particles in urban schools: Comparative assessment between Australia and Spain," *Environment International,* vol. 88, pp. 142-149, 2016.

[252] M. Viana, I. Rivas, X. Querol, A. Alastuey, J. Sunyer, M. Álvarez-Pedrerol, *et al.*, "Indoor/outdoor relationships and mass closure of quasi-ultrafine, accumulation and coarse particles in Barcelona schools," *Atmos. Chem. Phys.*, vol. 14, pp. 4459-4472, 2014.

[253] C. Reche, X. Querol, A. Alastuey, M. Viana, J. Pey, T. Moreno, *et al.*, "New considerations for PM, Black Carbon and particle number concentration for air quality monitoring across different European cities," *Atmos. Chem. Phys.*, vol. 11, pp. 6207-6227, 2011.

[254] C. Reche, M. Viana, T. Moreno, X. Querol, A. Alastuey, J. Pey, *et al.*, "Peculiarities in atmospheric particle number and size-resolved speciation in an urban area in the western Mediterranean: Results from the DAURE campaign," *Atmospheric Environment,* vol. 45, pp. 5282-5293, 2011/09/01/ 2011.

[255] M. Viana, I. Rivas, C. Reche, A. S. Fonseca, N. Pérez, X. Querol, *et al.*, "Field comparison of portable and stationary instruments for outdoor urban air exposure assessments," *Atmospheric Environment,* vol. 123, pp. 220-228, 2015/12/01/ 2015.

[256] G. Buonanno, M. Dell'Isola, L. Stabile, and A. Viola, "Uncertainty budget of the SMPS-APS system in the measurement of PM 1, PM 2.5, and PM 10," *Aerosol Science and Technology,* vol. 43, pp. 1130-1141, 2009.

[257] *EN 14907:2005. Ambient air quality-standard gravimetric measurement method for the determination of the PM<inf>2.5</inf> mass fraction of suspended particulate matter.*, Ref. No. EN 14907:2005: E, 2005.

[258] I. Rivas, M. Mazaheri, M. Viana, T. Moreno, S. Clifford, C. He, *et al.*, "Identification of technical problems affecting performance of DustTrak DRX aerosol monitors," *Sci Total Environ,* vol. 584-585, pp. 849-855, Apr 15 2017.

[259] X. Querol, A. Alastuey, S. Rodriguez, F. Plana, E. Mantilla, and C. R. Ruiz, "Monitoring of PM10 and PM2.5 around primary particulate anthropogenic emission sources," *Atmospheric Environment,* vol. 35, pp. 845-858, 2001.

[260] *EN 12341, 2001. Determination of the PM<inf>10</inf> fraction of suspended particulate matter,* 2001.

[261] P. Avino, G. Capannesi, and A. Rosada, "Characterization and distribution of mineral content in fine and coarse airborne particle fractions by neutron activation analysis," *Toxicological and Environmental Chemistry,* vol. 88, pp. 633-647, 2006.

[262] P. Avino, G. Capannesi, and A. Rosada, "Heavy metal determination in atmospheric particulate matter by Instrumental Neutron Activation Analysis," *Microchemical Journal,* vol. 88, pp. 97-106, 2008.

[263] P. Avino, D. Brocco, A. Cecinato, L. Lepore, and C. Balducci, "Carbonaceous components in atmospheric aerosol: Measurement procedures and characterization," *Annali di Chimica,* vol. 92, pp. 333-341, 2002.

[264] G. Buonanno, L. Stabile, P. Avino, and R. Vanoli, "Dimensional and chemical characterization of particles at a downwind receptor site of a waste-to-energy plant," *Waste Management,* vol. 30, pp. 1325-1333, 2010.

[265] F. Fuoco, L. Stabile, G. Buonanno, C. Trassiera, A. Massimo, A. Russi, *et al.*, "Indoor Air Quality in Naturally Ventilated Italian Classrooms," *Atmosphere,* vol. 6, p. 1652, 2015.

[266] C. Protano, M. Manigrasso, and P. Avino, "Second-hand smoke generated by combustion and electronic smoking devices used in real scenarios: Ultrafine particle pollution and age-related dose assessment.," *Environment International,* vol. in press, 2017.

[267] M. Manigrasso, M. Vitali, C. Protano, and P. Avino, "Temporal evolution of ultrafine particles and of alveolar deposited surface area from main indoor combustion and non-combustion sources in a model room," *Sci Total Environ,* vol. 598, pp. 1015-1026, Nov 15 2017.

[268] M. Mortamais, J. Pujol, B. L. van Drooge, D. Macià, G. Martínez-Vilavella, C. Reynes, *et al.*, "Effect of exposure to polycyclic aromatic hydrocarbons on basal ganglia and attention-deficit hyperactivity disorder symptoms in primary school children," *Environment International,* vol. 105, pp. 12-19, 2017.

[269] *Primary and General Secondary Education – 2016/17. Eurydice Facts and Figures.* , 2016.

[270] G. Buonanno, G. Giovinco, L. Morawska, and L. Stabile, "Lung cancer risk of airborne particles for Italian population," *Environ Res,* vol. 142, pp. 443-451, Aug 4 2015.

[271] *Technical Support Document for Cancer Potency Factors: Methodologies for Derivation, Listing of Available Values, and Adjustments to Allow for Early Life Stage Exposures.* , California Environmental Protection Agency, 2009.

[272] G. Zoppi, F. Bressan, and A. Luciano, "Height and weight reference charts for children aged 2-18 years from Verona, Italy," *European Journal of Clinical Nutrition,* vol. 50, pp. 462-468, 1996.

[273] F. Amato, I. Rivas, M. Viana, T. Moreno, L. Bouso, C. Reche, *et al.*, "Sources of indoor and outdoor PM2.5 concentrations in primary schools," *Sci Total Environ,* vol. 490, pp. 757-65, Aug 15 2014.

[274] C. Reche, M. Viana, I. Rivas, L. Bouso, M. Alvarez-Pedrerol, A. Alastuey, *et al.*, "Outdoor and indoor UFP in primary schools across Barcelona," *Sci Total Environ,* vol. 493, pp. 943-53, Sep 15 2014.

[275] G. Ghirga and M. Pipere, "Are children safe indoor from outdoor air pollution? A short review," *Open Journal of Pediatrics,* vol. 2, pp. 93-96, 2012.

[276] A. Y. P. Wardoyo, D. H. Santjojo, and I. I. H. Putri, "Indoor Outdoor Ultrafine Particle Measurements in Lecture Rooms," *International Journal of Basic & Applied Sciences,* vol. 12, pp. 198-201, 2012.

[277] M. Viana, I. Rivas, X. Querol, A. Alastuey, M. Álvarez-Pedrerol, L. Bouso, *et al.*, "Partitioning of trace elements and metals between quasi-ultrafine, accumulation and coarse aerosols in indoor and outdoor air in schools," *Atmospheric Environment,* vol. 106, pp. 392-401, 2015/04/01/ 2015.

[278] W. R. Chan, S. Parthasarathy, W. J. Fisk, and T. E. McKone, "Estimated effect of ventilation and filtration on chronic health risks in U.S. offices, schools, and retail stores," *Indoor Air,* vol. 26, pp. 331-43, Apr 2016.

[279] R. Goyal and P. Kumar, "Indoor–outdoor concentrations of particulate matter in nine microenvironments of a mix-use commercial building in megacity Delhi," *Air Quality, Atmosphere & Health,* vol. 6, pp. 747-757, 2013.

[280] M. Habil and A. Taneja, "Children's Exposure to Indoor Particulate Matter in Naturally Ventilated Schools in India," *Indoor and Built Environment,* June 28, 2011 2011.

[281] W. Zhang, Y. Tong, H. Wang, L. Chen, L. Ou, X. Wang, *et al.*, "Emission of Metals from Pelletized and Uncompressed Biomass Fuels Combustion in Rural Household Stoves in China," *Scientific Reports,* vol. 4, p. 5611, 07/08/online 2014.

[282] M. Scungio, G. Buonanno, L. Stabile, and G. Ficco, "Lung cancer risk assessment at receptor site of a waste-to-energy plant," *Waste Management,* vol. 56, pp. 207-215, 2016.

[283] A. Pacitto, L. Stabile, T. Moreno, P. Kumar, A. Wierzbicka, L. Morawska, *et al.*, "The influence of lifestyle on airborne particle surface area doses received by different Western populations," *Environmental Pollution,* vol. 232, pp. 113-122, 2018.

[284] U.S. Environmental Protection Agency, "Risk Assessment Guidance for Superfund: Volume I - Human Health Evaluation Manual (Part B, Development of Risk-based Preliminary Remediation Goals)," vol. 540/R-92/003, O. o. R. a. Development, Ed., ed. Washinghton, DC: United States Environmental Protection Agency, 1991.

[285] S. Rengasamy and B. C. Eimer, "Total Inward Leakage of Nanoparticles Through Filtering Facepiece Respirators," *The Annals of Occupational Hygiene,* vol. 55, pp. 253-263, 2011.

[286] S. Rengasamy, W. P. King, B. C. Eimer, and R. E. Shaffer, "Filtration performance of niosh-approved n95 and p100 filtering facepiece respirators against 4 to 30 nanometer-size nanoparticles," *Journal of Occupational and Environmental Hygiene,* vol. 5, pp. 556-564, 2008.

[287] Z. Zhuang, C. C. Coffey, P. A. Jensen, D. L. Campbell, R. B. Lawrence, and W. R. Myers, "Correlation Between Quantitative Fit Factors and Workplace Protection Factors Measured in Actual Workplace Environments at a Steel Foundry," *AIHA Journal,* vol. 64, pp. 730-738, 2003/11/01 2003.

[288] C. D. Crutchfield, E. O. Fairbank, and S. L. Greenstein, "Effect of test exercises and mask donning on measured respirator fit," *Appl Occup Environ Hyg,* vol. 14, pp. 827-37, Dec 1999.

[289] E. L. Floyd, J. B. Henry, and D. L. Johnson, "Influence of facial hair length, coarseness, and areal density on seal leakage of a tight-fitting half-face

respirator," *Journal of Occupational and Environmental Hygiene,* vol. 15, pp. 334-340, 2018/04/03 2018.

[290] S. A. Grinshpun, H. Haruta, R. M. Eninger, T. Reponen, R. T. McKay, and S.-A. Lee, "Performance of an N95 Filtering Facepiece Particulate Respirator and a Surgical Mask During Human Breathing: Two Pathways for Particle Penetration," *Journal of Occupational and Environmental Hygiene,* vol. 6, pp. 593-603, 2009/09/09 2009.

[291] L. E. Bowen, "Does That Face Mask Really Protect You?," *Applied Biosafety,* vol. 15, pp. 67-71, 2010.

[292] S. Rengasamy, B. Eimer, and R. E. Shaffer, "Simple respiratory protection - Evaluation of the filtration performance of cloth masks and common fabric materials against 20-1000 nm size particles," *Annals of Occupational Hygiene,* vol. 54, pp. 789-798, 2010.

[293] H. Jung, J. Kim, S. Lee, J. Lee, J. Kim, P. Tsai, *et al.*, "Comparison of filtration efficiency and pressure drop in anti-yellow sandmasks, quarantine masks, medical masks, general masks, and handkerchiefs," *Aerosol and Air Quality Research,* vol. 14, pp. 991-1002, 2014.

[294] W. Mueller, C. J. Horwell, A. Apsley, S. Steinle, S. McPherson, J. W. Cherrie, *et al.*, "The effectiveness of respiratory protection worn by communities to protect from volcanic ash inhalation. Part I: Filtration efficiency tests," *International Journal of Hygiene and Environmental Health,* vol. 221, pp. 967-976, 2018/07/01/ 2018.

[295] M. Nyhan, A. McNabola, and B. Misstear, "Evaluating artificial neural networks for predicting minute ventilation and lung deposited dose in commuting cyclists," *Journal of Transport & Health,* vol. 1, pp. 305-315, 2014/12/01/ 2014.

[296] S. Gao, J. Kim, M. Yermakov, Y. Elmashae, X. He, T. Reponen, *et al.*, "Performance of N95 FFRs Against Combustion and NaCl Aerosols in Dry and Moderately Humid Air: Manikin-based Study," *Ann Occup Hyg,* vol. 60, pp. 748-60, Jul 2016.

[297] J. D. Newnum, "The effects of relative humidity on respirator performance," *MS (Master of Science) thesis, University of Iowa, 2010,* 2010.

[298] F. Haghighat, A. Bahloul, J. Lara, R. Mostofi, and A. Mahdavi, *Development of a Procedure to Measure the Effectiveness of N95 Respirator Filters against Nanoparticles,* 2012.

[299] S. Yang and G. W. M. Lee, "Filtration characteristics of a fibrous filter pretreated with anionic surfactants for monodisperse solid aerosols," *Journal of Aerosol Science,* vol. 36, pp. 419-437, 2005/04/01/ 2005.

[300] M. Braniš and J. Šafránek, "Characterization of coarse particulate matter in school gyms," *Environmental Research,* vol. 111, pp. 485-491, 2011.

[301] M. Braniš, J. Šafránek, and A. Hytychová, "Indoor and outdoor sources of size-resolved mass concentration of particulate matter in a school gym-implications for exposure of exercising children," *Environmental Science and Pollution Research,* vol. 18, pp. 598-609, 2011.

[302] M. O. Ng, M. Qu, P. Zheng, Z. Li, and Y. Hang, "CO2-based demand controlled ventilation under new ASHRAE Standard 62.1-2010: a case study for a gymnasium of an elementary school at West Lafayette, Indiana," *Energy and Buildings,* vol. 43, pp. 3216-3225, 2011/11/01/ 2011.

[303] C. A. Ramos, H. T. Wolterbeek, and S. M. Almeida, "Exposure to indoor air pollutants during physical activity in fitness centers," *Building and Environment,* vol. 82, pp. 349-360, 2014/12/01/ 2014.

[304] P. Avino, M. Scungio, L. Stabile, G. Cortellessa, G. Buonanno, and M. Manigrasso, "Second-hand aerosol from tobacco and electronic cigarettes: Evaluation of the smoker emission rates and doses and lung cancer risk of passive smokers and vapers," *Science of The Total Environment*, vol. 642, pp. 137-147, 2018/11/15/ 2018.

[305] C. He, L. Morawska, J. Hitchins, and D. Gilbert, "Contribution from indoor sources to particle number and mass concentrations in residential houses," *Atmospheric Environment*, vol. 38, pp. 3405-3415, 2004.

[306] C. Howard-Reed, L. A. Wallace, and W. R. Ott, "The Effect of Opening Windows on Air Change Rates in Two Homes," *Journal of the Air & Waste Management Association*, vol. 52, pp. 147-159, 2002/02/01 2002.

[307] L. A. Wallace, S. J. Emmerich, and C. Howard-Reed, "Continuous measurements of air change rates in an occupied house for 1 year: the effect of temperature, wind, fans, and windows," *J Expo Anal Environ Epidemiol*, vol. 12, pp. 296-306, Jul 2002.

[308] S. Ruggieri, V. Longo, C. Perrino, S. Canepari, G. Drago, L. L'Abbate, *et al.*, "Indoor Air Quality in Schools of a Highly Polluted South Mediterranean Area," *Indoor Air*, vol. 0, 2018/12/23 2018.

[309] G. Buonanno, L. Stabile, L. Morawska, and A. Russi, "Children exposure assessment to ultrafine particles and black carbon: The role of transport and cooking activities," *Atmospheric Environment*, vol. 79, pp. 53-58, 11// 2013.

[310] B. Shi, L. E. Ekberg, and S. Langer, "Intermediate Air Filters for General Ventilation Applications: An Experimental Evaluation of Various Filtration Efficiency Expressions," *Aerosol Science and Technology*, vol. 47, pp. 488-498, 2013/05/01 2013.